

Reference 10.3

FC06876, Rev. 0

**“Performance of Low Temperature Overpressure Protection
System Analyses Using RELAP5: Methodology Paper”**

**PERFORMANCE OF
LOW TEMPERATURE OVERPRESSURE PROTECTION
SYSTEM ANALYSES USING RELAP5
AT COMBUSTION ENGINEERING-TYPE PWRs**

METHODOLOGY PAPER

3/15/02

Enercon Services
302 Pendleton Way
Oakland, Ca. 94563
510-632-1734

TABLE OF CONTENTS

| | | |
|-------|--|----|
| I. | INTRODUCTION AND PURPOSE | 3 |
| II. | OVERVIEW | 4 |
| III. | ANALYSIS CRITERIA | 5 |
| IV. | ACCEPTABILITY OF RELAP FOR LTOP ANALYSES | 6 |
| V. | DATA INPUTS | 12 |
| VI. | NRC LTOP ANALYSIS REQUIREMENTS | 15 |
| VII. | ANALYSIS DISCUSSION | 17 |
| VIII. | UNCERTAINTY AND THE LTOP SETPOINT CURVE | 26 |
| IX. | CONCLUSIONS | 29 |
| X. | REFERENCES | 30 |

I. INTRODUCTION AND PURPOSE

The Low Temperature Overpressure Protection (LTOP) systems at nuclear power plants provide peak pressure protection for transients that may occur while the Reactor Coolant System (RCS) is at reduced temperatures. The LTOP systems at Combustion Engineering (CE) Pressurized Water Reactors (PWR) typically consist of Power Operated Relief Valves (PORVs) on the Pressurizer with a pressure setpoint that decreases from its full power value when the LTOP system is enabled. This setpoint change is achieved by either a step change to a constant LTOP PORV setpoint value, or is a variable function of RCS temperature in accordance with a LTOP setpoint curve. The PORV acts to relieve pressure should any transient cause a pressure rise approaching the limiting allowable Pressure/Temperature curve (P/T curve). In many cases, the existence of a steam void in the pressurizer is also credited for the LTOP function for certain scenarios. Some CE plants use a shutdown cooling system relief valve for the LTOP function; these plants are not covered by this methodology paper.

There are two main types of LTOP initiation events. The first is a mass addition event, such as a spurious Safety Injection (SI) signal. In this event, all enabled safety injection pumps are hypothesized to start and inject fluid into the RCS. The pressure will rise as the added water increases the density of fluid in the fixed-volume RCS. When the pressure reaches the PORV setpoint, there is an instrumentation and mechanical time delay before the PORV opens. It is necessary to demonstrate first that the time delay will not cause a pressure overshoot that exceeds the P/T curve, and second that the flow rate of the PORV under the given conditions is sufficient to relieve enough fluid to offset the injection rate and maintain or decrease the RCS pressure.

The second type of LTOP initiating event is termed a heat addition event. The limiting scenario is the startup of a Reactor Coolant Pump (RCP) while the Steam Generators (SGs) contain hot secondary fluid. This situation can result after the RCS is put on shutdown cooling and no RCS fluid is circulated through the SGs; hence there is no cooling mechanism for the SGs while there is for the majority of the RCS. When the RCP is started, there is heat added both from the pump itself and from heat transfer from the hot SG. The added heat to the fixed-volume RCS will result in a pressure rise. In this case, the PORVs may open and relieve the pressure. The initial heat input can be very large if there is no administrative restriction on the delta-T between the primary and secondary system. In some cases, it may be necessary to hypothesize a steam void in the pressurizer at the time of first RCP start. A steam void helps maintain a relatively constant RCS pressure (while the steam bubble collapses) over the first few minutes while the RCS and SG temperatures equilibrate.

This report discusses the methodology of analyzing these transients using the RELAP5/MOD 3.2 (RELAP) personal computer code. It uses the Fort Calhoun nuclear power plant as an example plant (Reference 4). The purpose of the report is to describe the methodology, the required assumptions, and the model sensitivities so that RELAP can be applied for safety-related LTOP system analyses at CE plants that use PORVs as the pressure relieving device.

II. OVERVIEW

A RELAP model is created that represents the RCS up to the boundary of mass or heat injection, and to the boundary of mass relief (the PORV). Details of the modeling are described below. Every effort is made to assure that the model will be conservative in terms of predicting the peak pressure at the critical location. Sensitivity analyses are performed and described here to evaluate some of the modeling choices. Many of the other modeling conservative assumptions are taken from the NRC review of LTOP analyses performed by Combustion Engineering as described in Reference 1. These assumptions include a conservative decay heat, pressurizer heaters failed at full on power, conservative RCP heat addition, and the loss of shutdown cooling. These four assumptions, which cover all credible spurious heat sources, are applied to both the mass addition and heat addition cases.

In many cases, the plant operation is intentionally restricted for the purpose of LTOP. For example, at certain temperatures SI pumps can be intentionally disabled so that their spurious startup does not need to be considered. Similarly, the startup of the first RCP is not considered to be a credible spurious event, so plants can specify required conditions for the start of the first RCP, such as a minimum Pressurizer steam void or maximum primary to secondary temperature differential. When such plant restrictions are credited, the plant must have an assured method of satisfying the requirement, such as a governing Technical Specification. For example, Fort Calhoun Technical Specifications include limitations on minimum steam voids in the Pressurizer during the first RCP start, and on enabled High Pressure Safety Injection (HPSI) pumps at reduce RCS temperatures.

After the conservative RELAP model is created, mass addition and heat addition events can be simulated. Care is taken to select critical initial operating conditions to bound the worse cases in terms of peak pressure. Since the critical scenarios may not be known in advance, typically several different scenarios are proposed and evaluated throughout the LTOP enabled temperature range. The result of the scenario will be a peak pressure to be compared to the appropriate point on the P/T limit curve. The LTOP system is deemed adequate if all peak pressures are below the P/T limit.

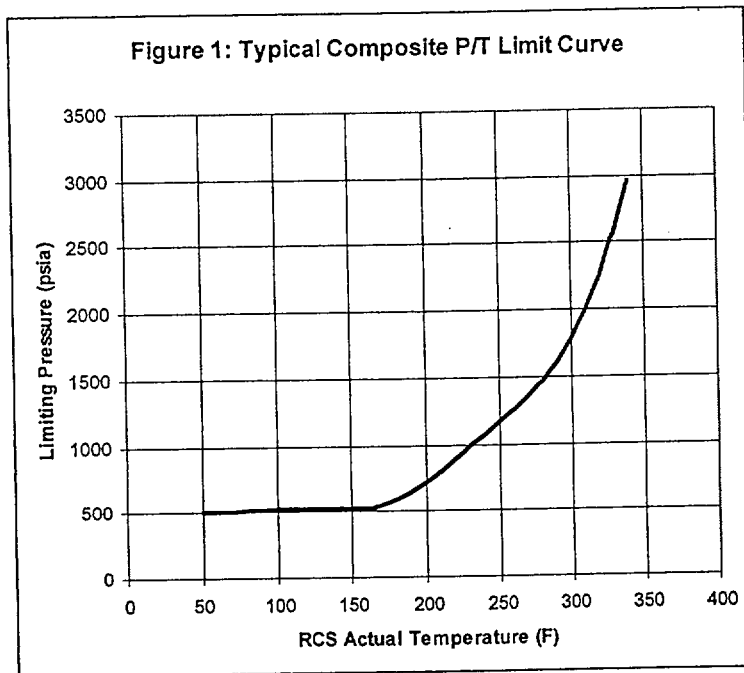
For some plants that specify a required Pressurizer steam void to start the first RCP, the transient will be run for ten minutes only. During this time, the RCS and SG temperatures will equilibrate and the heat addition will be effectively mitigated. However, the conservative methodology assumes a continued net heat input (from the decay heat, RCP heat, and Pressurizer heaters). This would eventually need to be mitigated, but the mass addition scenarios, which also include the same net heat input, would bound the transient.

Uncertainty in instrumentation and component performance is modeled conservatively. Unless otherwise described, a full bias due to uncertainty is applied to initial conditions and boundary conditions, for example, the maximum injection flow rate is used rather than a best estimate flow rate. For plants that use a variable LTOP PORV setpoint based on RCS temperature, the temperature and pressure errors are treated as described in Section VIII.

III. ANALYSIS CRITERIA

The purpose of the LTOP system is to limit pressure transients to below the P/T curve. P/T curves are developed in accordance with 10CFR50 Appendix G [Ref. 2] criteria based on Effective Full Power Years (EFPY) of Reactor Vessel operation. The P/T curves can be found in a plant's Technical Specifications or Pressure-Temperature Limitations Report (PTLR).

P/T curves are provided for both heatup and cooldown, and vary according to the heatup or cooldown rate. In general, it is possible to develop a composite P/T limit based on the maximum allowed heatup or cooldown rates. This composite curve is the minimum pressures allowed at the given RCS temperature for the maximum temperature change rates. For the purpose of the analysis, the curve is used without any uncertainty, i.e., it is the limiting actual pressure at the actual local temperature based on metallurgical concerns (see Figure 1).

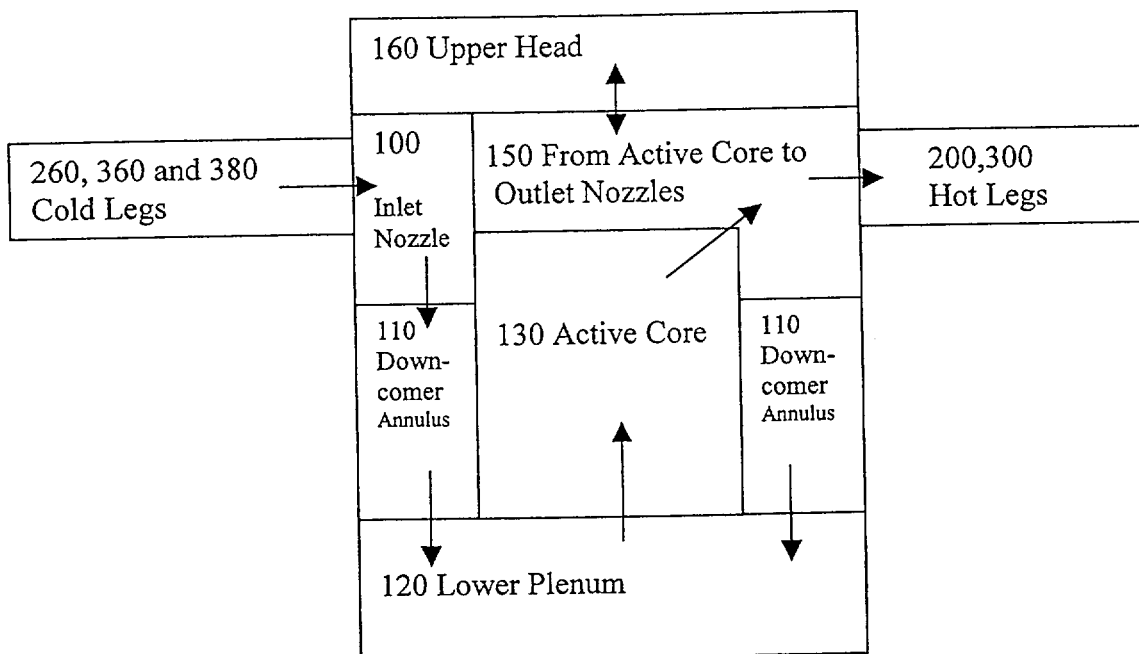


The P/T curve shown in Figure 1 may either be the pressure limit at the reactor vessel beltline, or it can be the pressure limit at the pressurizer. The reason for the latter approach is that only the Pressurizer is instrumented for pressure. When the P/T limit is based on the Pressurizer pressure, some conservative estimate must be made of the pressure difference between the location within the Pressurizer when pressure is measured, and the beltline Reactor Vessel pressure. This conservative pressure difference must include effects of elevation change and flow pressure drops under the maximum possible number of operating RCPs.

IV. ACCEPTABILITY OF RELAP FOR LTOP ANALYSES

A typical Relap model is shown in Figures 2, 3, and 4. Figure 2 shows the nodalization in the core. Figure 3 shows the left hand loop of a CE-type PWR. This type of reactor has one left hand hot leg, and two left hand cold legs, but since conditions would be identical in both cold legs for all scenarios, they are grouped into a single path. Figure 4 shows the right hand loop with the pressurizer and separately modeled cold legs. It will be noted that this nodalization is less detailed than SBLOCA models, but it is sufficient for the relatively simple transients involved in LTOP analysis.

Figure 2: Typical Nodalization of the Reactor Vessel



RELAP5/MOD3.2 has the ability to model single phase and two-phase flow situations in both nuclear and non-nuclear systems. RELAP5/MOD3.2 uses a non-homogeneous and non-equilibrium calculation model that is based on six equations which represent mass, momentum and energy for both the liquid and vapor phases. Additional features allow inclusion of reactor point kinetics, control systems, pumps, pressurizers, steam separators, and various types of valves.

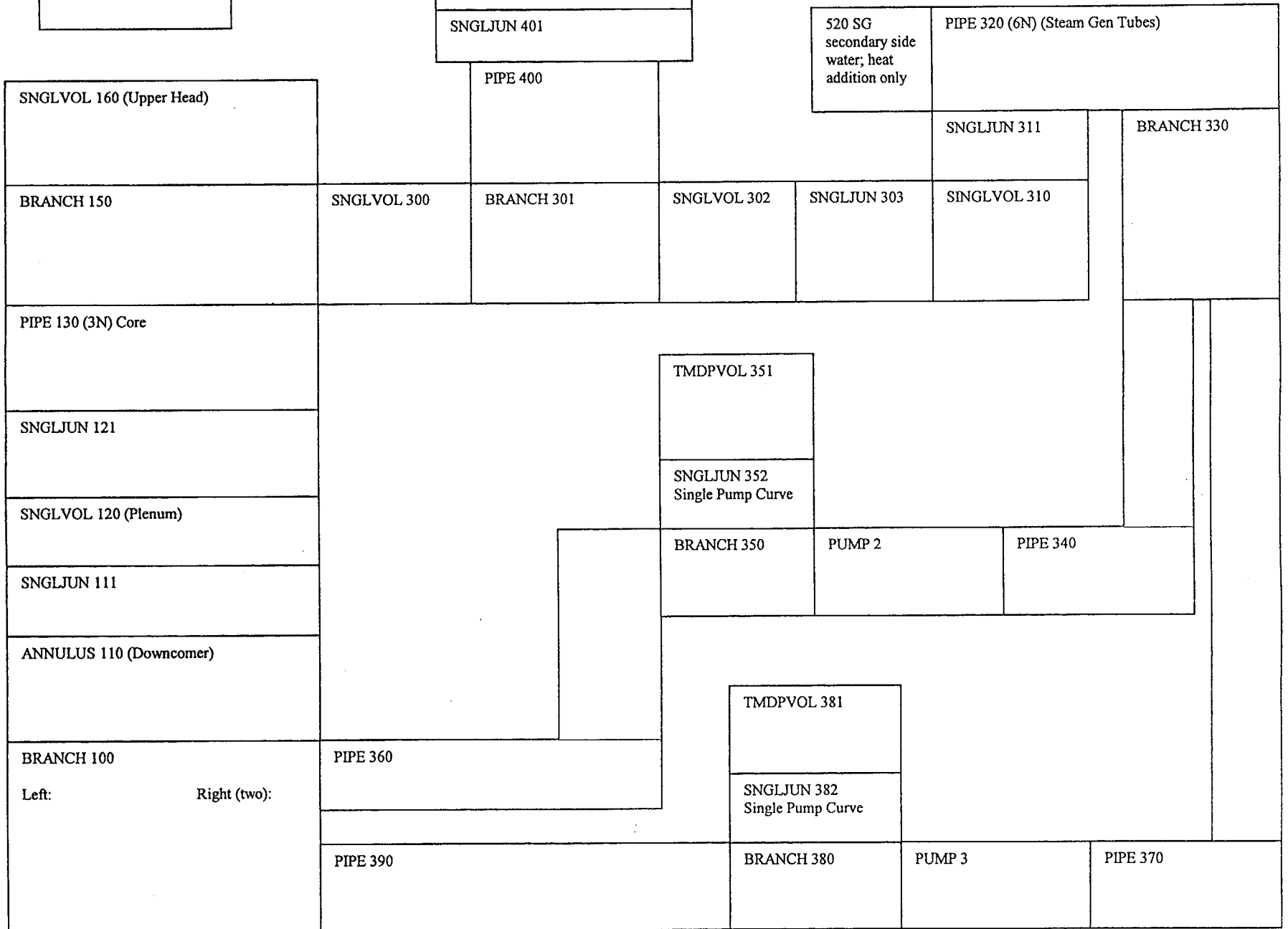
This version of the RELAP code is considered qualified for safety-related use under ENERCON's Quality Assurance Program. The associated V&V package that qualifies the code for general safety-related applications is on file in ENERCON's Atlanta office and is dated 2/19/98.

TMDPVOL 430
(PORV backpressure)

VALVE 420 (PORV)

PIPE 410 6N (Pressurizer)

Figure 4: Typical RELAP Schematic, CE Reference Plant, Right Side



The RELAP5/MOD3.2 code currently qualified is specifically able to accurately predict the plant transient due to a Pressurized Thermal Shock event that actuates LTOP systems in Light Water Reactors. It is assumed that the operation of the LTOP system can be considered a "controlled" Small Break Loss of Coolant Accident (SBLOCA). This assumption is validated by the fact that a small break LOCA has been generally defined to include any loss of integrity/break in the PWR pressure boundary which has a break area of 0.5 ft² or less. This range of break areas encompasses all small lines that penetrate the RCS pressure boundary including relief and safety valves, charging and letdown lines, drain lines and various instrumentation lines. Additionally, the initiator of the transient (a pressurized thermal shock) as well as the performance of the Pressurizer should be modeled accurately during the plant transient.

The RELAP code manual (in Volume 5 of Reference 3) provides abstracts of reference documentation that have shown the accuracy and capability of the RELAP code through its many years of use. Table 1 presents a list of abstracts that specifically identify the modeling of SBLOCAs, Pressurizers, and Pressurized Thermal Shock events. Examination of Table 1 shows that some of the published work was performed using RELAP5/MOD2. It should be noted that RELAP5/MOD3 was produced by improving and extending the modeling base that was established with the release of RELAP5/MOD2 in 1985. Code deficiencies identified by members of the International Code Assessment and Applications Program (ICAP) through assessment calculations were noted, prioritized, and subsequently addressed. Consequently, several new models, improvements to existing models and user conveniences were added to RELAP5/MOD2 to make MOD3 of the code. The RELAP5 code manual has a detailed list of some of these features and improvements that have been made to RELAP5/MOD2 and incorporated as RELAP5/MOD3.

Based upon the numerous publications that show the use of the RELAP5/MOD3.2 code for use in SBLOCA analysis, Pressurizer response analysis, and Pressurized Thermal Shock analysis it is deemed acceptable to use the RELAP5/MOD3.2 computer code for use in LTOP system analysis.

Table 1: List Of Selected Publications From NUREG/CR-5535, Volume 5, Revision 4 [Ref. 3] that show RELAP Modeling Of SBLOCA And Pressurizer Operations

SBLOCA References

1. Adams, J.P., et. al., 1986, "Numerical Simulation of PWR Response to a Small Break LOCA with Reactor Coolant Pumps Operating", *4th International Symposium on Multi-Phase Transport and Particulate Phenomena, Miami Beach, Florida, December 1986*, EGG-M-32686
2. Ardron, K.H., and P.C. Hall, 1988, "UK Experience with RELAP5MOD2," *15th Water Reactor Safety Information Meeting, Gaithersburg, Maryland, October 26, 1987*, February, Central Electricity Generating Board, Gloucester, England
3. Babcock & Wilcox Owner's Group Analysis Committee, 1986, *RELAP5/MOD2 Benchmark of OTIS Feed and Bleed Test #220899*, BAW-1903, March
4. Choi, H.R., et. al., 1988, "Impact of Safety Injection Flow Rate on Small Break LOCA Behavior." *Third International Topical Meeting on Nuclear Power Plant Thermal Hydraulics and Operations, Seoul, Korea, November 1988*, Korea Advanced Energy Research Institute
5. Fletcher, C.D., and C.M. Kullberg, 1985, *Break Spectrum Analysis for Small Break Loss-of-Coolant Accidents in a RESAR-3S Plant*, NUREG/CR-4384, EGG-2416, September
6. Gloude-mans, J.R., 1991, *Multiloop Integral System Test (MIST): Final Report, Vol. I: Summary of Key Results*, NUREG/CR-5395, April
7. Hall, P.C., and G. Brown, 1986, *RELAP5/MOD2 Calculations of OECD-LOFT Test LP-SB-01*, GD\PE-N\544, November, Central Electricity Generating Board, Barnwood, United Kingdom
8. Loomis, G.G., and J.E. Streit, 1985, *Results of Semiscale MOD-2C Small-Break (5%) Loss-of-Coolant Accident Experiments S-LH-1 and S-LH-2*, NUREG/CR-4438, EGG-2424, November
9. Makowitz, H. and W.H. Gray, 1987, "Investigation of Time Step Insensitivity for RELAP5/MOD2 SBLOCA Simulations," *Transactions of the American Nuclear Society, 55, pp.363-364*
10. Yuann, R.Y., K.S. Liang, and J.L. Jacobson, 1987, *RELAP5/MOD2 Assessment Using Semiscale Experiments S-NH-1 and S-LH-2*, NUREG/CR-5010, EGG-2520, October

Table 1 (continued): List Of Selected Publications From NUREG/CR-5535, Volume 5, Revision 4 [Ref. 3] that show RELAP Modeling Of SBLOCA And Pressurizer Operations

Pressurizer Operations References

1. Wang, S., C. Wu, and J. Wang, 1987, "Assessment of the RETRAN02/MOD3 and RELAP5/MOD2 Pressurizer Model," *Transactions of the American Nuclear Society*, November, pp. 704-705
2. Lin, J.C., et. al., 1985 "RELAP5/MOD2 Pressurizer Modeling," *ASME Winter Meeting, New Orleans, LA, December 1984*

Pressurized Thermal Shock References

1. Bolander, M.A., et. al., 1984, "RELAP5 Thermal-Hydraulic Analyses of Overcooling Sequences in a Pressurized Water Reactor," *International Meeting on Thermal Nuclear Reactor Safety, Karlsruhe, Federal Republic of Germany, September 1984*, KFK-3880/1, pp. 311-319
2. Fletcher, C.D., et. al., 1985, *RELAP5 Thermal-Hydraulic Analyses of Pressurized Thermal Shock Sequences for the H.B. Robinson Unit Pressurized Water Reactor*, NUREG/CR-3977, EGG-2341, April
3. Fletcher, C.D., et. al., 1985, *RELAP5 Thermal-Hydraulic Analyses of Overcooling Sequences for the H.B. Robinson Unit 2 Pressurized Thermal Shock Study*, NUREG/CR-3935, EGG-2335, May
4. Tuomisto, H., 1987, *Thermal-Hydraulics of the Loviisa Reactor Pressure Vessel Overcooling Transients*, June, Imatran Voima Oy, Helsinki, Finland
5. Tuomisto, H., et. al., 1986, "Thermal Hydraulic Analyses of Selected Overcooling Transients in the Probabilistic PTS Study of the Loviisa Reactor Pressure Vessel," *European Nuclear Conference '86 Transactions, Geneva, Switzerland, June 1986*, Technical Research Center of Finland

V. DATA INPUTS

The RELAP input deck model of the plant RCS is a series of data, for example, pipe lengths, pipe diameters, pump flow rates, etc. All data inputs must be from a verified, quality source, or must be bounded by a value that is known to be conservative. A list of sample required input data and a discussion of the direction of conservatism is provided in Table 2. In the application of this methodology, each datum must also have an accompanying reference source or development discussion. Additional discussion for key data sensitivities is provided in sections VI and VII.

Table 2: Inputs Assumed for the LTOP Analysis

| Name | Direction of conservatism |
|---|--|
| Mass and Energy Sources | |
| Plant Thermal Power | Use the maximum (licensed value plus 2%) to maximize the heat addition from decay heat. |
| Decay Heat | Use a conservative model to maximize the heat. An acceptable model is the ANS 1971 Std. The decay heat should be increased by an additional 20%, unless specific documentation is provided to assure the utilized decay heat is bounding and conservative. |
| RCP Heat Input | Use the maximum to increase heat addition to the RCS. |
| RCS and SG Temperatures for heat addition cases | Use the maximum expected temperature difference between the secondary and primary side. A bounding value is to use the maximum secondary side temperature at the time of shutdown cooling initiation, and the minimum RCS temperature for which a RCP may be started. Any lower temperature difference must be justified and administratively controlled |
| SG Heat Transfer Surface Area | Use the maximum for heat addition cases to maximize the heat added from the warmer secondary side to the RCS (do not use for mass addition). |
| SG number of tubes and tube volumes | Use the maximum for heat addition (either zero tube plugging or current level), minimum for mass addition (maximum permissible tube plugging level). For the former case, the maximum increases heat addition. For the latter case, the minimum reduces RCS volume. |
| SG tube thickness, heat capacity and conductivity | Use nominal tube thickness, conductivity, and heat capacity. For heat addition cases, heat flows from the secondary to the RCS through the tubes. For mass addition events, the tubes are modeled as insulated to prevent the secondary from acting like a heat sink and removing RCS energy. In both cases, small variations in these parameters are insignificant due to the small total thermal inertia and heat flow resistance. |
| Pressurizer Heaters | Use the maximum power for heaters plus backup heaters to maximize heat addition to the RCS. |

| Name | Direction of conservatism |
|--|---|
| Injection Flow Rate | Use the maximum pump flow rates. If a maximum has not been specified in previous plant safety analyses, the design flow rate plus 10% can be used or surveillance test data plus uncertainty. The maximum number of enabled pumps allowed by plant Technical Specifications or other limitations must be assumed. |
| PORV Data | |
| PORV Area | Since RELAP5 uses its own flow equations for PORV flow rate, and since these equations tend to be more realistic and less conservative than typical Relief Valve sizing equations, the actual PORV area should not be used. Instead, the RELAP program should be run to generate a valve area that provides the design flow rate. Typically, this will be on the order of 75% of the actual valve area (see Section VII). |
| PORV Opening Time | Use the maximum delay time. Unless quality data exists for PORV flow at partial opening, assume that the PORV remains completely closed until the full delay time (circuitry and mechanical) has passed. Then either model the PORV as instantly full open, or ramped open quickly (see Section VII to understand why the ramped model might be selected). |
| Uncertainty in Temperature Measurement | Appropriate temperatures, such as the LTOP enable temperature or HPSI pump enable temperatures, must be adjusted by the temperature uncertainty. For plants that use variable PORV LTOP setpoints based on RCS temperature, the LTOP setpoint must be offset as described in Section VIII. The temperature uncertainty used must be calculated by a standard instrument uncertainty method such as the square root of the sum of the squares. |
| Uncertainty in Pressure Measurement | The LTOP setpoint must be offset as described in Section VIII. The pressure uncertainty used must be calculated by a standard instrument uncertainty method such as the square root of the sum of the squares. |
| Location of Measured Pressure | The PORV setpoint is generally based on Pressurizer pressure. The RELAP model uses the minimum pressure to delay PORV opening. The minimum pressure is the midpoint pressure of the top element. If this elevation is below the actual PORV pressure tap, a non-conservatism caused by elevation difference must be identified in the LTOP analysis write up. |
| Location of Measured Temperature | For plants that use a variable LTOP setpoint based on RCS temperature, the analysis will conservatively use the warmest appropriate location to determine PORV lift setpoint (for example, if the temperature is measured in the cold leg, the warmest RELAP cold leg segment will be used). |

| Name | Direction of conservatism |
|--|--|
| Quench Tank Maximum Backpressure for PORV | Use a conservative maximum Quench Tank pressure for use in calculating PORV flow rates for cases where the PORV flow is not critical flow. |
| Miscellaneous Data | |
| All Piping and Vessel Sections | Use the minimum volumes for the RCS to maximize the relative effect of energy and mass addition. The only exception is for heat addition cases in the steam generators, where the RCS fluid is initially hot. These should use maximum volumes to increase the heat addition when the RCP is started. |
| Piping Flow Resistance | RCS piping resistances should be maximized between the reactor vessel beltline and the pressurizer, in order to maximize the pressure at the critical location relative to the pressure that is utilized to determine the PORV opening point. Piping resistances should be best-estimate or minimized elsewhere to maximize the RCS flow rate (see also pump head discussion below). |
| SI injection Temperature, Pressure and Density | In general, cooler injection flows involve greater mass, but warmer flows involve greater energy. Unless a bounding value is determined by sensitivity analyses, use a maximum T & P to determine the injection enthalpy, and a minimum T & maximum P to determine the density. |
| RCP performance | When available, the RCP design homologous curves can be utilized to determine fluid acceleration for heat addition cases. Conservatism is assured by using a fast time for pump speed (such as 1 second to go from 0 rpm to full speed rpm). When imposing the ramp rate as suggested, it is not necessary to model RCP motor torque. |
| RCP rated head and flow | Use a conservative maximum, such as 10% greater than design head, to increase the pressure difference between the reactor vessel beltline and the pressurizer. Note: the model requires a conservatively high RCS piping resistance between the beltline and the pressurizer. Therefore it may be necessary to increase the RCP head even greater than this value to get a desired high RCS flow rate. |
| Pressurizer Level Indication Uncertainty | Use a maximum uncertainty when specifying the required indicated Pressurizer level to satisfy the analytically assumed level, e.g., if the analysis assumes a minimum 40% steam void, the Technical Specification or other operational limit must specify a required indicated void of 40% plus uncertainty. |
| Operator Actions | If Operator Actions are required to mitigate the LTOP transient, these actions must be documented and assured consistent with operator actions credited in UFSAR Accident Analyses. |
| Single Failure | The single failure for LTOP is typically failure of one PORV to open on a two-PORV pressurizer. Other single failures should be considered based on case-by-case review of plant designs. |

VI. NRC LTOP ANALYSIS REQUIREMENTS

The Combustion Engineering Owners Group (CEOG) produced Report CE NPSD-683-A, Rev. 6, which defined the methodology to be used in LTOP analyses such as this. The NRC's review and approval of this document is a letter dated 3/16/2001 entitled "Safety Evaluation of Topical Report CE NPSD-683-A, Rev. 6, Development of a RCS Pressure and Temperature Limits Report (PTLR) for the Removal of P/T Limits and LTOP Requirements from the Technical Specifications" (TAC No. MA9561) [Ref. 1]. The NRC document stipulates the following requirements for LTOP analyses performed in accordance with the CEOG Report. The ENERCON RELAP LTOP methodology meets all of the subject requirements, with certain explanations as noted here.

1. Initial conditions are the most limiting allowed by Technical Specifications. *ENERCON applies instrument uncertainties to assure conservatism in the initial conditions. For example, if the Technical Specification requires that the RCS temperature be at least 250°F to enable 2 HPSIs, ENERCON assumes 2 HPSIs may be enabled at 250°F minus RCS indicated temperature uncertainty.*
2. Only one (1) PORV is credited with opening. *The RELAP model only includes one PORV.*
3. No credit is taken for letdown, RCS volume expansion, or RCS metal thermal inertia. *The RELAP model has no letdown flow path, no change in component volumes, and no thermal heat sinks.*
4. Water-solid conditions in the PZR are assumed unless Technical Specifications exist to require a steam or other gas volume. *ENERCON sets the model's initial conditions consistent with this guideline.*
5. Full Pressurizer heaters capacity must be assumed. *The RELAP model contains a heat slab component that provides the appropriate heat to the pressurizer water.*
6. Decay heat must be accounted for, with the maximum specified cooldown rate used to determine the time after shutdown. *ENERCON uses a conservatively minimal time to calculate decay heat, and then increases the value by 20% unless site documentation exists to assure an adequately conservative decay heat without this addition. The RELAP model contains a heat slab component that provides the appropriate heat to the reactor core water.*
7. PORV setpoint uncertainty must be treated consistent with RG 1.105 and ISA Standard S67.04-1994. *The analysis LTOP setpoint(s) is(are) protected by biasing the field setpoints to account for measurement uncertainty as described in Section VIII. The bias amount is based on plant documentation that calculates the appropriate uncertainties consistent with RG 1.105 and ISA Standard S67.04-1994.*
8. The mass-addition event is based on the maximum combined flow rate from HPSI pumps and charging pumps, where the flow rates are either the design flows plus 10% or flows based on IST with uncertainty or Safety Analysis limits. *The RELAP model uses conservative injection flow rates consistent with this requirement.*
9. If a Safety Injection Tank is available to inject fluid, it must be considered as a mass source. *The reference plant did not have Safety Injection Tanks that would*

impact the LTOP scenarios, so they did not appear in this sample model. If such a system is important to the scenario, the RELAP model will include the tanks as additional fluid sources.

VII. ANALYSIS DISCUSSIONS

Discussion is provided here for various sensitivities and how they have been conservatively addressed.

The Shutdown Cooling System, Decay Heat and Pressurizer Heaters

For both mass addition and heat addition cases, at the time of assumed transient initiation (typically 2 to 10 seconds into the scenario to allow for steady-state equilibrium to be established), it is assumed that there is a sudden failing of the shutdown cooling system coincident with a sudden failure (on) of the pressurizer heaters and backup heaters. In addition to these heat sources, heat is added for each operating RCP. Heat is added to the fluid at a constant MW rate by RELAP “heat slab” components.

The NRC identified that the decay heat should be added to the analysis as an additional conservatism. The decay heat is based on the fastest allowable time to the scenario’s initial RCS temperature using the formula:

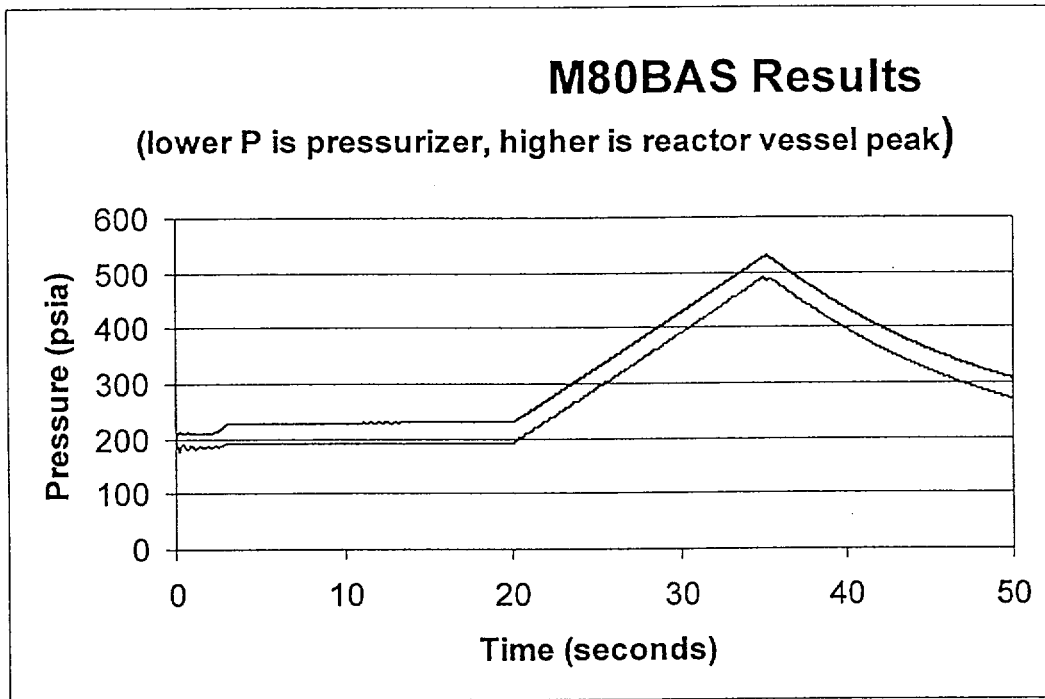
$$\text{Time} = (\text{Hot zero power temperature} - \text{scenario initial T}) / (\text{fastest cooldown rate})$$

Typically, this is done just for the maximum scenario initial T. The decay heat is then calculated using a conservative model, such as the ANS 1971 standard, and then increased by 20%.

Note: ENERCON has not had any occasion to vary from this conservative approach, but it is noted that the 1971 standard plus 20% decay heat is more conservative than required by Reference 1. Therefore, ENERCON reserves the right to decrease this conservatism with a case-by-case justification.

The impacts of this conservatism can be seen by a trial case. Reference 4 includes a base case model based on a reference CE plant labeled m80bas. The peak pressure with all model conservatisms for a mass addition event is calculated to be 490.25 psia, as shown in the below Figure 5. Sensitivity Case 1 (SA1) removes the heat inputs for the pressurizer heaters, decay heat, and RCP heat. The new peak pressure is just 483.93, or 6.5 psia lower without the conservative heat inputs. The graph for case SA1 would be very similar to Figure 5, but with a slightly lower pressurization rate. The peak pressure for case SA1 occurs at a time of 38.22 seconds, or about 3 seconds later than for the base case.

Figure 5: Reference Case Results showing a typical Pressure Trace for a Mass Addition Event. The initial 2 seconds are used to establish a steady-state without RCP flow, the next 18 seconds are to establish a steady-state with RCP flow. The Mass Addition causes a linear ramp until the PORV opens and immediately relieves pressure.



PORV Flow Rate

The flow rate through the PORV is based on design flow rate rather than valve orifice area. The reason for this is that the two-phase RELAP equations are less conservative than most relief valve sizing equations (see Ref. 3, Volume 4, Section 7.2, notably figure 7.2-8). If the actual area is used, the flow rate calculated by RELAP will be greater than the design flow rate. Instead, a case run must be made to investigate by trial and error what valve area gives the required flow rate. In practice, this is not difficult because the design flow is choked. Hence the area can be found by proportion with just a single trial. For example, at the reference site, the valve area was given in plant documents as 0.94 inch². The area that gave the correct design flow rate in RELAP turned out to be 0.77 inch².

Once the area is found by this approach, the RELAP code will handle all additional flow calculations.

Note: The exact flow rate through the PORV is not critical to the analysis if the flow is sufficient to halt the pressure rise. That is, if as soon as the PORV is full open, the flow out of the PORV is greater than the RCS volumetric increase (due either to mass addition or heat expansion), then the pressure will fall. Small errors in the PORV flow rate will

affect the rate of depressurization, but not the peak pressure. This analysis is only concerned with peak pressure. Should a transient result be found where the pressure is not immediately relieved at PORV lift, the RCS pressure will continue to rise until an equilibrium condition exists. Should this scenario occur, the accuracy of the PORV equation is important to the peak pressure. The analysis write up must determine if this case occurs, and, if so, must document through additional side calculations that the RELAP flow rate is acceptable.

PORV Opening Rate

The PORV flow area is conservatively assumed to be zero until the time at which the PORV is fully opened per plant data. Then the valve is modeled as though linearly ramped open from zero flow area to full flow area in some arbitrary brief period such as 0.5 seconds. Since the flow predicted during the ramping period is less than the full flow rate, this approach is conservative.

The reason for using a ramping open model rather than an instantaneous opening is not to add additional conservatism. When an instantaneous opening is used, the RELAP model predicts a negative pressure wave. Upon reflection, this negative pressure wave causes a small pressure spike in the Pressurizer pressure. As far as the pressurizer pressure is concerned, an instantaneous opening causes a slightly higher peak.

To demonstrate this, Sensitivity Case 2 (SA2) makes the PORV open rate $1e+6$ /second so that the valve opens in $1e-06$ seconds. The pressure when first opening is less than the base case (489.79 vs. 490.25 psia), but the reflected wave peak is 498.40 psia. It appears that the instant open case is more conservative, but it is not a conservatism worth including in the model for three reasons: it is unrealistic since the actual PORV takes a finite time to open, the resulting pressure graph contains a confusing oscillating pressure trace that is awkward to explain, and the pressure wave spike is limited to the pressurizer and does not impact the pressure in the reactor vessel, which is the critical pressure for LTOP concerns. Therefore the PORV is ramped open at a slow enough speed to avoid the pressure oscillation.

Reactor Coolant Pumps

Having RCPs running is conservative for the mass addition cases because they increase the pressure difference from the base of the Reactor Vessel to the top of the Pressurizer where the LTOP system gets its pressure input. An additional 10% is added to the rated head values in order to provide an additional conservative margin to the modeling of RCS flow. The addition of this margin would tend to increase the pressurization rate during the heat addition transient. However, it was determined through sensitivity studies that minor changes in RCS flow rate have negligible effect upon the results of the heat addition analysis. Specifically, a base case heat addition was run (HAbase). The Peak pressure in that analysis is 451.72 psia. In the sensitivity case SA3, the RCP rated flow was decreased by 10% from 47500 gpm to 42750 gpm. The new peak pressure is 450.61 psia.

For pump start up, the pump speed ramp rate is conservatively bounded by a zero-to-full speed acceleration in just 1 second (typical times are on the order of 30 seconds). This

manual acceleration means that the pump inertia entered in the RELAP deck is arbitrary. Although the pump reaches full rpm speed in 1 second, the system's inertia will make the RCS flow rate take an additional time period. This is conservative due to the 10% higher head and fast rpm acceleration. To demonstrate this, a fourth sensitivity analysis was run (SA4) with a pump that ramps to full speed over 30 seconds. The peak pressure was 451.72 in the base case HAbase. With the slower pump, the peak pressure is 449.64 psia.

Note: Since the pump model imposes a linear acceleration from zero to full rpm in 1 second, all the model inputs for pump rpm, rotational inertia, and torque are not used, and the data supplied to the model is arbitrary. That is, the model requires inputs for pump rpm, torque and moment of inertia, but the values are not used.

Mass Addition Cases – Initial Pressure

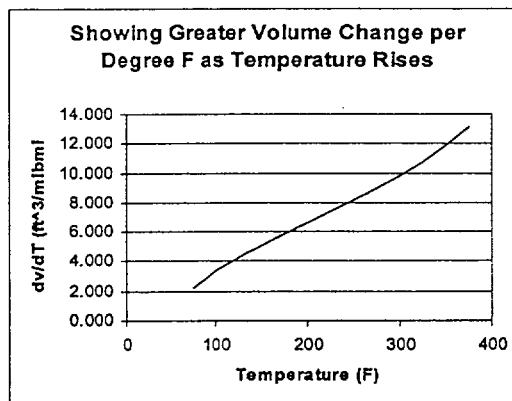
Exploratory runs demonstrate that the initial pressure does not have a significant impact on the peak pressure of a mass addition transient so long as the Pressurizer is water-solid at the time of PORV lift. This is because the mass addition inlet flow rate is a function of RCS pressure and is not a function of time. Whether the system is initially just below the PORV setpoint pressure, or whether the system ramps up to the PORV setpoint from some lower initial value, does not affect the pressure rise rate during the period between reaching the PORV setpoint and the delay time of the PORV opening. This was demonstrated by two cases in Reference 4 (m50p2 and m50p4), the first initiated at 200 psia, and the second at 400 psia. The peak pressure in the first case is 483.63 psia, and the peak in the second is 483.46 psia.

Mass Addition Cases – Initial Temperature

The case of m50p2 (initial temperature of 50°F) versus m80bas (initial temperature of 80°F) shows that this methodology predicts a slightly higher peak pressure as temperature rises. The 30°F temperature rise increases the peak pressure from 483.63 psia (m50p2) to 490.25 psia (m80bas), or 6.6 psi. An additional run in Reference 4 at 166°F demonstrates that the pressure rise due to the 116°F difference from m50p2 is about 16 psi.

The reason for this increase is that the change in volume for each Btu of energy addition is faster for water at 80 or 166°F than it is at 50°F. This is shown in Figure 6 at right, recognizing that the heat capacity, or dT/dh , is pretty close to constant over this temperature range. Thus the decay heat addition has a bigger impact for warmer initial temperatures. This is, in general, not a big impact because the P/T limit curve rises upward with temperature. It does show the need for a greater margin between PORV setpoint and the P/T limit curve as temperature rises.

Figure 6: Sensitivity of dv/dT to Temperature



Mass Addition Cases – Initial Pressurizer Bubble

Exploratory runs demonstrate that it is difficult to credit a steam bubble in the Pressurizer with assisting mass addition event mitigation. The RELAP model shows that when a bubble is present, the pressure starts to rise immediately following the start of mass injection. However, when the pressure rises sufficiently, the Pressurizer bubble collapses at a rate that offsets the mass addition, and pressure is constant. Pressure does not continue to rise until after the bubble is completely gone. Hence if the initial pressure is sufficiently below the PORV lift pressure, the bubble vanishes and the peak pressure is the same as if the initial condition was water solid.

Figure 7: Pressure Trace (from Ref. 4)

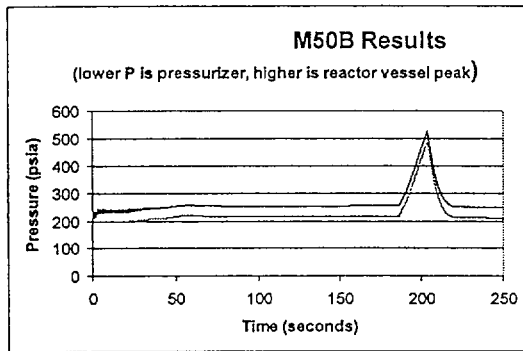
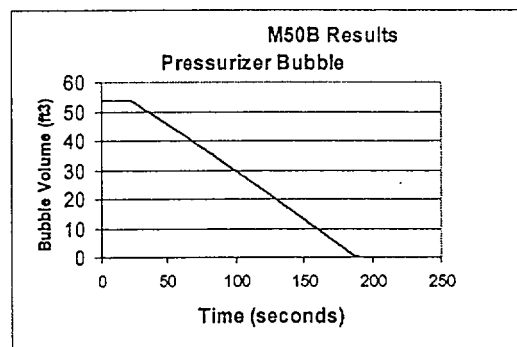


Figure 8: Bubble Size (from Ref. 4)



This phenomenon is particularly true for LTOP events because of the low density of the steam in the Pressurizer (relative to the steam density at 2100 psia). This low mass bubble is easier to condense than when the plant is operating at power. The condition of a water-solid lift is also specified in the NRC SER[Ref. 1].

Case m50b is a sensitivity case that uses m50p2 as a base case. The difference is in the presence of a small pressurizer bubble. The pressure is seen in Figure 7 to hold steady while the bubble collapses, and then to rise after the collapse as though the bubble had never been there (see Figure 8 to see that the bubble shrinks and vanishes). The peak pressure is 486.34 psia. This is slightly higher than the m50p2 and m50p4 cases, but that is an artifact of the conservative methodology which hypothesizes an imbalance in heat addition during the mass injection event (due to an assumed loss of shutdown cooling and high decay heat). Since the bubble takes longer to collapse, the RCS has warmed up a little, and the warmer RCS has already been shown to result in a higher peak pressure. In conclusion, the ENERCON methodology will be to run all mass addition cases assuming water solid conditions, and to investigate temperature effects through direct specification of the initial RCS temperature.

Mass Addition Events – SI Injection Temperature

It is difficult to identify the worst-case temperature for SI injection. The volumetric flow rate is constant, which means the mass flow rate is greater for colder temperatures. However, the injection water enthalpy is greater for higher temperatures. In order to assure a conservative choice, the modeler has two choices: either perform sensitivity analyses at numerous injection temperatures, or bound the possibilities by using a

maximum density such as water density barely above freezing (62.42 lbm/ft³), and an enthalpy associated with the maximum possible safety injection temperature and pressure. This is done by using the greater density when calculating the mass injection flow rate in lbm/s, but specifying maximum expected temperatures and pressures in the RELAP components for SI injection. SA5 evaluates the impact on the m80bas case of using colder injection water (just 50° instead of 250°F). The resulting peak pressure is 489.07 psia as compared to the base case 490.25 psia. In both cases, the boundary mass flow rate is based on a density of 62.42 lbm/ft³.

Heat Addition Events -- Effect of Temperature Rise on PORV Opening Setpoint

The effect of temperature rise during heat addition events can have a critical impact on the LTOP curve requirements if the PORV setpoint varies with RCS temperature. When the heat addition event occurs, the RCS temperature will rise. Since the LTOP system sets the PORV lift setpoint as a function of RCS temperature, the PORV will not lift until the setpoint associated with the higher temperature.

One way to avoid a significant restriction on the PORV LTOP setpoint curve is to mitigate heat addition transients before the Pressurizer steam void is lost. This is done by requiring a large void prior to the first RCP start via an operational requirement such as a Technical Specification, and determining that the void will not entirely collapse by the time that the Steam Generator and RCS temperatures equilibrate. After equilibration, the transient is effectively mitigated. Plants that wish to start RCPs with RCS in a water solid condition will need to impose maximum temperature differentials between the primary and secondary side to limit the energy input.

This concern does not apply to plants that have a flat PORV setpoint over the full range of LTOP temperatures.

Heat Addition Cases – Initial Conditions

Heat addition cases are primarily associated with cooldown transients. A conservative bounding assumption is that once the plant is placed on shutdown cooling, the Steam Generators maintain the previous temperature while the Reactor Vessel, Hot Leg, and Cold Leg are cooled. Should a RCP suddenly start up, the hot Steam Generator serves as a heat source and rapidly expands the RCS water as specific volume increases. In accordance with NRC guidance, the pump heat, Pressurizer heaters, and decay heat are all additional heat sources.

With the very conservative assumptions about temperature differentials, the initial energy input into the RCS can be huge. The full power delta-T might only be on the order of 50°F, but the heat addition assumptions can lead to initial delta-Ts on the order of 250°F. With these huge delta-Ts, even though only a single pump is running in one loop (with potential reverse flow in the other loop), the initial energy input can be on the order of 35% of full power. Figures 9, 10 and 11 are from Reference 4 Case hp503s30, which is the same case as HAbase described above.

Figure 9: High Initial Heat Addition

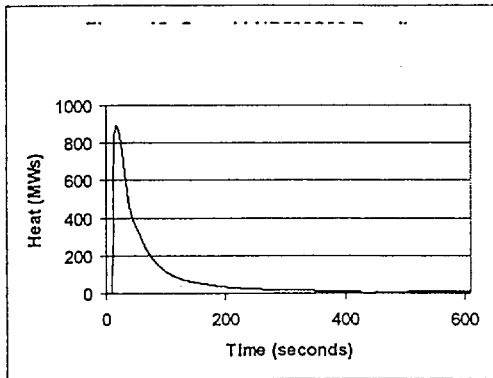


Figure 10: Rapid Bubble Collapse

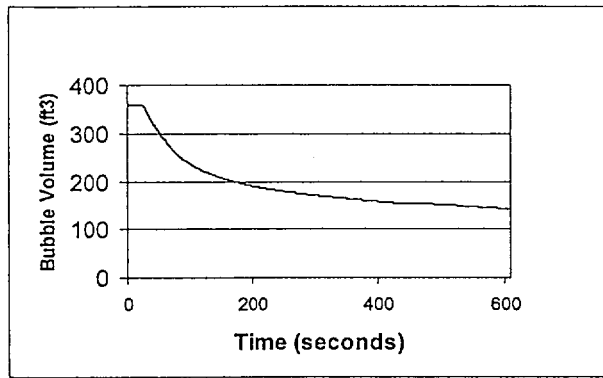
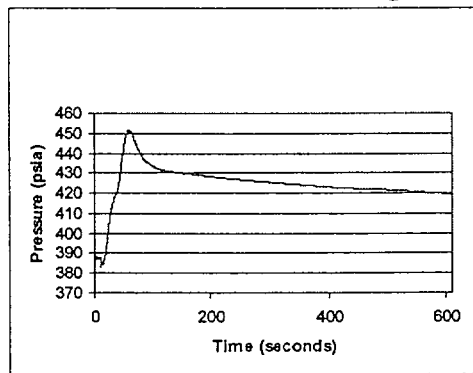


Figure 11: Pressure Held Constant during Bubble Collapse



As already noted, the methodology involves a net imbalance in heat addition due to the assumption of a loss of shutdown cooling and a high decay heat, RCP heat, and Pressurizer heaters failure (fails on). Thus the transient does not quite come to equilibrium after ten minutes (this is 610 seconds of simulation time because the RCP starts at 10 seconds). This continued transient is due to the conservative assumptions, and it is not the function of the LTOP system to mitigate this slow energy addition. At any rate, this is bounded by the mass addition event, which also includes this conservative assumption of a net heat input.

Heat Addition Cases – Secondary Side Assumption

The secondary side is conservatively modeled as isothermal water filling the full volume of the Steam Generator to maximize the latent heat delivered to the RCS. Thus, while the water volume is typically on the order of half or less of the total SG volume (the rest being steam space), this methodology assumes that the full volume is filled with water. The isothermal assumption is also a conservatism, in that the full mass of water serves as a heat source. In reality, if the steam generator were to be filled to the top, the top half of the steam generator would stratify and not be much of a heat source. This appears to be a large conservatism in that it approximately doubles the amount of heat energy, but it allows a significant simplification of the model. Without this assumption, the model would need to include secondary side water volumes (to model the stratification) and

thermal inertia in the steam generator metal mass (other than the steam tubes, which are already modeled).

Heat Addition Cases – Pressurizer Heaters

The assumption that Pressurizer heaters failed on full power is a net negative impact was investigated. Since mitigation of the heat addition cases relies on a steam bubble remaining long enough for the RCS and SG to equilibrate, it was considered that the Pressurizer heaters might have a net benefit. They tend to warm the pressurizer and promote the steam phase. On the other hand, the added energy also tends to expand the fluid and increase the pressure rise.

A sensitivity case was run (SA6) with no Pressurizer heaters to determine the impact. The peak pressure was 451.56 psia without heaters, as compared to 451.72 with heaters in HAbase. Hence the pressurizer heaters have a net negative affect on pressure, but a very small one. The bubble size 600 seconds after pump start was also a little better (146.7 ft³ without heaters vs. 141.8 ft³ with heaters in the base case). This is because the RELAP model spreads the heat out throughout the pressurizer water (no local boiling). The case with pressurizer heaters does have warmer pressurizer fluid, but it is still well subcooled due to the inrush of cooler RCS through the surgeline. At 610 seconds, the Pressurizer water volumes have the following temperatures with the Pressurizer heaters on (from bottom to top in degrees F: 268, 314, 350, 396, 423.33). Without the Pressurizer heaters, the temperatures are 240, 279, 342, 394, and 423.28.

The conclusion is that the pressurizer heaters have a small negative impact on both bubble size and peak pressure. However, this conclusion was based on a sensitivity run performed at the reference plant. Additional site specific sensitivity runs will be made to assure that this assumption is conservative at other plants.

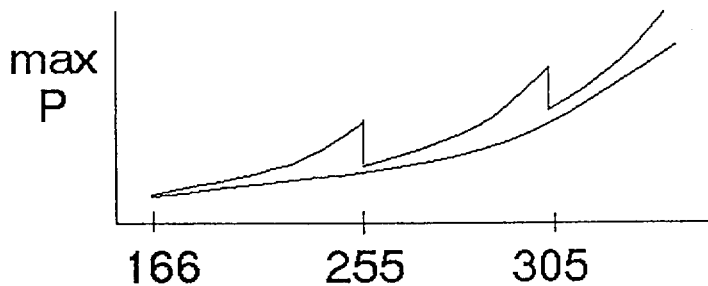
Heat Addition Cases – PORV Opens

It has been described how heat addition cases for large temperature differentials between the RCS and secondary side rely on a steam void to mitigate the transient without lifting a PORV. However, it may be that the PORV will open prior to the RCS-SG temperature equilibrium. This opening is possible if the PORV setpoint uncertainty causes the PORV to open at a lower pressure rather than at the maximum pressure. It is necessary to run a case at each site where the PORV will open (either by manipulating the initial conditions with high initial pressure or small void, or by changing the PORV setpoint). In terms of peak pressure, the limiting case is to manipulate the initial conditions. This is done in Reference 4, in case Hp504s30, by raising the initial pressure to close to the trip value, and reducing the bubble to less than Technical Specification size. The result shows that the PORV flow rate is adequate to mitigate the pressure transient, which is not surprising. The pressurization rate is slower with the bubble, and the steam volume released by a PORV is much greater than liquid volume. The volumetric release easily offsets the RCS expansion. In case Hp504s30, the maximum pressure is 476.3 psia, which is an overshoot of just 17.3 psi over the lift setpoint of 459 psia. This is a small overshoot compared to the mass addition cases.

Setpoint Curve Shape – Plants with LTOP Setpoints that follow the P/T Curve

There are distinct temperatures where the mass addition case can suddenly become more limiting due to additional mass injection. For example, at a certain plant, the number of enabled SI pumps might jump up incrementally at 255°F RCS T and 305°F. A jagged LTOP setpoint curve could be used in response to these sudden jumps in mass addition, but it would make the circuitry function more complicated, if even possible. Instead, the LTOP setpoint curve is typically developed as a conservatively lower monotonically-increasing curve. This approach also identifies a limited number of critical analysis temperatures (255°F and 305°F, in this example) simplifying the choice of initial temperatures for LTOP scenarios. The curve in Figure 12 shows conceptually the “tightest” LTOP setpoint curve allowed by analysis compared to the lower smooth curve used.

Figure 12: Conceptual Diagram of Highest Possible LTOP Setpoint Curve, and Recommended Smooth LTOP Setpoint Curve



VIII. UNCERTAINTY AND THE LTOP SETPOINT CURVE

Measurement uncertainty must be addressed because of possible process instrumentation measurement errors associated with the measured pressure and temperature that determine when the PORV open signal is generated. For plants with a flat PORV setpoint over the full range of LTOP events, the treatment is very simple. The field setpoint must be biased by the uncertainty. That is, if the analysis assumed a lift pressure of 460 psia and the uncertainty is 50 psia, the field setpoint must be 410 psia or less. The case is more complicated for plants with setpoint curves that follow the P/T limit curve by increasing the PORV setpoint with RCS temperature. This makes the uncertainty a function of both the pressure and the temperature error.

For the RELAP code analysis scenarios, the PORV setpoints and P/T limit curve are assumed to be correct with no adjustment for uncertainty. For example, if the PORV setpoint at 164°F is 459 psia and the P/T limit is 525 psia, the RELAP code will start to generate a PORV open signal following a mass injection event as soon as the top volume in the Pressurizer reaches 459 psia. The LTOP system is judged to be adequate if the peak Pressurizer pressure during the transient is below 525 psia.

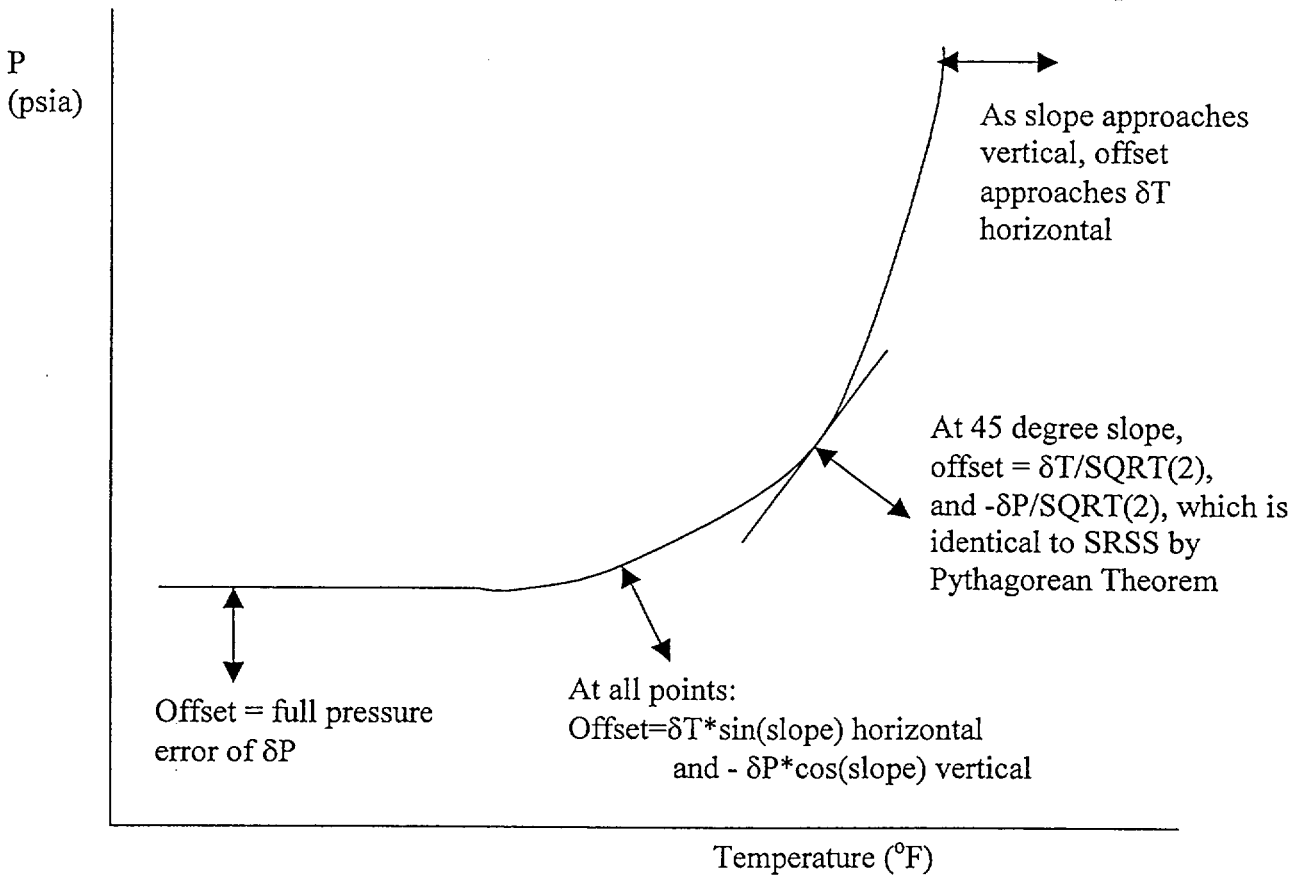
This approach is acceptable so long as it can be assured that when the actual RCS temperature is 164°F, a PORV open signal will be generated at or below a Pressurizer pressure of 459 psia. A conservative approach is to draw a setpoint curve through the point $(T+\delta T)$ and $(P-\delta P)$, where δT is the temperature error and δP is the pressure error. However, this is overly restrictive since it is highly unlikely that measurements will be at the extreme of both uncertainties. The temperature and pressure errors are independent random errors.

It is common to use statistical analysis to bound instrument uncertainties with a specific confidence limit, such as a 95% confidence limit (Ref. 5). Latitude is provided for reasonable statistical approaches based on "scientific judgment using all the relevant information available" (Ref. 5, subsection 4.1). In this case, we use an approach that is similar in concept to the square root of the sum of the squares (SRSS) reasoning.

SRSS would develop a net uncertainty based on $\delta T/T$ and $\delta P/P$ as $\text{SQRT}((\delta T/T)^2 + (\delta P/P)^2)$ assuming that the errors have equal weight in affecting the final result. That is not the case here. In the horizontal portion of the curve, the temperature error has no impact. As the curve approaches vertical, the pressure impact approaches zero. Instead a function is needed that approaches the pressure error only for the horizontal portion, the temperature error only as the curve approaches vertical, and $\text{SQRT}((\delta T/T)^2 + (\delta P/P)^2)$ when the curve has a 45 degree slope.

The solution is to offset the curve by $\delta T \cdot \sin(\text{slope})$ and $-\delta P \cdot \cos(\text{slope})$. Here the sine of the slope will be $\Delta P / \text{SQRT}(\Delta T^2 + \Delta P^2)$, and the cosine $\Delta T / \text{SQRT}(\Delta T^2 + \Delta P^2)$. Figure 13 shows conceptually how the LTOP setpoint curve is generated.

Figure 13: Conceptual Representation of the LTOP Setpoint Curve Development



For example, say two analysis pressure setpoints at RCS temperatures of 250°F and 251°F are 920 psia and 929 psia, respectively. That is, $\Delta T = 1^\circ\text{F}$ and $\Delta P = 9$ psi. Say the temperature error δT is 16.3°F and the pressure error δP is 66.3 psia. The corresponding point on the LTOP setpoint curve consists of a temperature of:

$$T + \text{offset} = T + \delta T * \Delta P / \text{SQRT}(\Delta T^2 + \Delta P^2) = 250 + 16.3 * 9 / \text{SQRT}(1 + 81) = 266.2^\circ\text{F}$$

The pressure is:

$$P - \text{offset} = P - \delta P * \Delta T / \text{SQRT}(\Delta T^2 + \Delta P^2) = 920 - 66.3 * 1 / \text{SQRT}(1 + 81) = 912.7 \text{ psia}$$

A check is made using a simple Monte Carlo simulation to verify that this approach will give acceptable results more than 95% of the time. The approach is as follows:

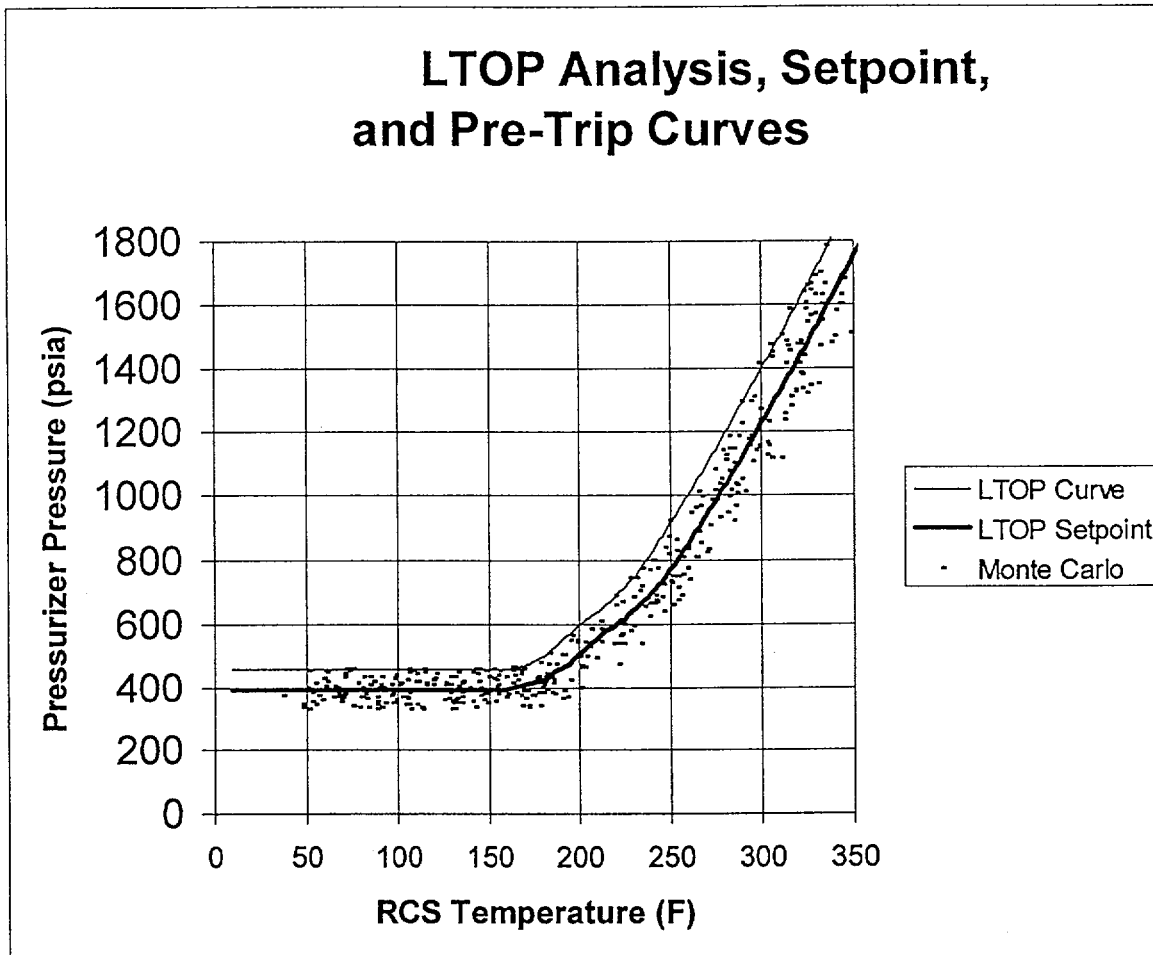
1. The LTOP analysis curve and the proposed LTOP setpoint curve are drawn on a Pressure versus Temperature graph (Figure 14). The setpoint curve is generated by offsetting each point in the LTOP curve by $+\delta T * \Delta P / \text{SQRT}(\Delta T^2 + \Delta P^2)$ °F and $-\delta P * \Delta T / \text{SQRT}(\Delta T^2 + \Delta P^2)$ psi as shown in the above example.
2. Random number generators are used to simulate actual pressure and temperature when the sensed P & T lie on the LTOP setpoint curve. For example, the actual

pressure = sensed pressure + (0.5 - rand()) * 2 * δP where rand() is a number between 0 and 1. The result of the term (0.5 - rand()) * 2 is therefore a number between -1 and +1. A similar equation is used to find actual temperature.

3. These measured point pairs are plotted as a cloud of scatter points. Some 100,000 such points are generated.
4. The result is verified to be within the analysis curve better than 95% of the time.

In 100,000 trials of the reference plant model, 96.8% of the points were within the LTOP curve. Figure 13 shows just 1000 of the 100,000 trials.

Figure 13: Results of Monte Carlo Analysis from Reference 4



X. CONCLUSIONS

The conclusion is that the ENERCON methodology of using RELAP5/MOD 3.2, for LTOP analyses is acceptable and conservative. The key conservatisms are discussed through this document, but can be summed up here:

1. Addition of a conservative pump heat, decay heat, and Pressurizer heaters heat for both mass injection and heat addition. No credit for shutdown cooling or letdown.
2. Conservative initial conditions, plus a wide range of initial conditions as necessary to bound the worst-case scenario.
3. Conservative PORV open setpoint (i.e., uncertainty applied to field setpoint to protect analysis setpoint), conservative time delay, calculated flow area to match design flow rate, and conservatively high backpressure. Only one PORV is credited.
4. The PORV is conservatively assumed to have zero flow area until the circuit and mechanical delay times to full open have passed.
5. Conservatively small RCS volumes (except for SG tube volume filled with hot RCS for heat addition cases, only), rigid RCS volumes (no expansion), and no thermal inertia credit for RCS metal mass or fuel mass.
6. Mass addition: conservative mass injection flow rates.
7. Mass addition: conservative mass injection density and enthalpy (even if non-mechanistic, i.e., even if the density is associated with a colder temperature than the enthalpy).
8. Mass addition: no heat transfer to secondary side.
9. Heat addition: conservative SG heat transfer area, water mass, and assumption of isothermal secondary-side water.
10. Heat addition: conservative fast ramp rate for RCP.

Additional key analysis features are as follows:

1. Mass addition: no Pressurizer void is hypothesized, since the voids do not impact the final peak pressure.
2. Heat addition: the initial conditions must include the maximum postulated delta-T between primary and secondary sides allowable by plant operation.
3. Heat addition: can credit a pressurizer bubble for the first RCP start if the bubble is required by Technical Specifications or otherwise assured.
4. Heat addition: although the pressurizer bubble may be credited in absorbing heat energy while the RCS and SG equilibrate, i.e., the PORV does not lift on water solid conditions while the SG is still at a much higher temperature than the RCS, there must be demonstrated acceptable results should a PORV open while a steam bubble still exists.

REFERENCES

1. "Safety Evaluation of Topical Report CE NPSD-683, Rev. 6, Development of a RCS Pressure and Temperature Limits Report (PTLR) for the Removal of P-T Limits and LTOP Requirements from the Technical Specifications" (TAC No. MA9561)
2. 10CFR50 Appendix G
3. RELAP5 Code Manual, NUREG/CR-5535, Revision 4
4. Fort Calhoun Low Temperature Overpressure Protection Final Report, ENERCON SERVICES, Rev.1, 3/15/02
5. NIST TN-1297, Guidelines for Evaluating and Expressing the Uncertainty of NIST Measurement Results, US National Institute of Standards and Technology, 1994.

Reference 10.15

Letter LTR-CI-02-14, Rev. 00

from WEC (S. T. Byrne) to OPPD (J. Jensen)

**“Extended Beltline Limit for Fort Calhoun Station Reactor
Pressure Vessel”**

February 15, 2002



Westinghouse Electric Company
Nuclear Services

2000 Day Hill Road
Windsor, CT 06095-0500
USA

Mr. James Jensen
Omaha Public Power District
Fort Calhoun Station
PO Box 550
Fort Calhoun, Nebraska 68023

February 15, 2002
LTR-CI-02-14, Revision 00

Subject: Extended Beltline Limit Assessment of
Fort Calhoun Station Reactor Pressure Vessel

Dear Mr. Jensen:

An assessment was performed of the Fort Calhoun reactor vessel materials. This was undertaken to support submittal and acceptance of a Pressure and Temperature Limits Report (PTLR) for Fort Calhoun Station. In the NRC Safety Evaluation (Reference 1) of CE NPSD-683, Revision 6, the Staff required that all of the ferritic materials that have accumulated neutron fluence in excess of 1.0×10^{17} n/cm² shall be assessed as beltline materials. In effect, any ferritic material in the beltline, as defined, would have to be considered in the establishment of the heat-up and cool-down (pressure-temperature) limits.

The assessment entailed the following:

1. The 1.0×10^{17} n/cm² bounds above and below the core were identified based on peak vessel fluence projections from Reference 2 and an estimate of the axial vessel fluence profile from Reference 3.
2. The material information was tabulated for plates, forgings and welds for all components within the 1.0×10^{17} n/cm² bounds.
3. The Adjusted Reference Temperature (ART) values were computed in accordance with 10CFR50.61 for 40 and 60 years for all materials within the 1.0×10^{17} n/cm² bounds. ART values were generated for all plates, forgings and welds within the 1.0×10^{17} n/cm² bound using the highest applicable fluence for that component.
4. For the plates and forgings without reported values for the copper content, the highest reported value for the plates and forgings, 0.17%, was assumed for chemistry factor determination.

Determination of Materials in the 1.0×10^{17} n/cm² Bounds

The peak fluence values were obtained from Reference 2 for times corresponding to end-of-license (August 2013) and to end-of-extended-license (August 2033). The axial vessel fluence variation from Reference 3 was used to adjust the peak fluence at each azimuth in

order to generate estimates of the fluence above and below the active height of the core. Application of the Reference 3 profile is illustrated in Figure 1. It is a plot of the neutron fluence at the 90-degree azimuth as a function of the distance below the centerline of the reactor coolant inlet and outlet nozzles. The highest values correspond to the active fuel length, and the relative fluence falls off rapidly above and below the active core height.

The Fort Calhoun vessel layout is shown in Figure 2 (from Reference 3). Using the axial fluence profiles in conjunction with the vessel layout, the following reactor vessel components were determined to lie outside the 1.0×10^{17} n/cm² bounds:

- closure head and included welds (closure head flange, torus, and dome)
- vessel flange and included weld
- inlet nozzles and included welds
- outlet nozzles and included welds
- bottom head and included welds (torus, and dome)

Included within the 1.0×10^{17} n/cm² bounds are materials from the upper shell plates, axial welds (1-410 A/C), and the intermediate-to-lower girth seam weld (8-410) in addition to the intermediate and lower shell plates and welds. The peak fluence for the upper shell plates and girth weld is approximately 2.8×10^{17} n/cm² and 3.8×10^{17} n/cm² for August 2013 and August 2033, respectively. The peak fluence at the upper shell axial welds is approximately 1.9×10^{17} n/cm² and 2.8×10^{17} n/cm² for August 2013 and August 2033, respectively.

The effect on the 1.0×10^{17} n/cm² bounds of increasing the peak (August 2033) fluence by 20% was also assessed. This is intended to encompass future events such as power uprate or fuel management changes that were assumed to increase the fast neutron fluence locally by 20%. It was determined that, even though the peak fluence in the upper shell plates and welds increased, the components lying outside the 1.0×10^{17} n/cm² bounds remained unchanged. (Furthermore it was determined that the fluence would have to increase by a factor of eight to include any additional materials in the 1.0×10^{17} n/cm² bounds.) In other words, no additional materials would need to be considered in the determination of limiting materials if the peak (August 2033) fluence was increased by 20%.

Determination of Limiting Materials in Extended Bounds

The determination of limiting materials within the 1.0×10^{17} n/cm² bounds is shown in Table 1. Determinations were made for August 2033. Table 1 provides a list of components by Code Number and gives the Chemistry Factor for each. The peak fluence in August 2033 for each component is given. The adjusted reference temperature is determined using Regulatory Guide 1.99, Revision 2 for each of the components using the peak fluence, chemistry factor, and initial RT_{NDT}. The margin added was 65.5⁰F for welds and 34⁰F for plates in accordance with Position 1.1 of Regulatory Guide 1.99, Revision 2.

In this assessment the limiting material is defined as the one with the highest adjusted reference temperature at the reactor vessel base or weld metal-clad interface. (It should be noted that for establishing pressure-temperature limits, the adjusted reference temperature is determined at the one-quarter and three-quarter thickness locations. In that case the limiting material is assessed at the two latter locations and not at the base or weld metal-clad interface.) From Table 1, the limiting material is lower shell weld 3-410 A/C based on the adjusted reference temperature of 268 °F. For the plates and welds located above the intermediate shell course, the predicted adjusted reference temperature is between 38 and 74 °F, values that are well below that of the limiting material.

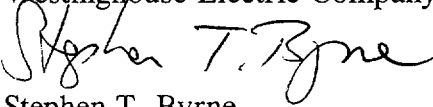
Conclusions

An assessment was made of all the materials within the bounds of the limits defined by a fluence of 1.0×10^{17} n/cm². This determination included consideration of the end of the current license in August 2013 as well as at the end of the extended license in August 2033.

It was determined that the upper-to-intermediate girth seam weld 8-410 and parts of the upper shell course plates and welds 1-410 A/C, would lie within the 1.0×10^{17} n/cm² bounds. This boundary did not extend to the reactor coolant inlet or outlet nozzles or below the lower shell course. The effect on the 1.0×10^{17} n/cm² bounds of increasing the August 2033 fluence by 20% (e.g., to accommodate power uprate or fuel management changes) was also assessed. It was determined that no additional materials would need to be considered in the determination of limiting materials if the peak fluence was increased by 20%. (It was determined that the fluence would actually have to increase by a factor of eight to include any additional materials in the 1.0×10^{17} n/cm² bounds.) An assessment was made to determine the limiting vessel material when all of the materials within the 1.0×10^{17} n/cm² bounds were considered. It was found that the limiting material is the lower shell axial weld seam 3-410 A/C.

The materials in the reactor vessel flange region (sections of the upper shell course plates, vessel flange, closure head flange, closure head torus, and included welds) are above the reactor vessel inlet nozzles. Therefore, the neutron fluence in the flange region is substantially less than 1.0×10^{17} n/cm² such that the bolt-up temperature can be based on the initial RT_{NDT} of the flange region materials.

If you have questions concerning the above please call me at (860) 731-6703.

Sincerely,
Westinghouse Electric Company

Stephen T. Byrne
Senior Consultant

References:

- 1) Nuclear Regulatory Commission letter dated March 16, 2001, Safety Evaluation of Topical Report CE NPSD-683, Revision 6, "Development of a RCS Pressure and Temperature Limits Report (PTLR) for the Removal of P-T Limits and LTOP Requirements from the Technical Specifications"
- 2) WCAP-15443, Rev. 0, "Fast Neutron Fluence for the Fort Calhoun Unit 1 Reactor Vessel", dated July 2000, prepared by Stan Anderson
- 3) CEN-189, Appendix A, "Evaluation of Pressurized Thermal Shock Effects due to Small Break LOCAs with Loss of Feedwater for the Fort Calhoun Reactor Vessel", December 1981, Combustion Engineering, Inc.

| Table 1- Determination of Limiting Vessel Materials (August 2033) | | | | | |
|--|---------------------------|--------------------------------------|-------------------------------|--|--|
| Component Name | Component Code No. | Initial RT_{NDT} (°F) | Chemistry Factor, (°F) | Peak Fluence (n/cm²) | Adjusted Reference Temperature (°F) |
| Lower Shell Plate | D-4812-1 | 0 | 83 | 3.45E19 | 144 |
| Lower Shell Plate | D-4812-2 | 0 | 65 | 3.45E19 | 120 |
| Lower Shell Plate | D-4812-3 | 0 | 65 | 3.45E19 | 120 |
| Inter.-to-Lower Shell Girth Weld | 9-410 | -56 | 188.41 | 3.45E19 | 259 |
| Lower Shell Axial Welds | 3-410 A/C | -56* | 208.68* | 2.43E19 | 268* |
| Inter. Shell Plate | D-4802-1 | 0 | 82.2 | 3.45E19 | 143 |
| Inter. Shell Plate | D-4802-2 | 18 | 72.0 | 3.45E19 | 147 |
| Inter. Shell Plate | D-4802-3 | 0 | 73.1 | 3.45E19 | 131 |
| Inter.-to-Upper Shell Girth Weld | 8-410 | -56 | 190.4 | 3.8E17 | 57 |
| Inter. Shell Axial Welds | 2-410 A/C | -56 | 89.03 | 2.43E19 | 120 |
| Upper Shell Plate | D-4801-1 | -16 | 81 | 3.8E17 | 38 |
| Upper Shell Plate | D-4801-2 | -16 | 81 | 3.8E17 | 38 |
| Upper Shell Plate | D-4801-3 | 10 | 121 | 3.8E17 | 74 |
| Upper Shell Axial Welds | 1-410 A/C | -56 | 215.5 | 2.8E17 | 55 |

* For the limiting weld wire heat combination only.

**Fig. 1 Axial Fluence Profile
August 2033 at 90 Degree Azimuth**

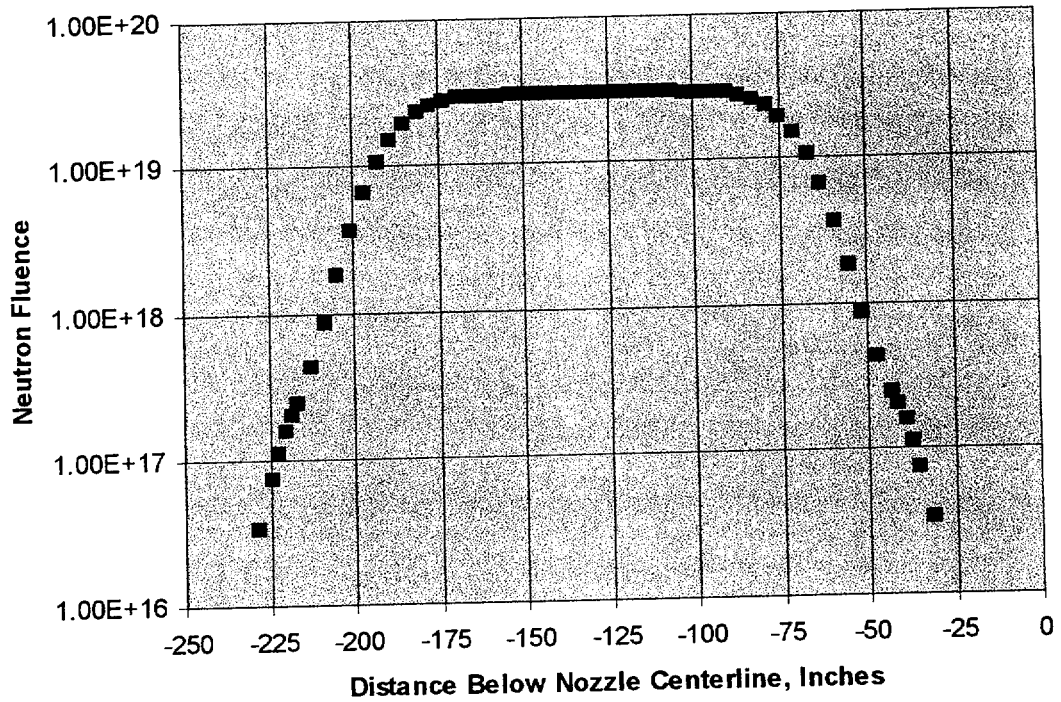
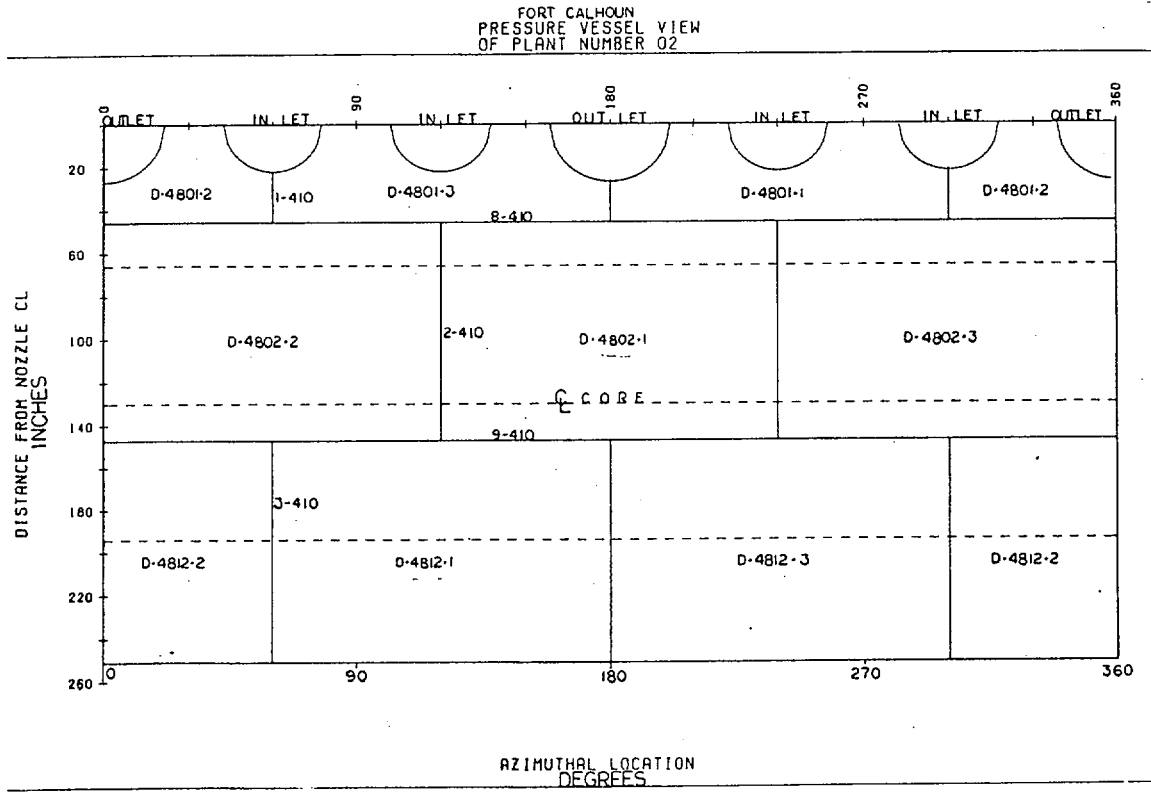


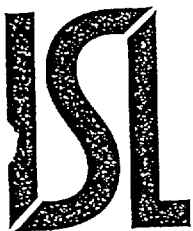
Fig. 2 Fort Calhoun Reactor Vessel Plan View



Reference 10.16

**Letter from ISL (W. Arcieri) to OPPD (F. J. Jensen),
"WCA-09-2002: Transmittal of RELAP5/Mod 3.2d,"**

August 2, 2002



INFORMATION SYSTEMS LABORATORIES

11140 Rockville Pike, Suite 500 • Rockville, MD 20852 • (301) 468-6425 • Fax: (301) 468-0883

August 2, 2002

OPPD - Fort Calhoun Nuclear Station
Highway 75 North
Fort Calhoun, NE 68023-0550
Attn: FREDRICK J. JENSEN III

SUBJECT: WCA-09-2002: Transmittal of RELAP5/MOD3.2d

Dear Mr. Jensen,

Enclosed is the CR-ROM that contains the transmittal of the RELAP5/MOD3.2d. The transmittal consists of source code and installation files to allow installation using the Fortran90 compiler on a Hewlett Packard workstation. Other changes made to the program since RELAP5/MOD3.2 are summarized in the "ChangeSummary.pdf" file included on the CD-ROM. The problem that you reported with the strip file has been corrected in this code version. It will also be corrected in RELAP5/MOD3.3. Your diligence in finding and reporting code problems is appreciated.

If you have any questions concerning this transmittal or require installation assistance, please contact me at ISL at (301) 255-2275 or via e-mail at billa@islinc.com.

Sincerely,

A handwritten signature in cursive script that reads "William Arcieri".

William Arcieri
Principal Engineer

cc: M. B. Rubin, USNRC (w/o enclosure)
D. Prelewicz, ISL (w/o enclosure)
D. Mlynarczyk, ISL (w/o enclosure)

File: 4421 - RELAP5 Transmittal File (2 copies)

Reference 10.17

**Readme.txt for the installation of RELAP5/Mod 3.2d from
Reference 10.16**

See the ChangesSummary.pdf file for a summary of the changes made to RELAP5/MOD3.2d from the earlier versions of RELAP5/MOD3.2.

RELAP5/MOD3.2d Installation Instructions

These instructions are for RELAP5 MOD3.2d. The installation requires approximately 78 MB (much of this can be deleted after installation if necessary) and takes anywhere from 30 minutes to a few hours.

We assume for these instructions that the transmittal is on a CD-ROM as a tar file. These files are about 55 Mbytes long.

STEPWISE INSTALLATION PROCEDURE

UNIX commands that may be used during the installation are enclosed in ().

Step 1. Change to the directory you want to contain the RELAP5 files. Copy the following files from the r5m3.2d tar file on the CD-ROM to your installation directory.

```
/Local Installation Directory
|-----> preinst
|-----> readme.txt
|----->/manuals
|----->/sampout
|----->/source
    |----->cnv32.f
    |----->dinstls
    |----->dutilty
    |----->envrl.s
    |----->goodies
    |----->indecks
    |----->selap.s
    |----->select.f
    |----->usplit.f
```

The indentation of cnv32f and the other files indicates that these file and/or subdirectories belong to the source subdirectory. There are 9 transmittal files in the source subdirectory. These transmittal files are listed below with their approximate size followed by a short description.

1. cnv32.f 11 KB Preprocessor for 32-bit computer changes to the source
2. dinstls 3 KB Top level installation C-shell script
3. dutilty 2 KB C-shell script to build the utilities:
 usplit.x, select.x, and cnv32.x
4. envrl.s 1747 KB Concatenated environmental library source files
5. goodies 50 KB Concatenated group of files that are used by the installation script
6. indecks 174 KB Concatenated input decks for checking the installation

Up to 4 parameters can follow the dinstls command. The first 3 parameters are required. The last parameter is optional and can be omitted.

Here is the usage command for dinstls:

```
usage: dinstls $1 $2 $3 $4
```

where the parameters are defined as follows:

```
$1 = machine type parameter
  cray = CRAY computer with bufin/bufout
  cray2 = CRAY computer without bufin/bufout
  decrisc = DEC RISC computer
  decrisc2 = DEC RISC computer with DEC compiler
  decalpha = DEC Alpha computer
  decalphao = DEC Alpha computer with nawk instead of awk
  decalp90 = DEC Alpha computer with Fortran 90 compiler
  hp = HP RISC computer
  hp90 = HP RISC computer using Fortan 90 compiler
  ibmrisc = IBM RISC computer, uses blkdta
  sgi = SGI RISC computer, defines both sun and sgi
  sgi64 = newer 64 bit SGI computer (in debug mode)
  stardent = STARDENT computer
  sun = SUN computer with Sun OS
  sunnew = SUN computer with Solaris OS
  vax = DEC VAX computer
```

```
$2 = code name parameter
  relap = RELAP5 code is installed
```

The arelap, asrelap, and srelap options, which are also in the dinstls script, will not work because the arelap requires a special property table and asrelap and srelap require the matpro.s file. The special property table and matpro.s file is not included in this distribution.

```
$3 = nuclear plant analyzer (NPA) parameter
  npa = NPA is included in installation
  nonpa = NPA is not included in installation
```

The next argument is optional. If it is not used, those options are deactivated.

```
$4 = GNU C compiler parameter (used on HP workstations only)
  GCC = use GNU gcc compiler to compile C source code
  nogcc = use UNIX C compiler to compile C source code (default)
```

This parameter only works when HP is used for \$1 machine type parameter. It is useful on HP computers that do not have the ANSI C compiler but do have the GNU C compiler.

Examples:

1: Basic installation on decrisc

```
dinstls decrisc relap nonpa
```

2: Basic installation on HP with ANSI C compiler

```
dinstls hp relap nonpa
```

3: Basic installation on HP with no ANSI C compiler

```
dinstls hp relap nonpa gcc
```

Step 5. When the code is completely installed using the dinstls command, three new directories are created under the /r5_mod3.2d/install directory. These are the envrl, selap, and run directories. The top levels of the directory structure now looks like:

```
/Local Installation Directory
|-----> preinst
|-----> readme.txt
|----->/manuals
|----->/sampout
|----->/source
    |----->cnv32.f
    |----->dinstls
    |----->dutilty
    |----->envrl.s
    |----->goodies
    |----->indecks
    |----->selap.s
    |----->select.f
    |----->usplit.f
|----->/install
    |----->cnv32.f
    |----->dinstls
    |----->dutilty
    |----->envrl.s
    |----->goodies
    |----->indecks
    |----->selap.s
    |----->select.f
    |----->usplit.f
    |----->/envrl
        |----->source and header files for
            environmental library
            and binary steam tables, tpfh2o
    |----->/selap
        |----->source and header files for relap5,
            makefiles, scripts, and executable
            code, relap5.x
    |----->/run
        |----->input (*.i), output (*.p), and
            restart (*.r) files from
            installation problems
```

ENVRL DIRECTORY

The envrl directory contains the source and header files that were used to make the environmental library, envrl.a. These source and header files came from the envrl.s file. The light and heavy water property tables, tpfh2o and tpf2o, are also in this directory.

SELAP DIRECTORY

The selap directory contains the source and header files that were used to make the relap5 libraries, relaplr.a, relaplq.a. The relap5 executable, relap5.x, and numerous other files that are also created during the installation such as the doitf and doith scripts are in this directory. The doitf script is used to run a Fortran source file through the two precompilers, select.x and cnv32.x and then to the compiler to generate the object file. The doith script is used to run a header file, .H file, through the two precompilers, select.x and cnv32.x to generate a .h file. The dloadr, dloadrn, dloads, and dloads_n scripts are used to link the newly compiled object files with the appropriate libraries to create a new executable file or files. The dloadr is used to create relap5.x, dloadrn is used to create relap5.x with the NPA links, dloads is used to create the scdap version of relap5, and dloads_n is used to create the scdap version of relap5 with the NPA links. These scripts are used when making changes to the source code.

RUN DIRECTORY

The run directory contains links to the relap5.x executable in the selap directory, and the water property tables, tpf2o and tpfh2o, in the envr1 directory. The run directory also contains the installation test problem input (*.i) output (*.p), and restart (*.r) files from running these installation problems. The output files should be checked to make sure all the installation problems ran successfully.

EXECUTION OF RELAP5

The basic command line usage statement for running RELAP5 is:

```
relap5.x -i indta -o outdta -r rstplt -w tpfh2o
```

where

```
indta = input file name (indta is the default name)
outdta = output print file name (outdta is the default
name)
rstplt = restart/plot file name (rstplt is the default
name)
tpfh2o = water properties file name (tpfh2o is the
default name)
```

Note:

For heavy water use -d tpf2o in addition to or instead of -w tpfh2o. If there is only one system and it contains heavy water, then use the -d option. If there are two systems, and one contains heavy water and one contains light water, then use both the -w and -d options.

Example: Run the Edward's pipe test problem from the installation set. The input deck name is edhtrk.i

```
relap5.x -i edhtrk.i -o edhtrk.p -r edhtrk.r
```

The default water properties table, tpfh2o, is correct for this problem so it is not included in the command line. The output print file will be called edhtrk.p and the restart file is called edhtrk.r. XMGR5 can be used to make plots from the restart file, edhtrk.r, because the restart file is really a combination file containing both restart and plot information.

REFERENCES:

To submit user problems or to review previous user problems, or for basic information on the usage of RELAP5, including command line options of RELAP5, see Volume II of the RELAP5 manual, which can be obtained via the World Wide Web in the NRC RELAP5 Home Page:

<http://www.nrc.gov/RES/RELAP5>

For other questions, contact
RELAP5 Hot Line: 301-231-5378

For submitting user problem reports, fill out the form on the Web page:
<http://www.nrc.gov/RES/RELAP5/>

or submit E-mail to:
relap5@nrc.gov

Reference 10.18

**Changesummary.pdf that summarizes the modifications to
RELAP5/Mod 3.2d from Reference 10.16**

RELAP5 MOD3.2d

August 2002

RELAP5/MOD3.2d, which is the current version of RELAP5/MOD3.2, evolved through a series of changes starting with the RELAP5/MOD3.2 program. The first in the series was RELAP MOD3.2a, which is RELAP5 MOD3.2 with the added ability to compile the code on the SGI 64 bit computer (sgi64) and the DEC alpha computer using the new awk (decalphao). RELAP5 MOD 3.2b is RELAP5 MOD3.2a with the added ability to compile the code on the HP computer using the f90 compiler. In the process of making and testing the changes to RELAP5/MOD3.2b, a coding error was discovered in the RPIPE.F subroutine. This error has probably been in the code since it was first written but it has no safety implications. RELAP5 MOD3.2c is RELAP5 MOD3.2b with this coding error in RPIPE.F corrected. RELAP5/MOD3.2d is RELAP5/MOD3.2c with corrections made to: 1) produce an input processing error if more than one mesh interval is specified in the fuel - cladding gap and 2) correct a formatting error in the header line in a strip file that prevented plotting with xmgr5.

There are nine files in the distribution CD and changes were needed in four of the files. The five files in which changes were not needed are: CNV32.F, DINSTLS, INDECKS, SELECT.F, and USPLIT.F. The following sections document the changes needed in the other four files.

dutilty

The DUTILTY script is used to compile the utility programs: CNV32.F, SELECT.F, and USPLIT.F. The DUTILTY script required the addition of an `ihp90i` option that used the f90 compiler. This option required changing the `i+Ti` option on the f77 compiler command line to `i+fp_exceptioni`. HP removed the +T option from the f90 compiler and added this new option in its place.

envr1.s

The call to IGETARG, which is in the HP library, now requires three arguments instead of the two arguments it required under f77. The additional argument is the length of the ARG variable. This was added to the code by defining a new variable, `L = LEN(ARG)`, and including L as the third argument in the IGETARG call.

All the thermodynamic property generation had their two underflow trapping statements:

```
on real*4 underflow call trap4
on real*8 underflow call trap8
```

replaced by one statement:

```
ON EXTERNAL ERROR IGNORE
```

This change was necessary in the following programs: STGBLOOD, STGD20, STGLYC, STGH2, STGH2O STGHE, STGK, STGLI, STGLIPB, STGN2, STGNA, STGNAK, and STGNH2.

goodies

Goodies had the `hp90` machine option added to the various scripts that are in the goodies file. These additions use the `fp_exception` f90 compiler command line option instead of the `f77` compiler command line option.

selap.s

The `DDOT.F` and `DNRM2.F` files had optional compiler statements added that set the returned function value to zero. These functions are not called, so this change has no effect on the answers, but the f90 compiler requires a return value for a function. The f77 compiler was not as strict about returning a value. The optional compiled statements that were added are:

```
$if,def,hp90
  ddot = 0.0 or dnr2 = 0.0
$endif
```

The UNDERFLOW trap statements in the RELAP5 program

```
on real*4 underflow call trap4
on real*8 underflow call trap8
```

were replaced by the statement

```
on external error ignore
```

A few format statements that had the `lp` and `gl3.5` run together without a comma, e.g.,

```
lp,gl3.5
```

needed a comma after the `lp` so that they now read

```
lp,g13.5
```

The error in `rpipe.F`

```
& if (xinit(i4+6).ne.0.0 .or. xinit(i4+7).ne.0.0 .or.
  xinit(i4+9).ne.0.0) imap(k+2) = ior(imap(k+2),4096)
```

had the `xinit(i4+9)` replaced by `xnit(i4+8)` so it now reads

```
& if (xinit(i4+6).ne.0.0 .or. xinit(i4+7).ne.0.0 .or.
  xinit(i4+8).ne.0.0) imap(k+2) = ior(imap(k+2),4096)
```

Changes were made to the `aatl.F` routine and the `htlinp.F` routines in the `selap.s` library in RELAP5/MOD3.2d. The changes made to `aatl.F` are made to identify the code version in the out-

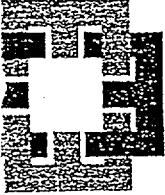
put and to correct the formatting in the strip file header line. The changes made to htlinp.F are made to produce an input error if the user specifies more than one mesh in the fuel rod gap. These changes do not affect the computations.

Reference 10.19

**Letter from ENERCON Services, Inc (D. R. Whitson) to OPPD
(J. Jensen)**

August 8, 2002,

“Quality Assurance for RELAP5/Mod 3.2”



ENERCON SERVICES, INC.
An Employee Owned Company

5100 E. Skelly Dr., Suite 450
Tulsa, OK 74135
(918) 665-7693
(918) 665-7232 - Fax
(800) 735-7693

August 8, 2002
DRW-02-027

Mr. James Jensen
Omaha Public Power District
Fort Calhoun Station
PO Box 550
Fort Calhoun, NE 68023-0550

Subject: Quality Assurance for RELAP5/Mod 3.2

Dear Mr. Jensen:

Enercon recently completed an LTOP analysis for OPPD's Fort Calhoun Station using RELAP5/Mod 3.2. This letter documents the Quality Assurance methods and controls that were applied to this work.

Per contract, our work for this project was conducted under the Enercon Services Quality Assurance Program. Specifically, Enercon's Corporate Standard Procedure (CSP) 3.02, "Control of Computer Software" governs the requirements for use of software in safety-related applications. Section 3.1 of this procedure allows that software previously developed by entities other than Enercon may be used in safety-related activities provided assurance of the accuracy and applicability of the software is provided, approved by the Project Manager and maintained in the project files. For programs such as RELAP, the CSP would require that the software to be reviewed and verified by Enercon personnel, and that the software can be shown to be accurate and applicable for the intended application. Note that this requires review and approval for use in each application or project. The use of RELAP for the LTOP application was reviewed and approved per Enercon procedure.

For the OPPD project, the standard test cases provided for RELAP5/Mod 3.2 by INEEL were run to check the accuracy of the RELAP code on Enercon's machines. These cases were:

ANS79
EDHTRK
EDHTRKN
EDRST
ESDTRIP
PUMP2
TYPPWR
TYPPWRN

All of the above cases were run satisfactorily. Any differences between the output on Enercon's machines and the INEEL results were justified and determined to be acceptable.

To ensure the RELAP code would properly model two-phase flow as compared to an alternate information source, a RELAP model was developed to emulate the test apparatus described in Dr. Ralph W. Pike's Ph.D. Thesis, "The Adiabatic, Evaporating, Two-Phase Flow of Steam and Water in Horizontal Pipe" (July 1962, Georgia Institute of Technology).

The thesis test runs for equilibrium conditions, non-equilibrium conditions and critical flow were modeled in RELAP and benchmarked. The results of RELAP showed good comparison to the test conditions and results. Any discrepancies between the model and test were explained and were considered satisfactory.

It must be noted that before any calculation is performed using the RELAP code, the RELAP code manual is researched to determine if any previous models/analyses using RELAP similar to the analyses to be performed has been accomplished. If previous analyses have been performed, the title of the work is identified and noted in the Computer Certification form that is included in the QA file for the project.

Certain modifications were made to the code for the LTOP project. To increase the speed of the code compilation, various extraneous programs from the INEEL environmental file, *envr1.s*, were removed. These have no effect on the RELAP code. To be compatible with the NDP Fortran compiler, changes to various environmental file subroutines regarding the timing function, write statements, date, and clock were made. Also for compatibility, modifications to RELAP source subroutines to change the page header title and error trapping routines for Hewlett-Packard computers were made. Missing carriage returns from Subroutine *level* and *std2x6* were also added. Other changes to the code were the correction of errors in the *plotr5* subroutine. None of the above modifications changed the methodology of the code or the numerics.

The Enercon Services Quality Assurance Program has been audited to the requirements of 10 CFR 50 Appendix B on numerous occasions. The Enercon program has been audited by nuclear utilities under the auspices of NUPIC in 1999 and again in 2001. These audits included control of software within their scope, and auditors examined the RELAP quality assurance package as evidence of the Enercon program. No findings related to the RELAP package were generated by either audit.

Enercon appreciates this opportunity to be of service. If you have any questions, please contact me at (918) 665-7693 or through my email address, dwhitson@enercon.com.

Sincerely,



Douglas R. Whitson
Client Services Manager

Reference: 10.20

**R5-02-01, Validation Report for NEPTUNUS Pressurizer using
RELAP5/Mod 3.2,**

April 12, 2002

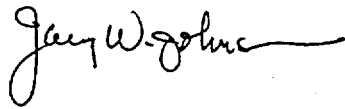
Validation Report

R5-02-01

Title: NEPTUNUS Pressurizer

April 12, 2002

Code Version: MOD3.2



Manager: _____

Date: April 12, 2002

G. W. Johnsen, RELAP5-3D
Code Development

1.0 INTRODUCTION

The NEPTUNUS pressurizer experiment is one of a series of separate effects tests used to assess the performance of the RELAP5 code in modeling nuclear reactor thermal-hydraulic behavior. NEPTUNUS is a scaled model pressurizer located in the Laboratory of Thermal Power Engineering at the Delft University of Technology in the Netherlands. Test Y05 simulated successive insurges, combined with spray, and outsurges in a pressurizer. The assessment tests the accuracy of the interfacial heat and mass transfer models that come into play at the surface of the moving liquid level and in the steam space above the liquid level. To a lesser extent, it also tests the internal wall heat transfer modeling.

Section 2 describes the test facility and the test procedure, section 3 describes the RELAP5/MOD3 model, section 4 discusses and analyzes the results, section 5 summarizes conclusions, and section 6 lists the references. Appendix A contains a listing of the RELAP5/MOD3 input file.

2.0 FACILITY AND TEST DESCRIPTION

This section describes the test facility and the test conditions, both of which were obtained from a paper by H. A. Bloemen in which an analysis of test Y05 using RELAP5/MOD1 was discussed¹.

The NEPTUNUS pressurizer test facility is about 1/40-scale on a volume basis and consists of a pressure vessel with a surge line at the bottom and a spray line at the top. The basic flow paths in the facility are shown in Figure 1. The flow in the spray line was controlled by a pump connected to a vessel containing hot water. The surge line was connected through a buffer vessel to a cold water vessel pressurized with nitrogen. The flow in the surge line was controlled by varying the nitrogen pressure. The buffer vessel was used to keep a boundary between the hot (548 K) water surging into and out of the pressurizer and the cold (ambient) water in the vessel pressurized with nitrogen. The boundary between the hot and cold fluid was kept in the buffer vessel to prevent thermal shock to the system piping. The spray line and surge line nozzles contained thermal sleeves to prevent thermal shock to the vessel. The flows and fluid temperatures in each line were measured.

The geometric details of the carbon steel test vessel are shown in Figure 2. The vessel was 2.51 m high and 0.8 m in diameter. The surge line nozzle diameter was 0.084 m and the spray line nozzle diameter was 0.027 m. Heater elements with a total power of 17 kW were installed to compensate for environmental heat losses.

The test was initiated with the vessel partially filled (to a level of 1.12 m) with water at 600 K; then an insurge of 548 K water flowed into the vessel, followed shortly by the initiation of spray flow. The temperature of the spray varied from 500 K to 591 K. The test consisted of four successive insurges, combined with spray flow, and outsurges. The magnitude and timing of the spray and surge line flows are shown in Figure 3.

The measured data in the vessel were very limited. One pressure and four fluid temperatures were all that were reported¹. These data were digitized from the report for comparison with the calculations. The exact location of the measurements was not documented, but in Bloemen's report they were compared with calculated results between the 1.52 m and 1.72 m elevations.

3.0 RELAP5/MOD3 MODEL

Figure 4 shows the RELAP5/MOD3² nodalization diagram of the NEPTUNUS pressurizer. The pressurizer was modeled using thirteen volumes and twelve junctions. The wall of the pressurizer was modeled using thirteen heat slabs to simulate the environmental heat loss and the condensation effect due to the cold pressurizer wall. Two time dependent volumes were used to simulate the boundary conditions of the cold water supply vessel and spray vessel. The surge line flow rate and the spray rate were modeled using two time dependent junctions. The test-specified surge flow rate and spray rate were input to RELAP5/3D as boundary conditions.

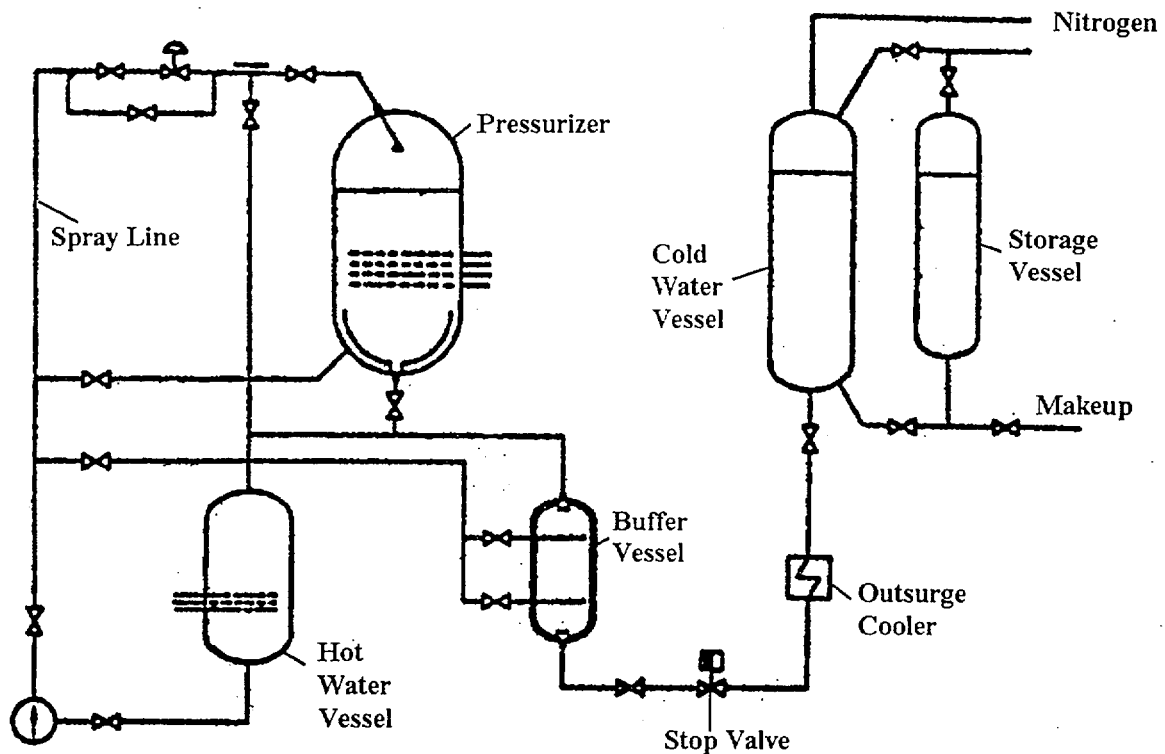


Figure 1. NEPTUNUS Facility Diagram

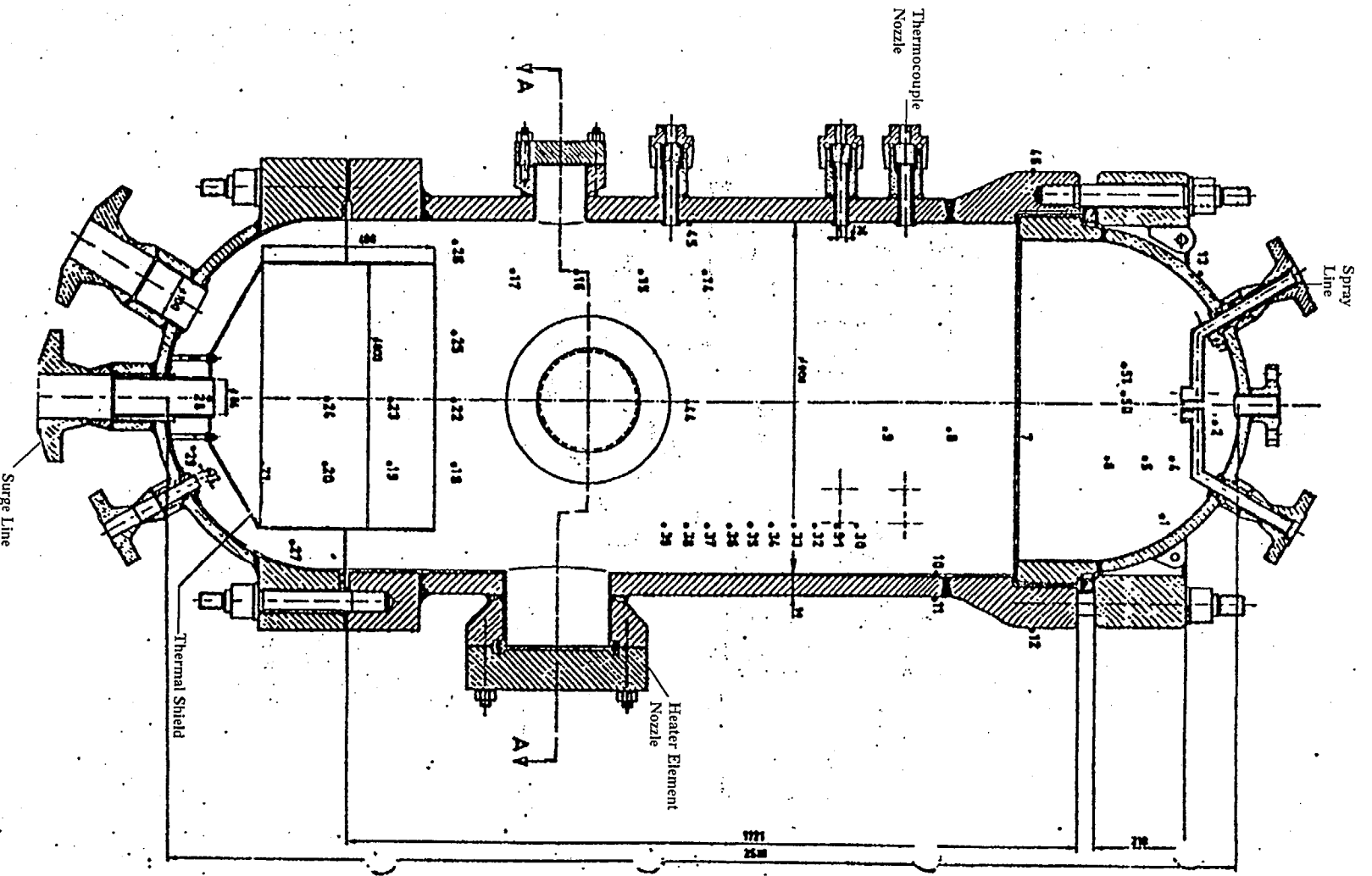


Figure 2. NEPTUNUS Pressurizer

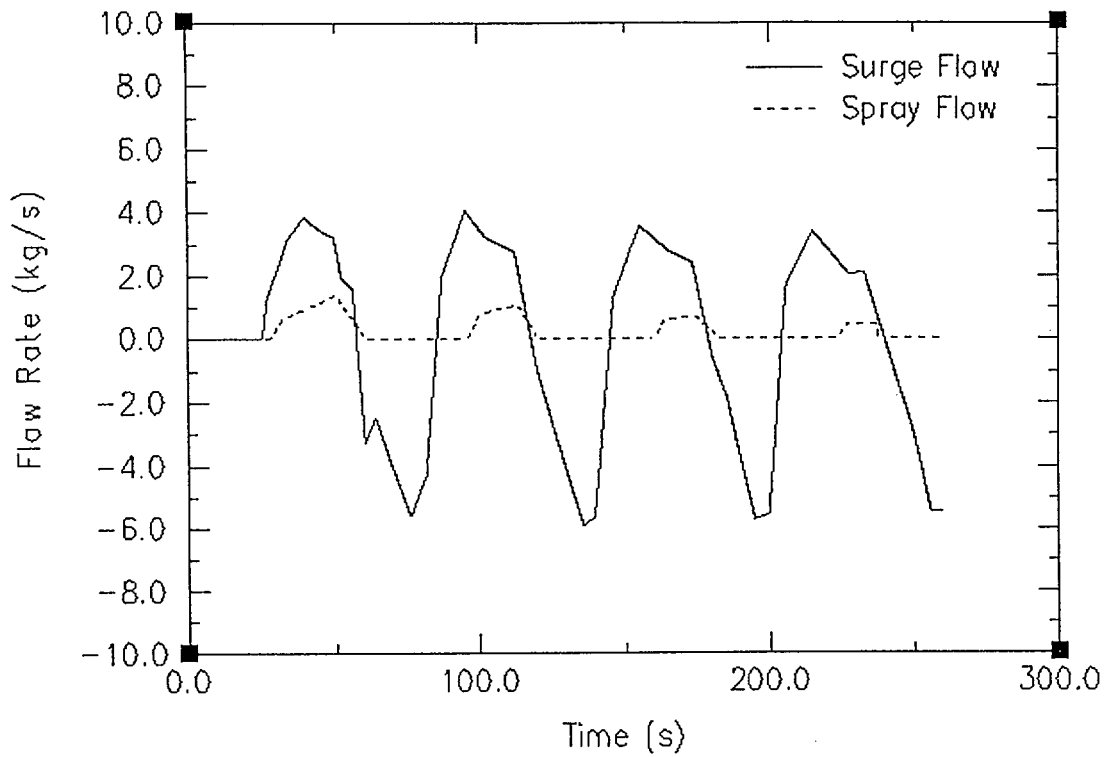


Figure 3. Prescribed surge and spray flows in Test Y05 based on measured data

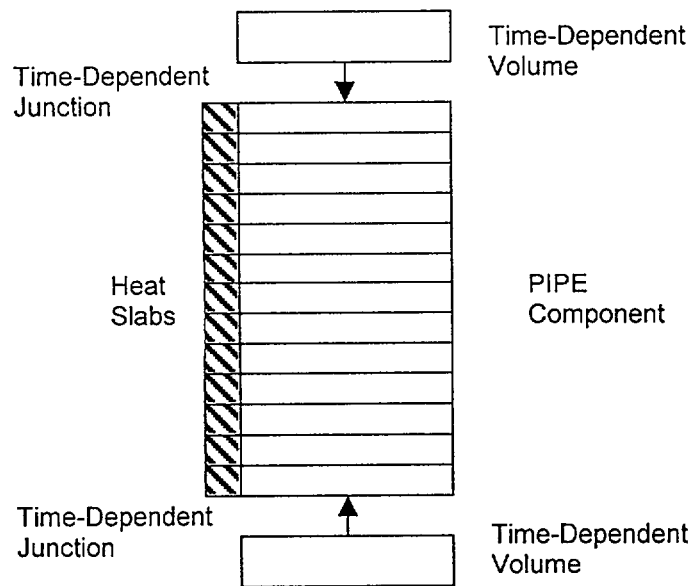


Figure 4. RELAP5/MOD3 Nodalization Diagram

4.0 RESULTS

Figure 5 compares the calculated and measured pressure near the top of the pressurizer. RELAP5/MOD3 reproduces the overall trend well, but over-predicts the peak pressures that occur during the insurge phases. This is caused by insufficient condensing of the steam when the spray is activated.

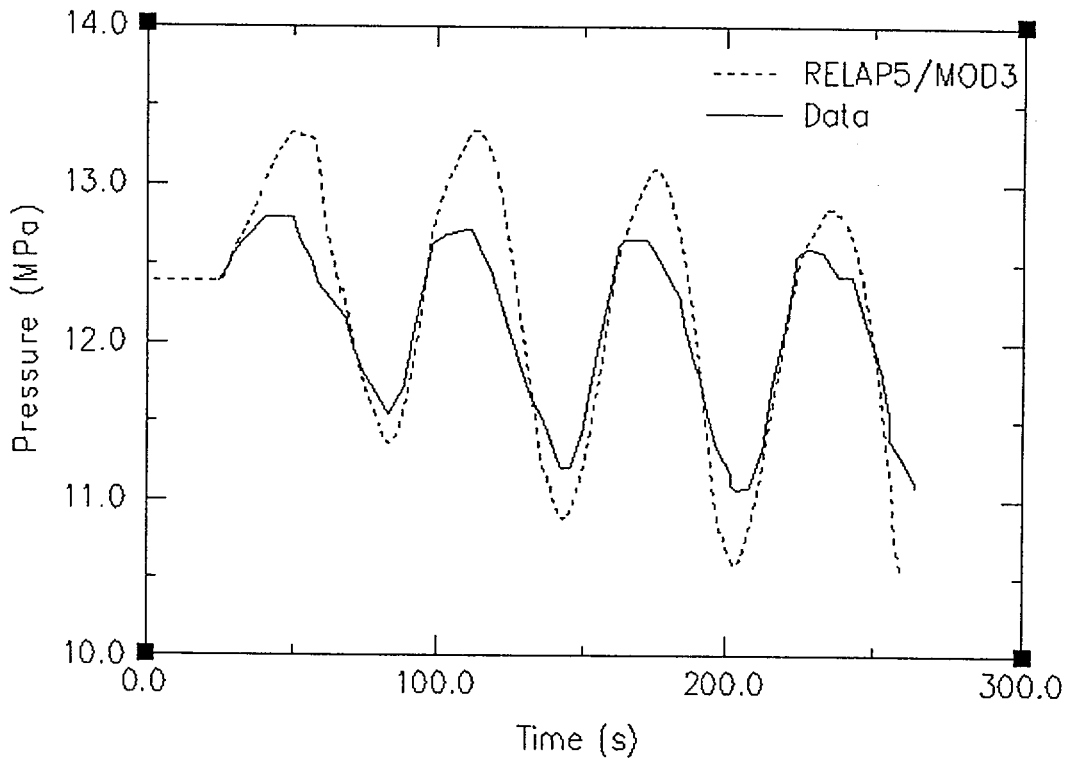


Figure 5. Calculated and measured pressurizer pressure

This conclusion is supported by the comparison of calculated and measured steam space temperature near the top of the pressurizer shown in Figure 6, and comparisons of steam space temperature and saturation temperature from the test and calculation shown in Figures 7 and 8, respectively. The calculation shows a significant degree of superheating in the steam space during all of the insurges. In the experiment, little superheating occurs during the first and second insurges, where the spray interval closely matches the insurge interval (see Figure 3). During the third and fourth insurge the spray is delayed, allowing time for the steam to superheat in the experiment.

The apparent *degree* of disagreement in the temperature data is probably somewhat exaggerated. When the spray is on in the experiment, it can impinge on the thermocouple located in the steam space, thereby giving a false reading for steam temperature. The RELAP5/MOD3 calculated temperature shown in Figures 6 and 8 is the average steam temperature at the location where the thermocouple was located.

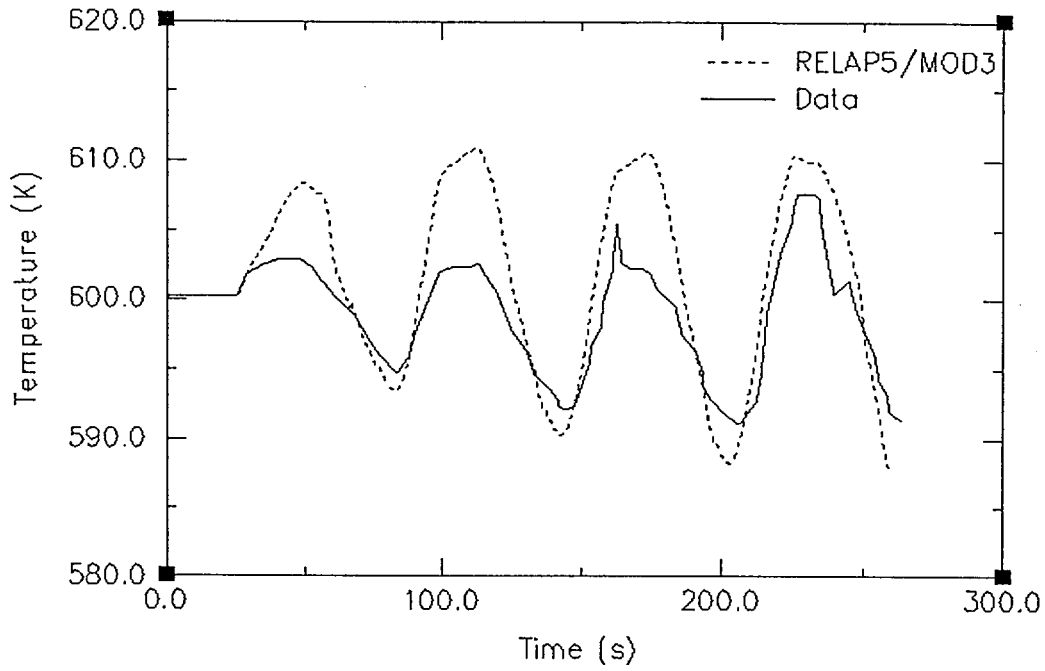


Figure 6. Calculated and measured temperature near the top of the pressurizer

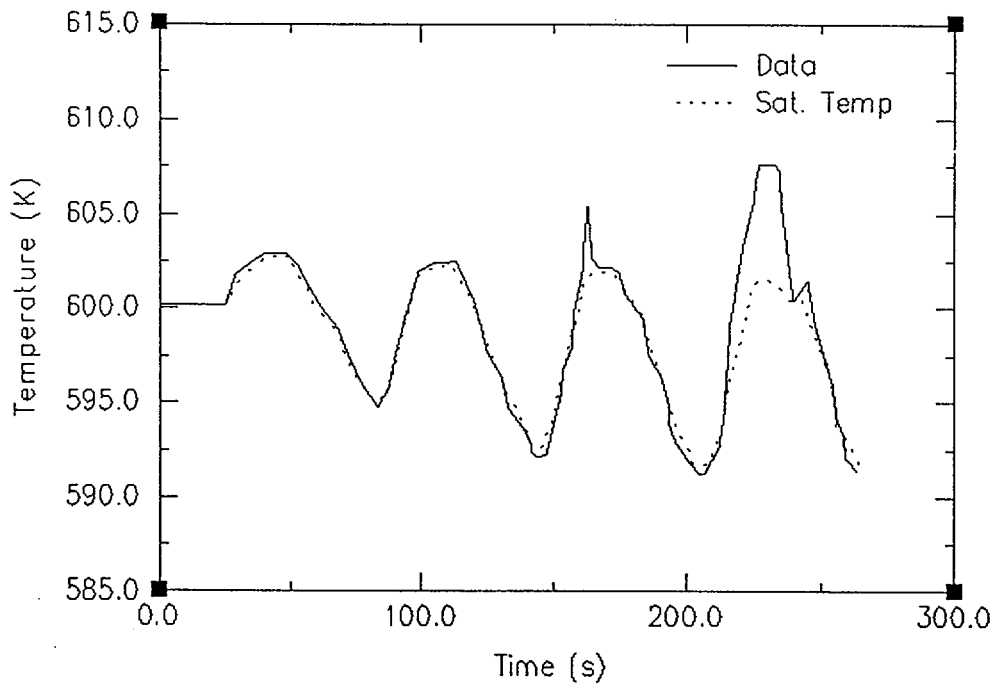


Figure 7. Comparison of steam space temperature and saturation temperature (test data)

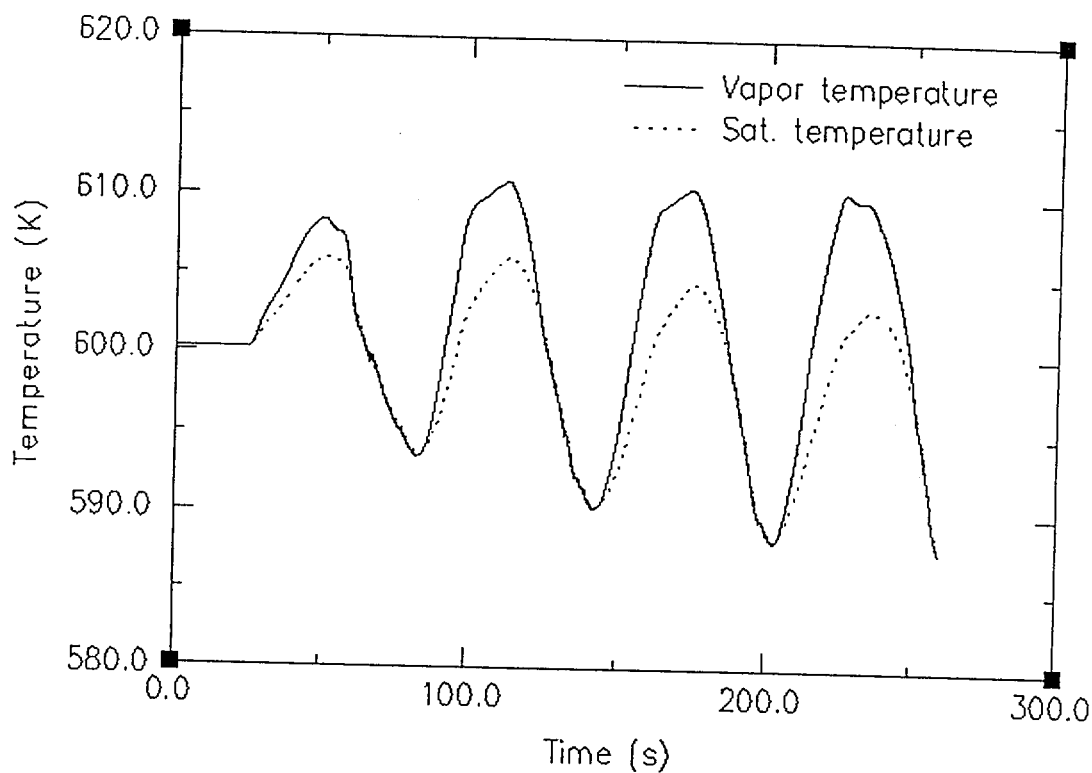


Figure 8. Comparison of steam space temperature and saturation temperature (RELAP/MOD3)

The insufficient condensing of steam while the spray is operational indicates an under-prediction of the heat/mass transfer in the steam space, where the "cold" spray droplets are interacting with "hot" steam. The interfacial heat transfer coefficients are clearly too low.

The RELAP5-3D³ code includes a PRIZER component specifically designed to model pressurizers. It includes the capability to alter the interfacial heat/mass transfer in the steam space. Figure 9 compares the NEPTUNUS pressure data to the MOD3 calculation and a RELAP5-3D calculation. In the latter, the interfacial heat/mass transfer was increased through user input. The agreement with the data is seen to be improved. However, the calculated peaks are high for the first two insurges and low for the third and fourth. Also, the minimum pressures are under-predicted throughout.

5.0 CONCLUSIONS

An assessment of the RELAP5/MOD3 code has been conducted by simulating the Neptunus Y05 pressurizer experiment. The results show that the code predicts the correct overall trends but exaggerates the maximum and minimum pressures that occur during the insurge/outsurge cycles. In this respect, the results could be considered conservative. The principal reason the peak pressures are overstated is insufficient condensation occurring in the steam space when the spray is activated. This was confirmed by running the same problem with RELAP5-3D, in which the interfacial heat/mass transfer can be altered by the user through data input. When the interfacial

heat/mass transfer was increased, the agreement with the data improved. This increased interfacial heat/mass transfer is applied all the time, whether the spray is activated or not. It would be more physically realistic if the heat/mass transfer were dependent on whether the spray was on or off.

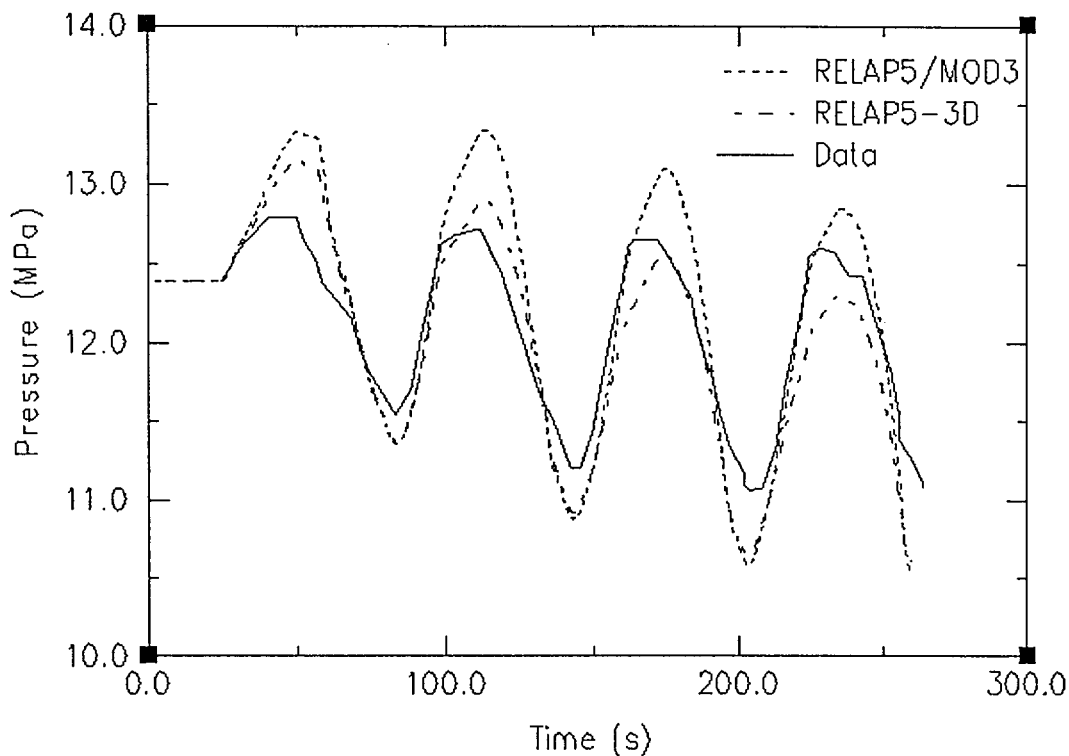


Figure 9. Calculated and measured pressurizer pressure

5.0 REFERENCES

1. H. A. Bloemen, *Verification of the Pressurizer Model in RELAP5/MOD1*, Energieonderzoek Centrum Nederland, Memo No. 0.375.10 GR 26 (OD 79-24), May 1983.
2. The RELAP5 Development Team, *RELAP5/MOD3 Code Manual*, NUREG/CR-5535, INEL-95/0174, August, 1995.
3. The RELAP5 Development Team, *RELAP5-3D Code Manual, Rev. 1.3.a*, INEEL-EXT-98-00834, February, 2001.

APPENDIX A. LISTING OF RELAP5/MOD3 INPUT FILE FOR NEPTUNUS Y05

```

=neptunus y05
0000100 new transnt
0000201 260.00 1.e-6 0.050 402 1 1000 1000
*
0000301 p      002010000
0000302 tempg  002010000
0000303 velfj  004000000
0000306 p      002090000
0000307 tempg  002090000
0000308 tempf  002090000
0000311 rhofj  004000000
0000313 rhofj  005000000
0000316 velfj  002120000
0000317 velgj  002120000
0000318 p      002120000
*
0000501 time 0 ge null 0 25.0 1
0000502 time 0 ge null 0 25.0 1
*
0010000 surge tmdpv01
0010101 0.18550 2.5 0.0 0.0 90.0 2.5 4.e-5 0.0 10
0010200 3 501
0010201 0.00 125.0e+5 548.0
0010202 300.00 125.0e+5 548.0
*
0020000 press pipe
0020001 13
0020101 0.03398 1
0020102 0.28274 3
0020103 0.50265 10
0020104 0.41169 13
0020301 0.11900 1
0020302 0.20000 3
0020303 0.20083 9
0020304 0.15500 10
0020305 0.13600 11
0020306 0.12450 13
0020601 90.0 13
0020801 0.00004 0.0 13
0021001 00 13
0021101 1100 1
0021102 1000 2
0021103 1100 3
0021104 1000 9
0021105 1100 10
0021106 1000 12
0021201 2 12390000.0 0.0 0.0 0.0 0.0 6
0021202 2 12390000.0 1.0 0.0 0.0 0.0 13
0021301 0.0 0.0 0.0 12
*
0030000 spray tmdpv01
0030101 0.50265 2.5 0.0 0.0 90.0 2.5 4.e-5 0.0 10
0030200 3 501
0030201 0.00 128.00e+5 593.98

```

| | | | |
|---------|--------|-----------|--------|
| 0030202 | 2.74 | 128.00e+5 | 593.98 |
| 0030203 | 5.00 | 123.00e+5 | 506.48 |
| 0030204 | 8.92 | 128.00e+5 | 500.23 |
| 0030205 | 19.38 | 128.00e+5 | 529.40 |
| 0030206 | 37.19 | 128.00e+5 | 537.73 |
| 0030207 | 49.20 | 128.00e+5 | 578.57 |
| 0030208 | 71.40 | 128.00e+5 | 598.15 |
| 0030209 | 72.67 | 128.00e+5 | 533.57 |
| 0030210 | 97.97 | 128.00e+5 | 539.82 |
| 0030211 | 110.69 | 128.00e+5 | 580.65 |
| 0030212 | 135.00 | 128.00e+5 | 593.57 |
| 0030213 | 137.35 | 128.00e+5 | 535.5 |
| 0030214 | 159.94 | 128.00e+5 | 539.82 |
| 0030215 | 169.12 | 128.00e+5 | 579.4 |
| 0030216 | 198.34 | 128.00e+5 | 593.98 |
| 0030217 | 200.88 | 128.00e+5 | 537.73 |
| 0030218 | 215.99 | 128.00e+5 | 539.82 |
| 0030219 | 230.53 | 128.00e+5 | 584.40 |
| 0030220 | 300.00 | 128.00e+5 | 591.07 |

*

| | | | | |
|---------|---------------|-----------|-----------|------|
| 0040000 | surj4 tmdpjun | | | |
| 0040101 | 001000000 | 002000000 | 0.5542e-2 | |
| 0040200 | 0 502 | | | |
| 0040201 | 0.00 | 0.00 | 0.00 | 0.00 |
| 0040202 | 1.42 | .27968 | .27968 | 0.00 |
| 0040203 | 8.82 | .73981 | .73981 | 0.00 |
| 0040204 | 14.28 | .90581 | .90581 | 0.00 |
| 0040205 | 19.38 | .81559 | .81559 | 0.00 |
| 0040206 | 24.32 | .75604 | .75604 | 0.00 |
| 0040207 | 26.96 | .45291 | .45291 | 0.00 |
| 0040208 | 30.83 | .37712 | .37712 | 0.00 |
| 0040209 | 35.00 | -.79394 | -.79394 | 0.00 |
| 0040210 | 38.76 | -.60447 | -.60447 | 0.00 |
| 0040211 | 50.91 | -1.43450 | -1.43450 | 0.00 |
| 0040212 | 56.19 | -1.13316 | -1.13316 | 0.00 |
| 0040213 | 61.95 | .45651 | .45651 | 0.00 |
| 0040214 | 70.40 | .95272 | .95272 | 0.00 |
| 0040215 | 77.18 | .76146 | .76146 | 0.00 |
| 0040216 | 87.30 | .64778 | .64778 | 0.00 |
| 0040217 | 95.00 | -.22735 | -.22735 | 0.00 |
| 0040218 | 110.79 | -1.47239 | -1.47239 | 0.00 |
| 0040219 | 114.67 | -1.43450 | -1.43450 | 0.00 |
| 0040220 | 121.18 | .30134 | .30134 | 0.00 |
| 0040221 | 130.33 | .84266 | .84266 | 0.00 |
| 0040222 | 140.20 | .65319 | .65319 | 0.00 |
| 0040223 | 148.47 | .56297 | .56297 | 0.00 |
| 0040224 | 155.00 | -.11368 | -.11368 | 0.00 |
| 0040225 | 160.45 | -.45651 | -.45651 | 0.00 |
| 0040226 | 169.96 | -1.40563 | -1.40563 | 0.00 |
| 0040227 | 175.00 | -1.39119 | -1.39119 | 0.00 |
| 0040228 | 180.70 | .38073 | .38073 | 0.00 |
| 0040229 | 190.22 | .79755 | .79755 | 0.00 |
| 0040230 | 202.54 | .47817 | .47817 | 0.00 |
| 0040231 | 207.83 | .49441 | .49441 | 0.00 |
| 0040232 | 225.00 | -.72176 | -.72176 | 0.00 |
| 0040233 | 230.72 | -1.32984 | -1.32984 | 0.00 |
| 0040234 | 237.72 | -1.36774 | -1.36774 | 0.00 |

```

*
0050000 spr tmdpjun
0050101 003000000 002010000 0.4016e-5
0050200 0 501
0050201 0.00 0.0000 0.0000 0.0
0050202 2.74 0.0000 0.0000 0.0
0050203 6.99 183.2918 183.2918 0.0
0050204 24.96 432.2958 432.2958 0.0
0050205 35.86 0.0000 0.0000 0.0
0050206 70.96 0.0000 0.0000 0.0
0050207 75.49 252.4651 252.4651 0.0
0050208 88.51 338.9193 338.9193 0.0
0050209 95.58 0.0000 0.0000 0.0
0050210 135.35 0.0000 0.0000 0.0
0050211 138.75 190.2141 190.2141 0.0
0050212 149.79 224.8008 224.8008 0.0
0050213 157.86 0.0000 0.0000 0.0
0050214 198.33 0.0000 0.0000 0.0
0050215 202.58 155.6275 155.6275 0.0
0050216 212.77 155.6275 155.6275 0.0
0050217 212.77 0.0000 0.0000 0.0
0050218 300.00 0.0000 0.0000 0.0
*
10011000 1 2 2 1 0.042
10011100 0 1
10011101 1 0.322
10011201 1 1
10011301 0.0 1
10011400 0
10011401 600.0 2
10011501 002010000 0 1 1 0.114 1
10011601 0 0 0 1 0.114 1
10011701 0 0.0 0.0 0.0 1
10011801 0.0 10.0 10.0 0.0 0.0 0.0 0.0 1.0 1
10011901 0.0 10.0 10.0 0.0 0.0 0.0 0.0 1.0 1
*
10021000 1 2 2 1 0.208
10021100 0 1
10021101 1 0.322
10021201 1 1
10021301 0.0 1
10021400 0
10021401 600.0 2
10021501 002010000 0 1 1 0.119 1
10021601 0 0 0 1 0.119 1
10021701 0 0.0 0.0 0.0 1
10021801 0.0 10.0 10.0 0.0 0.0 0.0 0.0 1.0 1
10021901 0.0 10.0 10.0 0.0 0.0 0.0 0.0 1.0 1
*
10031000 2 2 2 1 0.3
10031100 0 1
10031101 1 0.533
10031201 1 1
10031301 0.0 1
10031400 0
10031401 600.0 2
10031501 002020000 10000 1 1 0.200 2

```

10031601 0 0 0 1 0.200 2
10031701 0 0.0 0.0 0.0 2
10031801 0.0 10.0 10.0 0.0 0.0 0.0 0.0 1.0 2
10031901 0.0 10.0 10.0 0.0 0.0 0.0 0.0 1.0 2
*
10041000 2 2 2 1 0.4
10041100 0 1
10041101 1 0.455
10041201 1 1
10041301 0.0 1
10041400 0
10041401 600.0 2
10041501 002040000 10000 1 1 0.20083 2
10041601 0 0 0 1 0.20083 2
10041701 1 0.0 0.0 0.0 2
10041801 0.0 10.0 10.0 0.0 0.0 0.0 0.0 1.0 2
10041901 0.0 10.0 10.0 0.0 0.0 0.0 0.0 1.0 2
*
10091000 1 2 2 1 0.4
10091100 0 1
10091101 1 0.455
10091201 1 1
10091301 0.0 1
10091400 0
10091401 600.0 2
10091501 002060000 0 1 1 0.20083 1
10091601 0 0 0 1 0.20083 1
10091701 1 1.0 0.0 0.0 1
10091801 0.1 10.0 10.0 0.0 0.0 0.0 0.0 1.0 1
10091901 0.0 10.0 10.0 0.0 0.0 0.0 0.0 1.0 1
*
10101000 3 2 2 1 0.4
10101100 0 1
10101101 1 0.455
10101201 1 1
10101301 0.0 1
10101400 0
10101401 600.0 2
10101501 002070000 10000 1 1 0.20083 3
10101601 0 0 0 1 0.20083 3
10101701 0 0.0 0.0 0.0 3
10101801 0.0 10.0 10.0 0.0 0.0 0.0 0.0 1.0 3
10101901 0.0 10.0 10.0 0.0 0.0 0.0 0.0 1.0 3
*
10051000 1 2 2 1 0.400
10051100 0 1
10051101 1 0.489
10051201 1 1
10051301 0.0 1
10051400 0
10051401 600.0 2
10051501 002100000 0 1 1 0.165 1
10051601 0 0 0 1 0.165 1
10051701 0 0.0 0.0 0.0 1
10051801 0.0 10.0 10.0 0.0 0.0 0.0 0.0 1.0 1
*
10061000 1 2 2 1 0.362

10061100 0 1
10061101 1 0.5225
10061201 1 1
10061301 0.0 1
10061400 0
10061401 600.0 2
10061501 002110000 0 1 1 0.136 1
10061601 0 0 0 1 0.136 1
10061701 0 0.0 0.0 0.0 1
10061801 0.0 10.0 10.0 0.0 0.0 0.0 0.0 1.0 1
10061901 0.0 10.0 10.0 0.0 0.0 0.0 0.0 1.0 1
*
10071000 2 2 2 1 0.362
10071100 0 1
10071101 1 0.397
10071201 1 1
10071301 0.0 1
10071401 600.0 2
10071501 002120000 10000 1 1 0.249 2
10071601 0 0 0 1 0.249 2
10071701 0 0.0 0.0 0.0 2
10071801 0.0 10.0 10.0 0.0 0.0 0.0 0.0 1.0 2
10071901 0.0 10.0 10.0 0.0 0.0 0.0 0.0 1.0 2
*
10081000 1 2 2 1 0.002
10081100 0 1
10081101 1 0.397
10081201 1 1
10081301 0.0 1
10081400 0
10081401 600.0 2
10081501 002130000 0 1 1 0.035 1
10081601 0 0 0 1 0.035 1
10081701 0 0.0 0.0 0.0 1
10081801 0.0 10.0 10.0 0.0 0.0 0.0 0.0 1.0 1
10081901 0.0 10.0 10.0 0.0 0.0 0.0 0.0 1.0 1
*
20100100 c-steel
20200100 power 501 1.0 1.0
20200101 0.0 0.0
20200102 100.0 0.0
.

Reference 10.21

**INEEL/EXT-02-00589, May 2002, SCDAP/RELAP5-3D Code Manual,
Volume 5: Assessment of Modeling of Reactor Core Behavior During
Severe Accidents, Appendix A12, "TMI-2 Accident"**

A12. TMI-2 ACCIDENT

A12.1 Introduction

The TMI-2 Accident Test Problem provides under full scale conditions an assessment of virtually every in-core damage progression model in the SCDAP/RELAP5/MOD3.3 code. Since the accident was not an experiment, the measured behavior of the reactor during the accident was limited. Nevertheless, the limited amount of information obtained during the accident and the post-accident examinations of the reactor provide a significant amount of information for assessing at least in an indirect manner most of the in-core damage progression models in the code. The TMI-2 accident involved spacer grid meltdown, cladding ballooning, control rod meltdown, fuel rod oxidation, hydrogen production, cladding meltdown, fuel melting, molten pool formation, quenching of hot and embrittled fuel rods, and molten pool slumping. The measurements obtained during the accident and inferences made from observations after the accident only provide quantitative assessment of a few of the damage progression models, such as models that calculate total hydrogen production, location of previously molten frozen material, and total amount of molten material. Nevertheless, since one damage progression event in the overall chain of damage progression events is dependent upon all the other previous damage progression events in the chain, the correct calculation of a few of the damage progression events cannot be made without a correct calculation of the other damage progression events. So an indirect assessment can be made of virtually every in-core damage progression model in the code.

A12.2 Description of TMI-2 Accident Problem

All major components of the TMI-2 primary system were represented in the TMI-2 Accident Test Problem. The RELAP5 module was used to simulate the thermal-hydraulics of the reactor vessel, primary coolant loops, steam generators, and pressurizer. Steam generator secondary side coolant levels, pressures, and feedwater temperatures, and primary side makeup and letdown flow rates were supplied as boundary conditions. The SCDAP module was used to simulate the reactor core, which was divided into five radial regions by grouping similarly powered fuel assemblies together.

The TMI-2 accident is generally divided into four distinct phases for analysis purposes.^{A12-1} Phase 1 (0 - 100 min) is a small-break loss-of-coolant accident (LOCA) through the stuck-open pilot-operated relief valve (PORV). One or more reactor coolant system (RCS) pumps operated continuously during Phase 1 of the accident, thereby providing adequate core cooling. Phase 2 (100 - 174 min) is a continuation of a small break LOCA without the RCS pumps. Core uncover, heatup, and initial melting occurred during Phase 2. Phase 3 (174 - 200 min) begins with a restart of reactor coolant pump 2B. Approximately 30 m³ of coolant was injected into the reactor vessel in less than one minute, cooling the peripheral fuel assemblies and forming an upper core debris bed with significant zircaloy oxidation. Heatup of the degraded core region, with the formation and growth of a pool of molten material, continued during Phase 3. Phase 4 (200 - 300 min) begins with the initiation of high pressure injection (HPI). The central region of the partially molten core material was not coolable by HPI even though the water level reached the level of the hot legs by 207 min. Between 224 and 226 min, the crust encasing and supporting the molten core region is believed to have failed, allowing molten material to relocate to the lower plenum. Summaries of the measured and observed reactor core damage are given in References A12-2 and A12-3.

The RELAP5 portion of the TMI-2 model was derived from an Oconee plant model described in Reference A12-4. Both TMI-2 and Oconee are PWR's having a two-by-four coolant loop configuration, i.e., two primary coolant loops, each containing one hot leg and two cold legs. Both plants were built by Babcock & Wilcox in the 1970's and have nearly identical design and operating characteristics. Consequently, the Oconee RELAP5 model was easily adapted to represent TMI-2. Figure A12-1 through Figure A12-4 are nodalization diagrams of the reactor vessel, primary piping, steam generators, and pressurizer respectively.

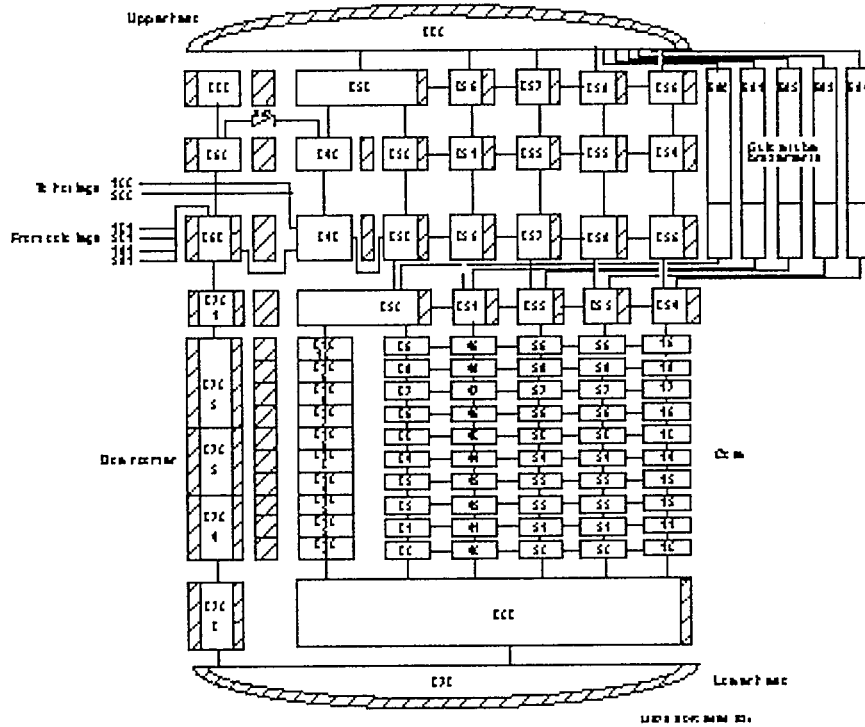


Figure A12-1. RELAP5 nodalization of the reactor vessel and core.

The RELAP5 vessel model (Figure A12-1) represent all major components of the reactor vessel, including the inlet annulus, downcomer, lower plenum, core, core bypass, upper plenum, upper head, reactor vessel vent valves, and the control rod guide tube brazements. The core is divided into five parallel channels, each consisting of ten subvolumes (branch components 10 through 59). Lateral flow between adjacent core channels is simulated using the RELAP5 crossflow model. Annulus component 570 represents the downcomer and pipe component 510 the core bypass. Branch components 505 and 575 represent the lower plenum. The upper plenum is also divided into five parallel regions that are connected laterally by crossflow junctions. This arrangement allows for the development of in-vessel natural circulation under appropriate conditions. Valve component 542 represents the reactor vessel vent valves and pipe components 580 through 584 the guide tube brazements. Fifty-one heat structures were used to model the thermal behavior of reactor vessel metal structures.

Figure A12-2 is a nodalization diagram of the primary coolant loop A, which consists of one hot leg (components 100 through 114), one steam generator (discussed subsequently), two pump suction legs (pipe components 135 and 165), and two cold legs (components 140 through 151 and 170 through 181).

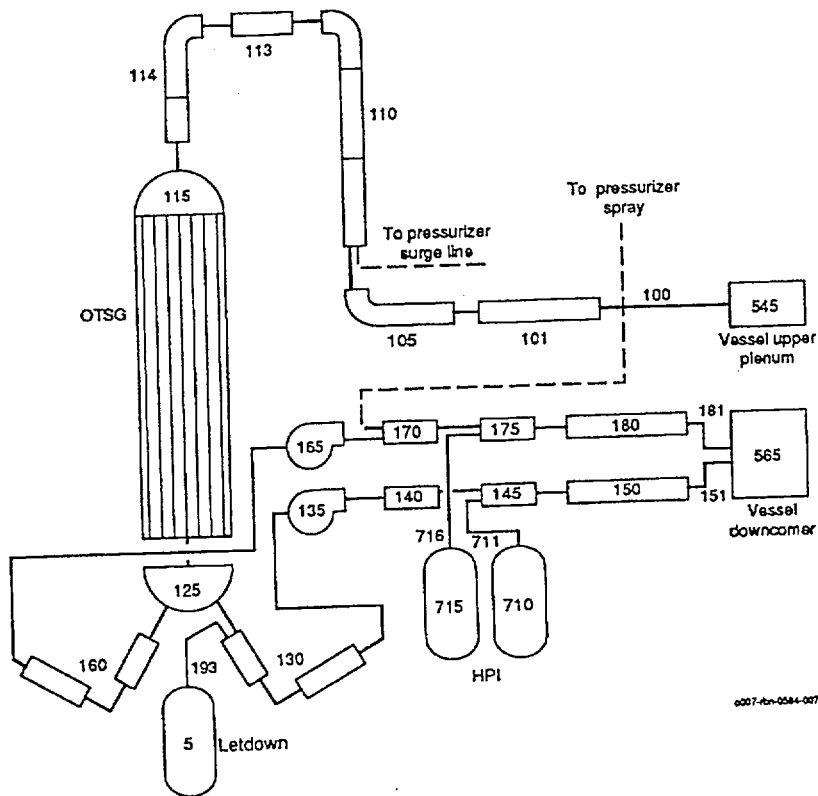


Figure A12-2. RELAP5 nodalization of primary coolant loop A.

Primary loop B is identical to loop A, except it does not contain a letdown flow path (time-dependent junction 193) or connections to the pressurizer spray and surge lines. The component numbers for loop B are also increased by 100 (e.g., the primary pumps are numbered 235 and 265 rather than 135 and 165). The high pressure injection (HPI) system is represented by time-dependent volumes 710 and 715, which are connected to the cold legs by time-dependent junctions 711 and 716. HPI flow is assumed to be split equally between the A and B loops while makeup flow is injected only into the B loop. Eighteen heat structures (per loop) were used to model the thermal behavior of the primary piping.

The nodalization of steam generator A is shown in Figure A12-3. Steam generator B is identical except that all component numbers are increased by 100. The boiler region is divided into two parallel flow channels: an inner channel (volumes 310 through 323), connected to 90% of the steam generator tubes, and an outer channel (volumes 360 through 373), connected to 10% of the steam generator tubes. Crossflow junctions connect the two boiler regions. Auxiliary feedwater is normally injected into the top of the 10% region. Pipe component 120 represents the primary side of the steam generator tube bundle, while branch components 115 and 125 represent the inlet and outlet plena. The steam generator downcomer is modeled by component 305, and components 345 and 350 represent the steam line. To preheat the feedwater, a portion of the steam flow is bled into the downcomer through an aspirator near mid-boiler (modeled with a junction between component 365 and 305). Valve component 821 represents the main steam valve. Forty-three heat structures were used to model the thermal behavior of steam generator metal structures (including the tube bundle).

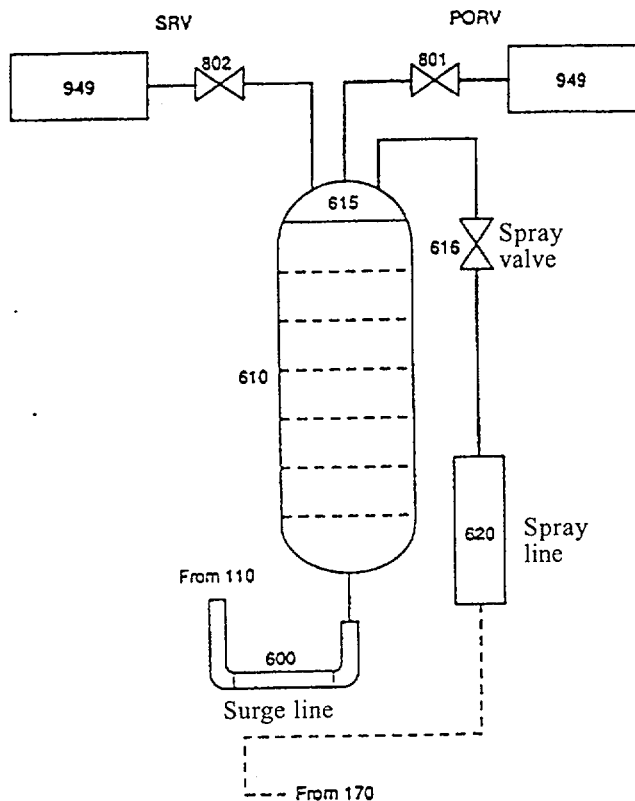


Figure A12-4. RELAP5 nodalization of the pressurizer.

represents the containment building, which is initially filled with air at 101 kPa. Twelve heat structures are used to model the thermal behavior of the pressurizer shell, upper and lower heads, and the surge line; one heat structure is used to simulate operation of the pressurizer heaters; and five heat structures are used to model the thermal behavior of the containment building.

It should be noted that critical flow through the PORV is modeled using the homogeneous (single velocity) two-phase flow option in RELAP5. Previous TMI-2 calculations using SCDAP/RELAP5^a have shown that this option better predicts the PORV flow history reported in the TMI-2 initial and boundary conditions (ICBC) data base^{A12-6} than other options. [The PORV flow rates reported in Reference A12-7 were calculated using the Henry-Fauske critical flow model for subcooled conditions and the homogeneous equilibrium critical flow model (HEM) for two-phase conditions.] It should also be noted that for all calculations reported here, a servo valve was installed between the pressurizer and the surge line at 117 min to prevent the pressurizer from draining. In preliminary calculations, the pressurizer drained completely after the PORV block valve was closed at 139 min, which effectively terminated core heatup. More accurate representations of the surge line and pressurizer might eliminate some of the problems encountered in this and previous TMI-2 analyses. For example, the junction connecting the surge line to

a. C. A. Dobbe, private communication, EG&G Idaho, Inc., March 15, 1994.

hot leg A should be oriented horizontally rather than vertically (to reflect its true alignment) and the countercurrent flow limitation (CCFL) model should be activated at the junction connecting the surge line to the pressurizer, rather than at the hot leg junction. Also, the CCFL input parameters (currently set to default values) should be reviewed for applicability.

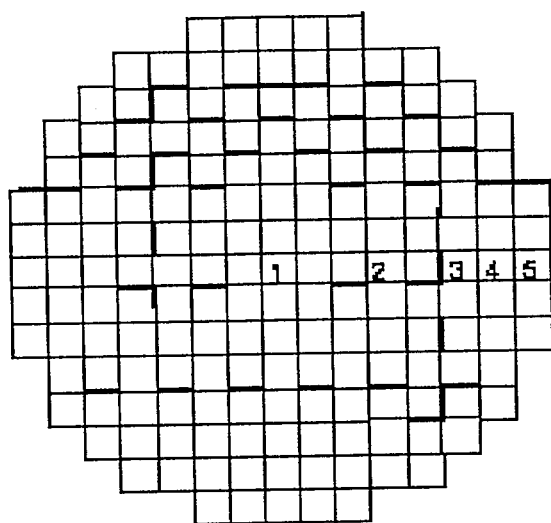
The TMI-2 core was divided into five regions for this analysis by grouping similarly powered fuel assemblies together. Figure A12-5 is a cross-section of the core illustrating each region and its average radial power peaking factor. Table A12-1 lists the average axial power peaking factors for each region. Both the axial and radial peaking factors were derived from detailed peaking factor data presented in Appendix A of Reference A12-6.

Table A12-1. TMI-2 axial power peaking factors.

| Distance from bottom of fuel (m) | Power factor | | | | |
|----------------------------------|--------------|----------|----------|----------|----------|
| | Region 1 | Region 2 | Region 3 | Region 4 | Region 5 |
| 0.183 | 0.665 | 0.674 | 0.729 | 0.690 | 0.670 |
| 0.549 | 0.933 | 0.919 | 0.962 | 0.951 | 0.944 |
| 0.914 | 1.134 | 1.099 | 1.112 | 1.132 | 1.145 |
| 1.280 | 1.216 | 1.164 | 1.112 | 1.168 | 1.213 |
| 1.646 | 1.248 | 1.202 | 1.138 | 1.192 | 1.238 |
| 2.012 | 1.262 | 1.221 | 1.153 | 1.206 | 1.248 |
| 2.377 | 1.225 | 1.232 | 1.251 | 1.241 | 1.222 |
| 2.743 | 1.078 | 1.124 | 1.174 | 1.131 | 1.083 |
| 3.109 | 0.792 | 0.853 | 0.880 | 0.834 | 0.794 |
| 3.475 | 0.448 | 0.512 | 0.488 | 0.455 | 0.442 |

One SCDAP fuel rod component is used to represent all the fuel rods in each core region. One SCDAP control rod component is used to represent all the full and part-length control rods, all the guide tubes (including those containing burnable poison rods), and all the instrument tubes in each core region (except region five which contains no control rods). The control rod radii in regions one through four have been adjusted so that the total mass of zircaloy, Ag-In-Cd absorber, and stainless steel is conserved (the burnable poison mass is neglected). In core region five, a dummy fuel rod component is used to represent all the guide and instrument tubes. By specifying a small fuel diameter and zero power, this component essentially behaves as a hollow zircaloy tube. The SCDAP grid spacer model is used to represent the eight inconel spacer grids that are uniformly distributed along the length of each fuel assembly.

Much of the SCDAP input data was obtained from Reference A12-8 and is summarized in Table A12-2. Table A12-3 lists the total number of fuel assemblies, fuel rods, control rods, burnable poison rods, and orifice rods in each core region.



| <u>Region</u> | <u>Radial Peaking Factor</u> |
|---------------|------------------------------|
| 1 | 1.245 |
| 2 | 1.136 |
| 3 | 1.074 |
| 4 | 1.061 |
| 5 | 0.733 |

MC20-000-0004-001

Figure A12-5. Cross-sections of core showing fuel assembly grouping and radial peaking factors.

Table A12-2. Total fuel assemblies, fuel rods, and control rods in each core region.

| Core regions | Fuel assemblies | Fuel rods | Full-length control rods | Part-length control rods | Burnable poison rods | Instrument tubes | Orifice rods |
|--------------|-----------------|-----------|--------------------------|--------------------------|----------------------|------------------|--------------|
| 1 | 13 | 2704 | 144 | 0 | 64 | 13 | 0 |
| 2 | 28 | 5824 | 256 | 0 | 192 | 28 | 0 |
| 3 | 40 | 8320 | 192 | 128 | 320 | 40 | 0 |
| 4 | 48 | 9984 | 384 | 0 | 384 | 48 | 0 |
| 5 | 48 | 9984 | 0 | | 128 | 48 | 640 |
| Total | 177 | 36816 | 976 | 128 | 1088 | 177 | 640 |

Table A12-3. SCDAP input parameters.

| Parameter | Value |
|--|------------------------|
| Fuel rods | |
| Active height (m) | 3.568 |
| Rod pitch (m) | 1.443×10^{-2} |
| Cladding inner radius (m) | 4.788×10^{-3} |
| Cladding outer radius (m) | 5.461×10^{-3} |
| Fuel pellet radius (m) | 4.699×10^{-3} |
| Fuel density (% T.D.) | 92.5 |
| Mass of He fill gas (estimated) (kg) | 1.265×10^{-4} |
| Upper and lower plenum void volume (m ³) | 1.490×10^{-5} |
| Control rods | |
| Guide tube inner radius (m) | 6.325×10^{-3} |
| Guide tube outer radius (m) | 6.731×10^{-3} |
| Cladding inner radius (m) | 5.055×10^{-3} |
| Cladding outer radius (m) | 5.588×10^{-3} |
| Absorber radius (m) | 5.004×10^{-3} |
| Instrument tubes | |
| Tube inner radius (m) | 5.601×10^{-3} |
| Tube outer radius (m) | 6.261×10^{-3} |
| Grid spacers | |
| Grid spacer mass (kg) | 0.86 |
| Grid spacer height (m) | 3.30×10^{-2} |
| Grid spacer thickness (m) | 5.08×10^{-4} |

Table A12-4 compares the initial conditions in the SCDAP/RELAP5 model to those recommended in the ICBC data base.^a with the exception of steam generator pressures and temperatures, the calculated (or specified) initial conditions are in good agreement with the data base. For steady-state calculations, a control system is used in the SCDAP/RELAP5 model to automatically adjust steam generator pressures (by varying the flow areas of the main steam valves) until user-specified cold leg temperatures are obtained. For simplicity, the target coolant temperature for all four cold legs was specified to be 565 K. Table A12-5 compares the calculated initial conditions on the secondary side of each steam generator to

a. All initial conditions correspond to the time of turbine trip: 04:00:37 hours on March 28, 1979.

the initial conditions recommended in Reference A12-9. It is seen that the calculated steam generator pressures are in much better agreement with the Reference A12-9 data than with the ICBC data base.^a Calculated steam generator coolant levels, however, differ considerably from those reported in Reference A12-9. For future calculations, it is recommended that the steam generator models should be adjusted to better represent the Reference A12-9 data. One way to accomplish this may be to increase the pressure drop across the tube support plates as was done for a TMI-2 analysis performed with the CATHARE code.^{A12-10}

Table A12-4. TMI-2 initial conditions at turbine trip.

| Parameter | ICBC data base | SCDAP/RELAP5 |
|---|----------------|--------------|
| Reactor power (MW) | 2700 | 2700 |
| Primary system pressure (MPa) | 15.2 | 15.2 |
| Pressurizer level (m) | 5.77 | 5.76 |
| Pressurizer heater power (MW) | 1.39 | 1.39 |
| Cold leg temperature 1A (K) | 561 | 565 |
| Cold leg temperature 2A (K) | 548 | 565 |
| Hot leg temperature loop A (K) | 592 | 593 |
| Hot leg temperature loop B (K) | 592 | 593 |
| Makeup flow (kg/s) | 5.44 | 0.0 |
| Letdown flow (kg/s) | 4.18 | 0.0 |
| PORV flow (kg/s) | 2.59 | 0.0 |
| Feedwater temperature (K) | 513 | |
| Steam generator A pressure (MPa) | 7.31 | 6.34 |
| Steam generator B pressure (MPa) | 7.24 | 6.28 |
| Steam generator A steam temperature (K) | 586 | 576 |
| Steam generator B steam temperature (K) | 585 | 582 |

a. The pressures reported in Reference A12-9 are average steam line pressures measured 10 to 0.1 min before turbine trip.

Table A12-5. Steam generator initial conditions.

| Parameter | Reference A12-9 | SCDAP/ RELAP5 |
|---|-----------------|------------------|
| Steam generator A feedwater flow (kg/s) | 722 | 723 |
| Steam generator B feedwater flow (kg/s) | 718 | 717 |
| Steam generator A pressure (MPa) ^a | 6.38 | 6.34 |
| Steam generator B pressure (MPa) ^a | 6.24 | 6.28 |
| Steam generator A steam temperature (K) | 586 | 576 |
| Steam generator B steam temperature (K) | 586 | 582 |
| Steam generator A riser level (cm) | 526 | 197 |
| Steam generator B riser level (cm) | 538 | 183 |
| Steam generator A downcomer level (cm) | 660 | 559 |
| Steam generator B downcomer level (cm) | 669 | 543 |
| Steam generator A power (MW) | 1346 | 1332 |
| Steam generator B power (MW) | 1339 | 1378 |

A0.2.1 Boundary Conditions

All boundary conditions, except HPI/makeup flow rates, were obtained from the ICBC data base (Reference A12-6). The HPI/makeup flow rate history reported in Reference A12-11 was adjusted until the time of core uncover (as inferred from hot leg temperature measurements), the time of initial fuel rod cladding failure (as inferred from containment radiation measurements), and the primary system pressure history were predicted reasonable well.^a Figure A12-6 compares the HPI/makeup flow rate history used for the best-estimate SCDAP/RELAP5 calculation discussed subsequently to that recommended in Reference A12-6. In a previous SCDAP/RELAP5 analysis of the TMI-2 accident,^{A12-12} using a previous version of the code, better results were obtained by reducing the makeup flow rate from 4 to 2 kg/s between 100 and 174 min. In an analysis performed with the MELPROG/TRAC code,^{A12-13} it was concluded that the makeup flow rate recommended in Reference A12-6 was too high between 12 and 100 min. For that analysis, the flow was reduced from 6.5 to 1 kg/s between 12 and 100 min (which was the nominal value given in the original issue of the ICBC data base). Core power as a function of time for the first 400 s following reactor scram was estimated using the reactor (point) kinetics and decay heat models in the RELAP5 code. The decay power from 617 minutes onward was obtained from Reference A12-14. Figure A12-7 shows the reactor power versus time curve in the SCDAP/RELAP5 model.

a. The uncertainty in HPI/makeup flow is large, particularly between 100 and 174 min.^{A12-11} Consequently, as noted in Reference A12-12, it isn't possible to determine which assumptions are better.

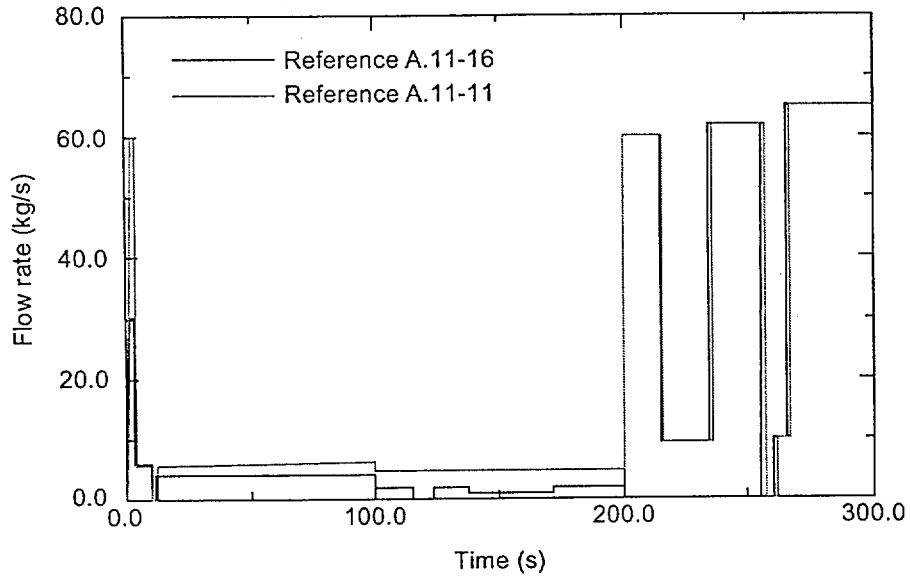


Figure A12-6. Makeup flow history for TMI-2 calculation.

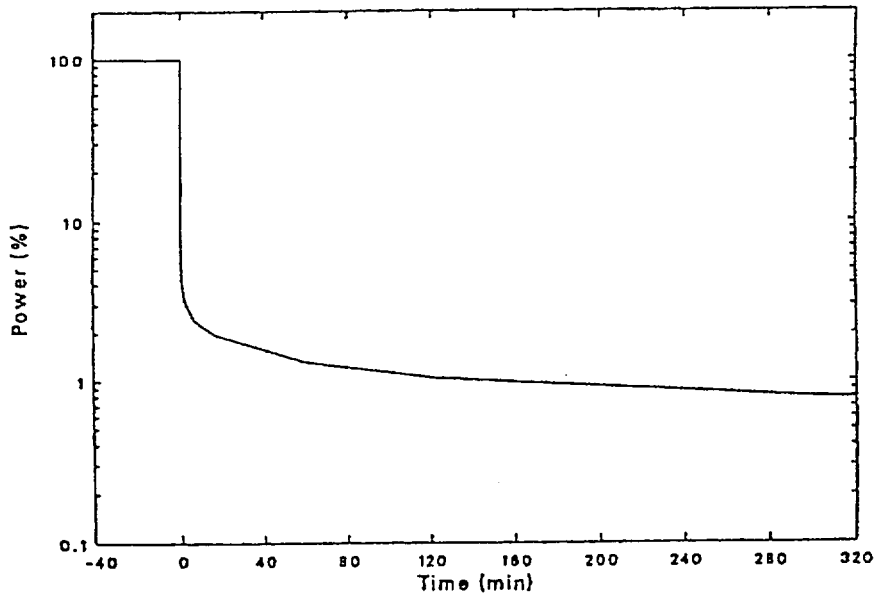


Figure A12-7. Reactor power versus time curve used for TMI-2 calculation.

A12.3 Assessing Using TMI-2 Accident

The timing of the opening and closing of the PORV block valve is an important boundary condition for the TMI-2 accident. Figure A12-8 is a plot that shows the times at which the block valve was opened and closed and the calculated rate of mass flow through the valve for the periods of time that it was open. The plot also shows the calculated rate of flow through the PORV valve. The calculated rate of flow through the open PORV valve ranged from 5 to 35 kg/s.

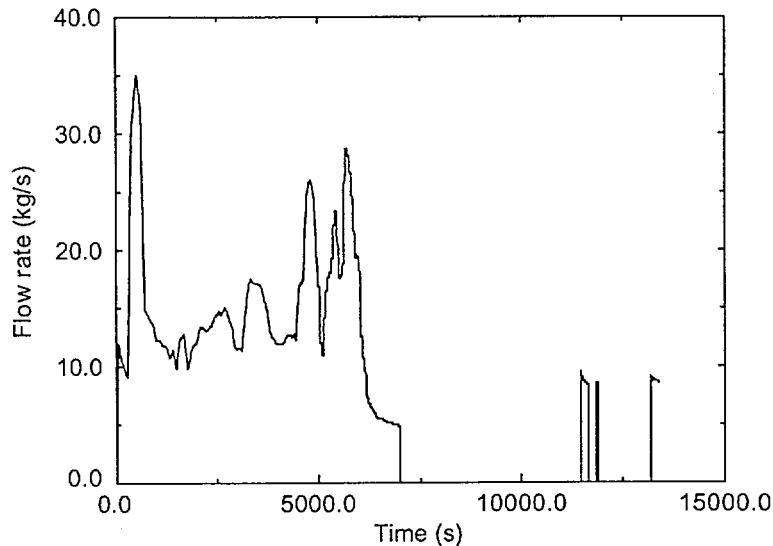


Figure A12-8. Timing of closure of PORV block valve and history of calculated rate of flow through PORV valve.

The SCDAP/RELAP5 MOD3.3 solution to the TMI-2 Accident test Problem is presented next. The calculated timing of the damage progression is described and calculated results are presented for which measurements are available for comparison and assessment. These calculated results are; (1) location of core material, (2) maximum amount of molten material, (3) reactor system pressure, and (4) hydrogen production. Default values were used for all the modeling parameters subject to being defined by the code user.

The damage to the TMI-2 reactor core began with the ballooning and rupture of the cladding of the fuel rods and advanced to the slumping of a significant amount of molten core material to the lower head of the reactor vessel. The MOD3.3 calculated and measured progression of damage are compared in Table A12-6. The results of the MOD3.2 calculation of the TMI-2 accident are included in the table. After core uncover was calculated to occur at 6270 s, core damage was calculated to occur quite rapidly. Cladding failure due to ballooning was calculated by MOD3.3 to begin at 8445 s. MOD3.2 calculated cladding failure to be due to chemical attack by the Inconel spacer grids and to not occur until 9417 s. After cladding failure, double-sided oxidation of the cladding was calculated by MOD3.3 to occur in the vicinity of the cladding failure. The melting of fuel and the formation of a molten pool were calculated by MOD3.3 to begin at 9500 s. MOD3.2 calculated molten pool formation to begin at 10,330 s. The start-up of the

2B-pump at 10,446 s was calculated by both MOD3.3 and MOD3.2 to cause a rapid increase in the pressure of the primary coolant system and to accelerate the rate of hydrogen production. These calculations are in agreement with the measurements. MOD3.3 calculated 9,530 kg of molten material in the core region at the start of the 2-B pump and 27,600 kg of molten material in the core just before the slumping of core material to the lower head at 12,890 s. MOD3.2 calculated 1734 kg of molten material in the core region at the start-up of the 2B-pump and 37,400 kg of molten material in the core just before the slumping of core material to the lower head at 13,379 s. The post-accident examination of the TMI-2 reactor indicated that 40,800 kg of the reactor core was molten at some time. Inferences from the measured system pressure and other measurements indicate that 15,800 kg of molten material slumped to the lower head at 13,500 s. Both the MOD3.3 and MOD3.2 calculated masses of molten material and the time of slumping are in approximate agreement with the measured values. The MOD3.3 calculated location of molten core material was in fair agreement with the post-accident observation of the TMI-2 reactor. The elevations of the bottom surface of the in-core molten pool at the centerline of the core were calculated and observed to be 1.10 m and 0.11 m, respectively. The highest location in the core to become molten was calculated to be 2.9 m and to be located along the centerline of the core. The molten pool was calculated to extend in the radial direction from the centerline of the reactor vessel to the periphery of the reactor core. The bottom surface of the molten pool at the periphery of the core was calculated by MOD3.3 to be at the elevation of 2.2 m. These calculated results are in agreement with the post-accident observation of the TMI-2 core.

Table A12-6. Calculated timing and sequence of core damage progression.

| Damage progression parameter | Measured or inferred | MOD3.2 | MOD3.3 |
|--|----------------------|--------|--------|
| Beginning of long term core uncoverly (s). | - | 6,390 | 6,270 |
| Beginning of cladding failure due to ballooning (s). | - | 9,417 | 8,445 |
| Beginning of spacer grid slumping (s). | - | 9,418 | 9,112 |
| Beginning of molten pool (s). | - | 10,330 | 9,530 |
| Cumulative hydrogen production at start-up of 2B-pump at 10,446 s (kg). | 300 | 275 | 365 |
| Primary coolant system pressure at start-up of 2B-pump (MPa). | 8.20 | 5.03 | 6.96 |
| Mass of molten material at start-up of 2B-pump (kg). | - | 1734 | 15,000 |
| Increase in primary coolant system pressure after start-up of 2B-pump (MPa). | 6.30 | 5.21 | 7.00 |
| Final cumulative hydrogen production (kg). | 460 | 453 | 417 |
| Mass of core material that was molten during some period of accident (kg). | 40,800 | 37,400 | 27,600 |

Table A12-6. Calculated timing and sequence of core damage progression. (Continued)

| Damage progression parameter | Measured or inferred | MOD3.2 | MOD3.3 |
|--|----------------------|--------|--------|
| Elevation of bottom of molten region relative to bottom of core (m). | 0.71 | 1.46 | 1.10 |
| Smallest distance from side of molten pool to periphery of core (m). | 0.0 | 0.0 | 0.0 |
| Time at which bulk of material in molten material slumped to lower head (s). | 13,500 | 13,379 | 12,890 |
| Mass of molten material that slumped to lower head (kg). | 15,800 | 37,400 | 27,600 |
| Percent of molten material that slumped to lower head (%). | 39 | 100 | 100 |

MOD3.3 calculated a greater rise of the water level in the reactor core after activation of the 2B-pump than did MOD3.2. Both MOD3.3 and MOD3.2 calculated damage progression to be a strong function of the calculated collapsed liquid level in the reactor vessel. Figure A12-9 are plots of the MOD3.3 and MOD3.2 calculated collapsed liquid levels as a function of time. A temporary core uncover was calculated by MOD3.3 to begin at 4800 s and the long term uncover was calculated to begin at 6330 s. After 6330 s, the core continued to uncover until the 2-B pump activation at 10,446 s. The collapsed liquid level was calculated by MOD3.3 to be 0.3 m above the bottom of the reactor core just before activation of the 2-B pump. MOD3.2 calculated the collapsed liquid level just before start-up of the 2B-pump to be 0.2 m above the bottom of the reactor core. After activation of the 2-B pump, MOD3.3 calculated the water level to rise 3.0 m and MOD3.2 calculated the water level to rise 0.8 m. This difference in calculated rise in water level is due to MOD3.3 calculating a significantly greater fraction of the reactor core to be molten at the start-up of the 2B-pump than MOD3.2. Both MOD3.3 and MOD3.2 calculated activation of the HPIS at 12,012 s to cover the entire reactor core with water within 600 s.

The level of water in the pressurizer has an influence on the level of water in the reactor vessel. Figure A12-10 is a plot of the measured water level in the pressurizer and the levels calculated by MOD3.3 and MOD3.2. In the period of 10,000 s to 13,000 s, both MOD3.3 and MOD3.2 calculated a lower level of water in the pressurizer than the measured level.

MOD3.3 calculated severe core damage to begin about 800 s earlier than MOD3.2. The onset of melting of the reactor fuel and the beginning of molten pool formation is a mark of the beginning of severe core damage. The timing of damage progression is indicated by plots of the history of the maximum temperature in the reactor core and of the effective radius of the molten pool, as shown in Figures A12-11 and A12-12, respectively. The effective radius is the radius of a hemisphere with a volume equal to the calculated volume of molten material. The MOD3.3 and MOD3.2 calculated timings for the beginning of fuel melting were 9530 s and 10,330 s, respectively. MOD3.3 calculated a significantly more rapid heatup of the reactor core after the beginning of oxidation than did MOD3.2. In the temperature range of 1800 K to 2200 K, when rapid oxidation occurs, MOD3.3 calculated a heatup rate of nearly 50 K/s. The MOD3.2

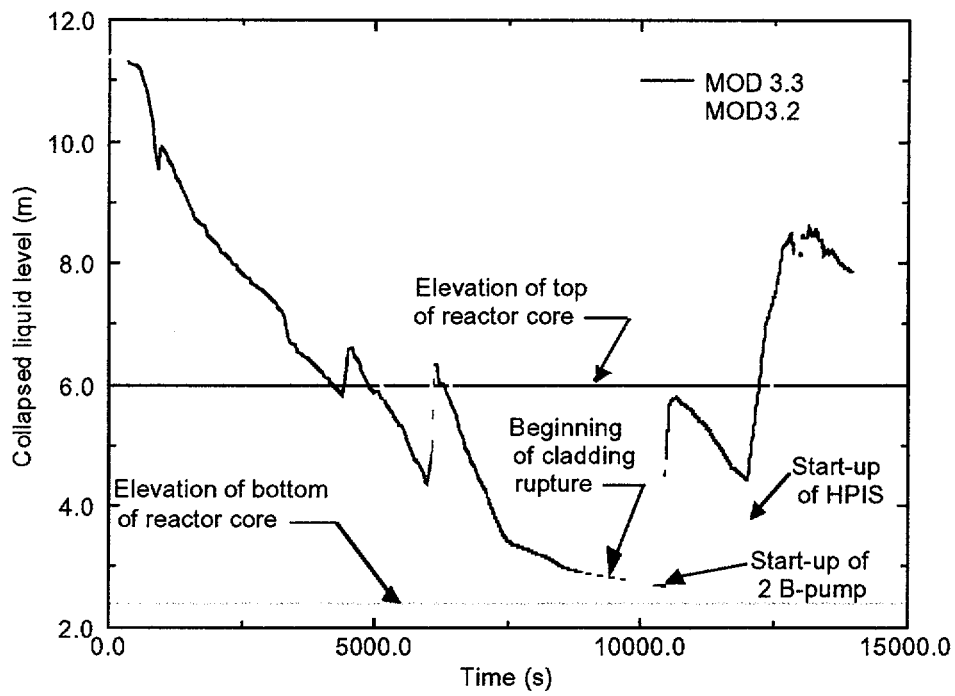


Figure A12-9. History of calculated collapsed liquid level in reactor vessel.

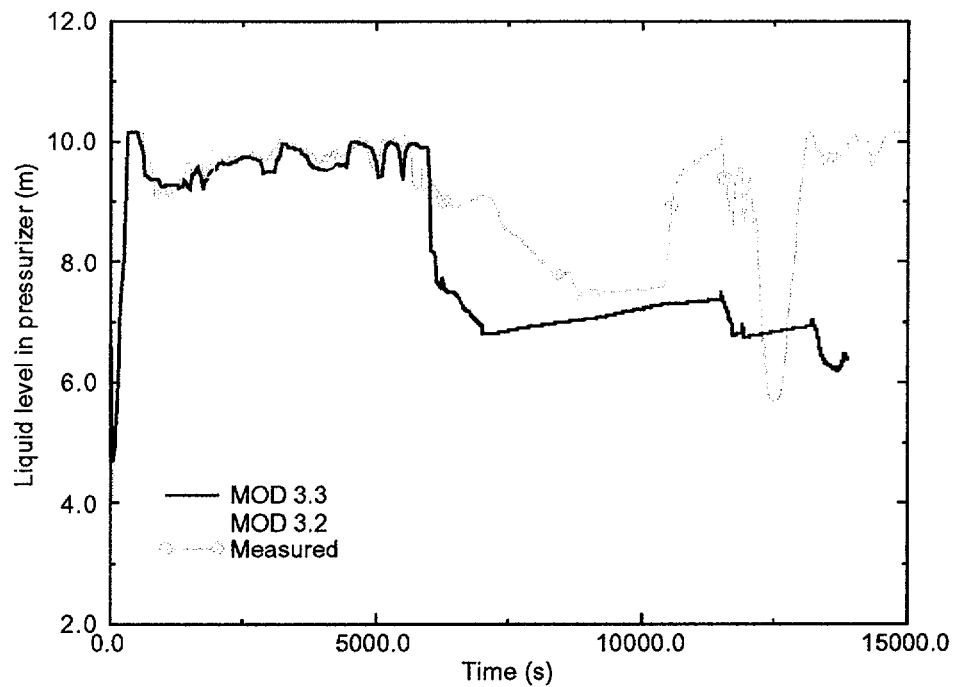


Figure A12-10. Comparison of calculated and measured liquid level in pressurizer.

calculated rate of heatup in this range of temperature was significantly less than that calculated by MOD3.3. Both MOD3.3 and MOD3.2 calculated that activation of the 2B-pump at 10,446 s did not result in any reduction in the maximum core temperature. A reduction in temperature was calculated to not occur because a significant part of the core was in the form of a large molten pool and because of an increase in oxidation of fuel rod cladding due to cracking of oxide layers and more flow of steam. The activation of HPIS at 12,012 s was calculated to not cause any cooling of the molten part of the reactor core. MOD3.3 calculated no further melting of fuel after 10,480 s (34 s after activation of 2B-pump), while MOD3.2 calculated fuel melting to occur until 13,000 s. MOD3.3 calculated the maximum effective radius of the molten pool to be 1.20 m. This value is in general agreement with the corresponding measured value of 1.40 m.

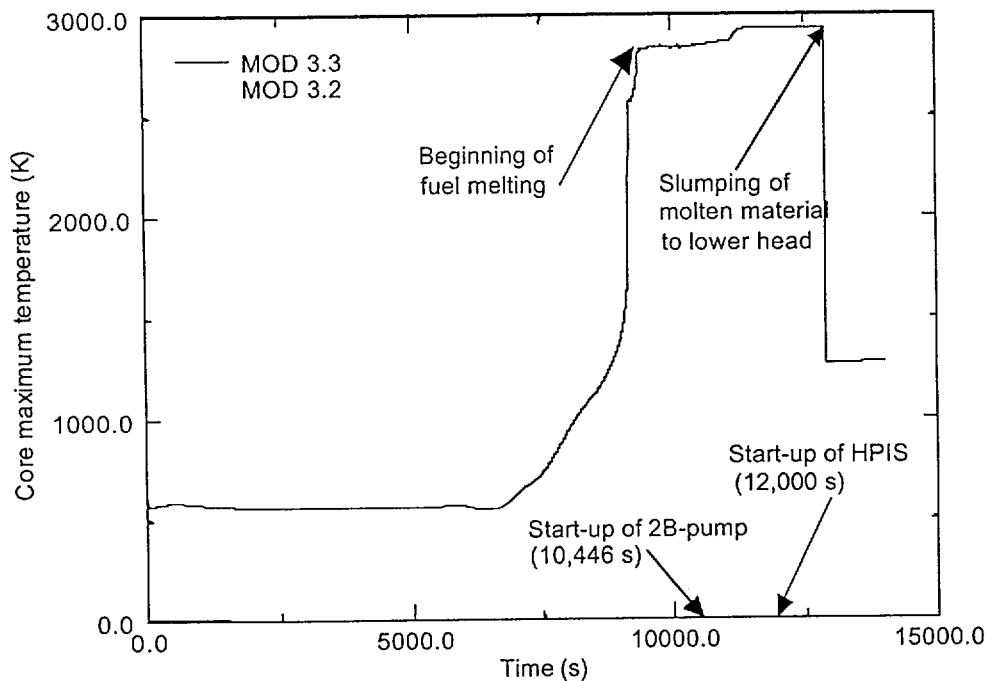


Figure A12-11. History of calculated maximum temperature in reactor core.

The MOD3.3 calculated and measured histories of the primary coolant system pressure were in partial agreement. The measured and calculated pressure histories are compared in Figure A12-13. The MOD3.2 calculated pressure history is also shown. The calculated and measured pressures were in good agreement from the start of the accident until 7,500 s. In the period of 7,500 s to start-up of the 2B-pump at 10,446 s, the calculated pressure was significantly less than the measured pressure. The coolant system pressure was calculated to increase about 7 MPa after start-up of the 2B pump. This calculated increase in pressure was in general agreement with the measured pressure increase of 6.3 MPa. The increase in pressure was calculated to be due to steam generated by pumping of water into the hot reactor core and by heatup of the reactor core by an acceleration in the oxidation of fuel rod cladding. In the period of 10,500 s to activation of HPIS at 12,012 s, the pressure was calculated and measured to gradually decrease a few MPa. After activation of the HPIS, the pressure was calculated and measured to increase a few MPa.

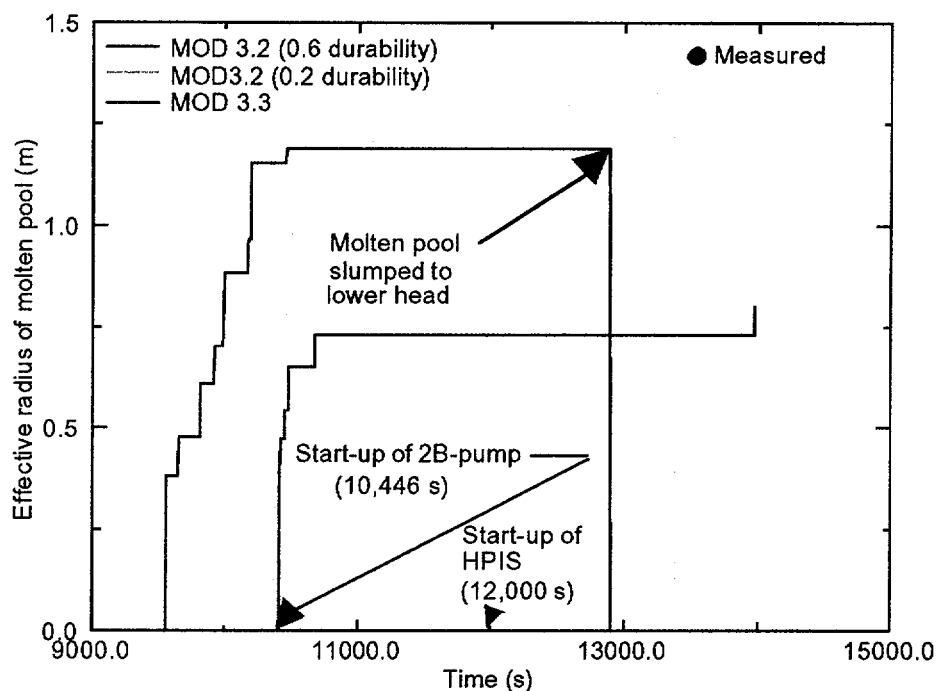


Figure A12-12. History of calculated effective radius of molten pool.

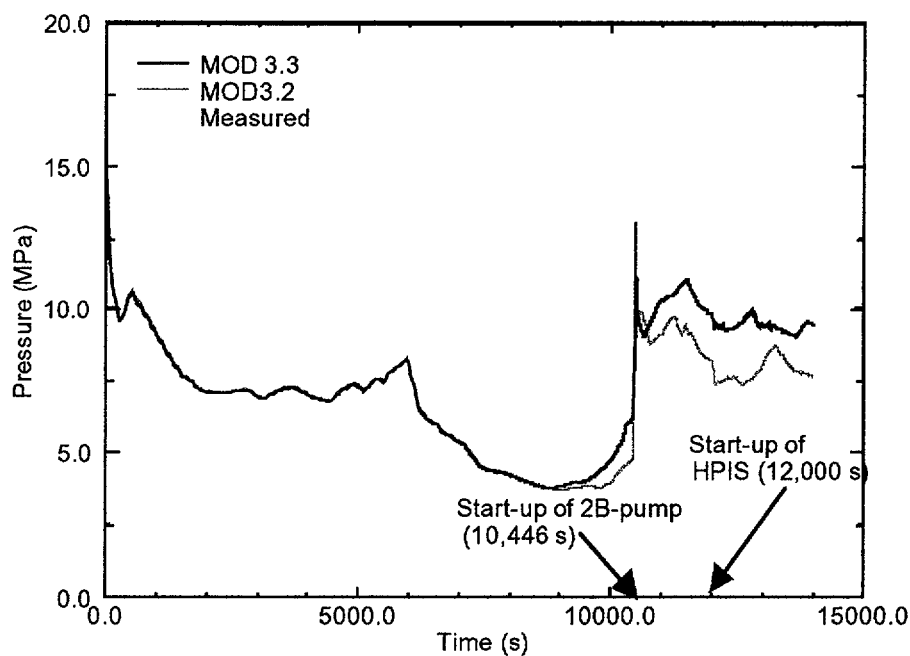


Figure A12-13. Calculated and measured pressures of primary coolant system.

The MOD3.3 calculated pressure history of the primary coolant system was improved using the boundary conditions for the TMI-2 accident applied by Annunziato et al.^{A12-17} The TMI-2 accident has a large degree of uncertainty in boundary conditions that influence the pressure of the primary coolant system. The accident has uncertainties in boundary conditions such as make-up flow rate, performance of the 2B-pump, flow rate through the PORV, and time of its closure. Since there are uncertainties in these boundary conditions, the TMI-2 accident was also calculated by MOD3.3 using the boundary conditions used by Annunziato et al. The pressure history calculated by a slightly earlier version of MOD3.3 with these boundary conditions is compared with the measured pressure history in Figure A12-14. The calculated pressure history in the period of 7500 s to 10,000 s was in general agreement with the measured pressure history. Other aspects of reactor behavior, such as the total hydrogen production and total mass of molten material, were also in general agreement with measurements and the post-accident observation.

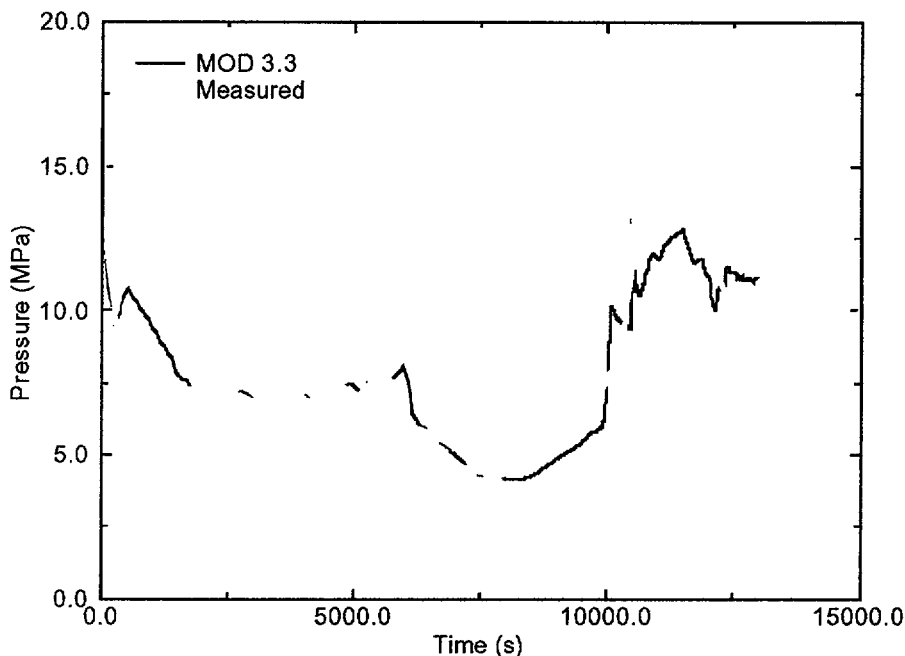


Figure A12-14. Comparison of calculated and measured pressure histories of primary coolant system for case of boundary conditions from Annunziato.

The calculated hydrogen production was in general agreement with the hydrogen production estimated from post-accident observations and inferences. The MOD3.3 calculated cumulative hydrogen production is compared with the measured hydrogen production in Figure A12-15. The MOD3.2 calculated hydrogen production is also shown in the figure. MOD3.3 calculated the rapid production of hydrogen to begin sooner than MOD3.2. Nevertheless, both the MOD3.3 and MOD3.2 calculations of hydrogen production are in approximate agreement with the measured hydrogen production. At the start-up of the 2B-pump, the MOD3.3 and MOD3.2 calculations of cumulative hydrogen production were 275 kg and 365 kg, respectively. The measured hydrogen production at the start-up of the 2B-pump was 300 kg. The MOD3.3 calculated and measured total hydrogen productions were 417 kg and 460 kg, respectively. Both MOD3.3 or MOD3.2 calculated that no significant amount of hydrogen production occurred 50 s after the start-up of the 2B-pump (10,500 s). Hydrogen production was calculated to not

occur after 10,500 s because the portions of the core with intact fuel rods and some metallic cladding were too cool to rapidly oxidize. This behavior is shown in Figure A12-16, where the MOD3.3 calculated temperature histories are shown of the fuel rods in the outer most fuel assemblies of the reactor core at the elevations of 3.11 m and 3.47 m, respectively. As shown in this figure, hydrogen production at the 3.11 m and 3.47 m elevations was calculated to stop due to the cooling caused by the start-up of the 2B-pump. The oxide layer at this location was calculated to be too thin to crack during the reflood caused by start-up of the 2B-pump.

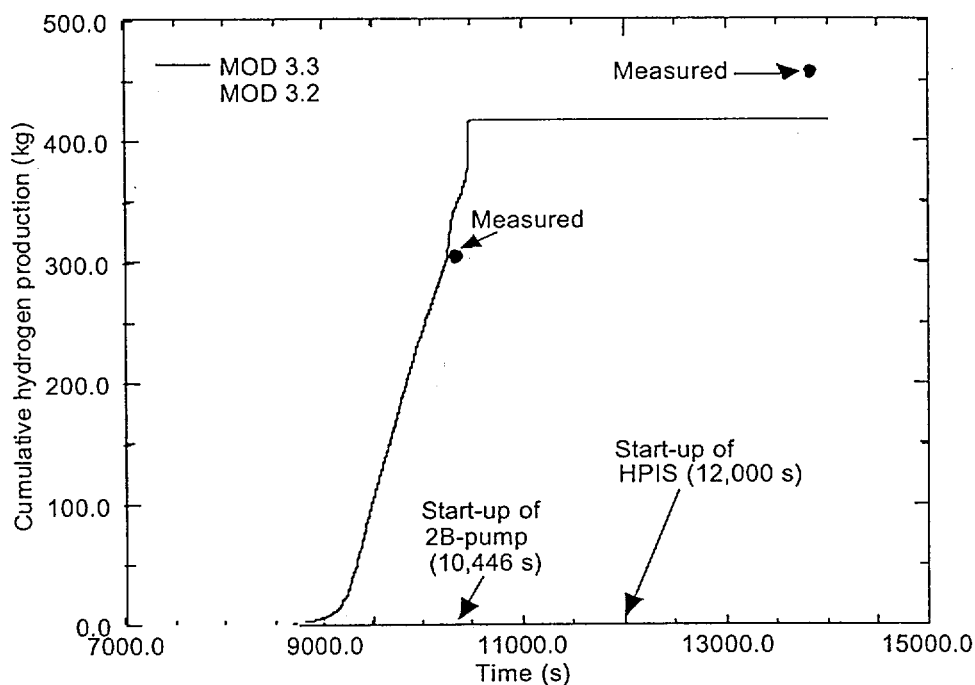


Figure A12-15. Calculated hydrogen production during TMI-2 accident.

The MOD3.3 calculation of the disintegration of fuel rods into porous debris was in agreement with the post-accident observation of the locations in the reactor core with porous debris. Porous debris regions were calculated to form in the outer most fuel assemblies in the elevation interval of 0.5 m to 1.2 m and across the entire diameter of the reactor core in the elevation interval of 2.6 m to 3.6 m. The calculation of porous debris in the elevation interval of 2.6 m to 3.6 m was consistent with the post-accident observation of the state of the reactor core.

The porous debris thermal hydraulic models in MOD3.3 performed properly after activation of the HPIS, which resulted in two-phase coolant conditions in porous debris in the upper part of the reactor core. The calculated temperature history at a location with porous debris is shown in Figure A12-17. The plot applies for the location 2.7 m in elevation and in the fourth ring of fuel assemblies. This location disintegrated from intact fuel rods to porous debris soon after start-up of the 2B-pump, and thus was porous debris at the time of start-up of HPIS. As a result, the flow losses and heat transfer at this location during the reflood period beginning with the start-up of HPIS were calculated with the porous debris thermal hydraulic models implemented into MOD3.3. The debris had a porosity of 0.46 and a particle

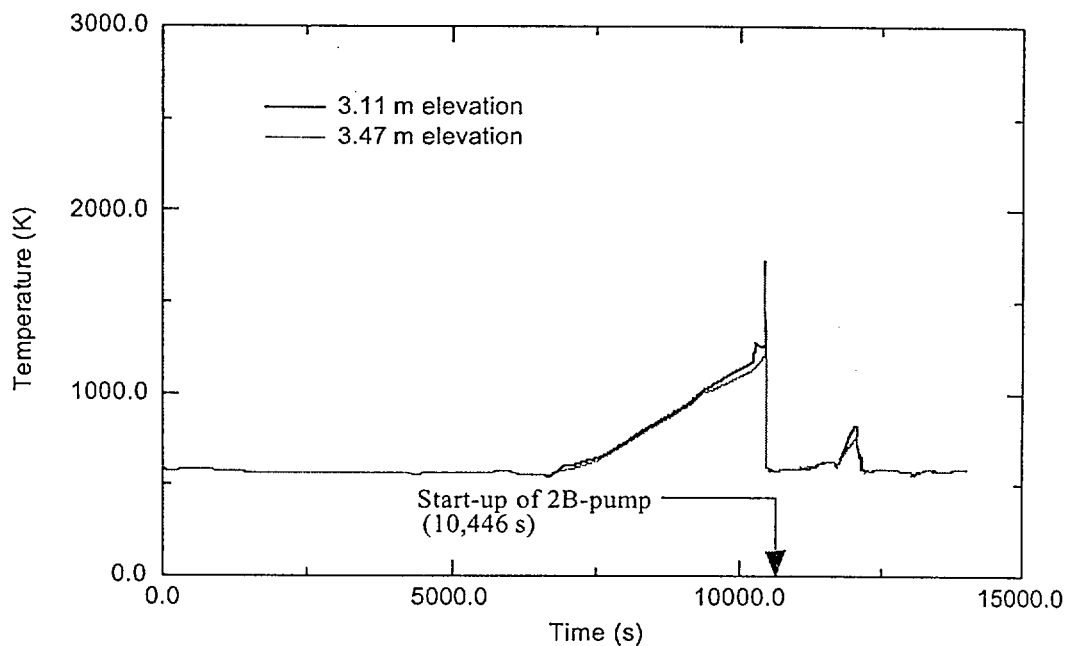


Figure A12-16. MOD3.3 calculated temperature histories of fuel rods in upper part of outer most fuel assemblies in reactor core.

diameter of 3.5 mm. Since the molten pool was located below this location and blocked the upward flow of water from the HPIS, the debris was flooded from the top down. The calculated temperature history of this location following reflood of the reactor core beginning at 12,012 s was consistent with that seen in experiments on the quenching of porous debris, as described in Section A8.

The implementation into MOD3.3 of the integral diffusion model for fuel rod oxidation caused it to calculate a more rapid progression of damage to the reactor core than calculated by MOD3.2. The onset of severe damage was calculated to begin at 9530 s by MOD3.3 and at 10,330 s by MOD3.2. This difference is due to the integral diffusion model for oxidation in MOD3.3 calculating a more rapid heatup due to oxidation at locations with a rich supply of steam than that calculated by the parabolic kinetics model for oxidation in MOD3.2. These differences in calculated behavior also occurred in the analyses of severe fuel damage experiments described in Sections A2 through A4.

The MOD3.3 calculation of the TMI-2 accident was improved by the implementation into MOD3.3 of the stress-based model for calculating the time of failure of an oxide layer retaining the melted metallic part of the fuel rod cladding. While MOD3.2 applied one model for failure of the oxide layer for analysis of severe fuel damage experiments and another model for the analysis of the TMI-2 accident, MOD3.3 applied the same oxide failure model for analysis of severe fuel damage experiments and the TMI-2 accident. The calculations of the oxide failure model have a strong influence on the calculations of hydrogen production and the extent melting of fuel assemblies. With the stress-based model for calculating oxide failure, MOD3.3 calculated hydrogen production and extent of melting in general agreement with measurements for both severe fuel damage experiments and the TMI-2 accident. On the other hand, when using the same oxide failure model for the TMI-2 analysis as used for analysis of severe fuel damage

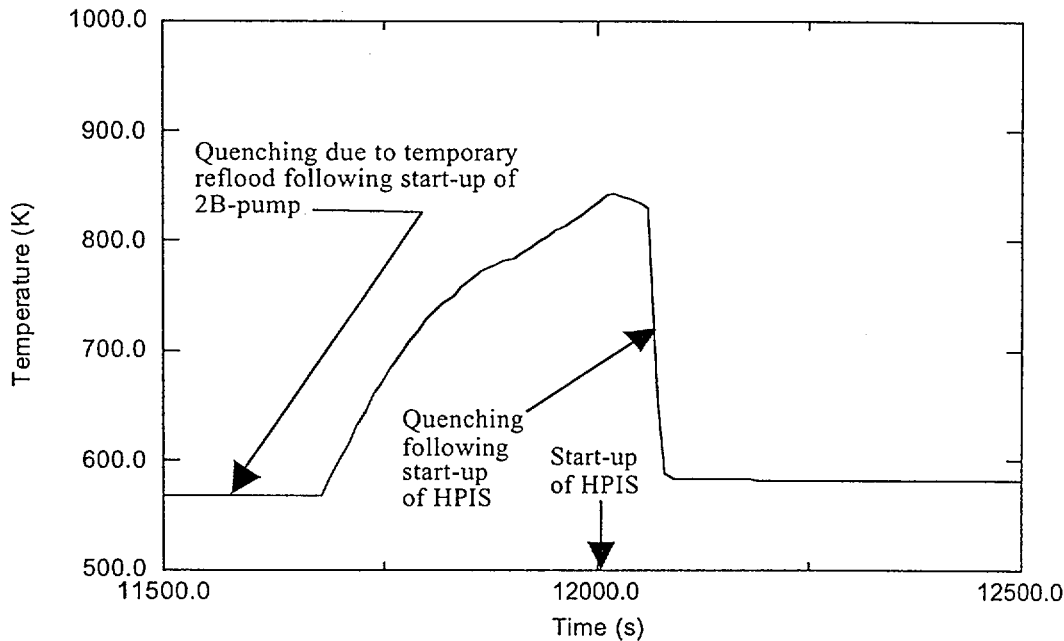


Figure A12-17. MOD 3.3 calculated temperature history of location with porous debris (2.7 m elevation of fourth ring of fuel assemblies).

experiments, MOD3.2 underpredicted by a factor of two the extent of melting of the reactor core, and did not predict any slumping of molten core material to the lower head.

Another difference in calculated reactor core behavior between MOD3.3. and MOD3.2 was in the calculated ballooning and rupture of fuel rods; MOD3.3 calculated ballooning and rupture of fuel rod cladding to occur significantly earlier than MOD3.2. This difference in calculated behavior is due to corrections made in MOD3.3 to the model for ballooning of the fuel rod cladding.

A12.4 Conclusions

The MOD3.3 calculation of the TMI-2 accident showed that its new models result in calculated behavior of the reactor core and primary coolant system in general agreement with measurements and post-accident observations. The calculated and measured hydrogen productions were 417 kg and 460 kg, respectively. The calculated and measured masses of molten material in the core region were 27,600 kg and 40,800 kg, respectively. The MOD3.3 calculation of the locations of porous debris regions in reactor core was for the most part in agreement with the observed locations of porous debris. The calculated temperature behavior of the porous debris was consistent with temperature behavior observed in debris quenching experiments. The calculated and measured rapid increase in primary coolant system pressure following the start-up of the 2B-pump were in good agreement. Except for an intermediate period of the accident, the calculated primary coolant system pressure was in good agreement with the measured pressure for all periods of the accident. An adjustment of boundary conditions within their range of

uncertainty resulted in good agreement of calculated and measured pressure also during this intermediate period. The calculated location of molten material in the core region and the timing of the slumping of this molten material to the lower head were in general agreement with inferences from measurements and the post-accident observation of the reactor core.

The MOD3.3 calculations of the TMI-2 accident differed from the MOD3.2 calculations in some aspects of behavior. MOD3.3 calculated damage progression in the reactor core to occur significantly more rapid than MOD3.2. This difference is due to oxidation of fuel rod cladding in MOD3.3 being calculated by the integral diffusion model instead of by the parabolic kinetics model in MOD3.2. MOD3.3 calculated the ballooning and rupture of fuel rod cladding to occur significantly earlier than MOD3.2. This difference is due to corrections to the ballooning model implemented into MOD3.3. The stress-based model in MOD3.3 for the failure of an oxide layer retaining melted cladding resulted in good agreement of calculations with measurements for both the analysis of the TMI-2 accident and the analyses of severe fuel damage experiments. On the other hand, MOD 3.2 underpredicted the extent of core melting by a factor of two when using for the TMI-2 analysis the same oxide failure model as used for the analyses of severe fuel damage experiments. In the modeling of phenomena causing damage to fuel assemblies during severe accident conditions, MOD3.3 does not require a distinguishing of models for the analyses of severe fuel damage experiments from the models for the analyses of nuclear power plants; one set of models applies for both types of analyses, and all of the models used for nuclear power plant analyses have been assessed using severe fuel damage experiments.

A12.5 References

- A12-1. D. F. Guessing, "The Three Mile Island Analysis Exercise," *Nuclear Technology*, 87, August 1989, pp. 298-301.
- A12-2. J. M. Broughton, P. Kuan, D. A. Petti, and E. L. Tolman, "A Scenario of the Three Mile Island Unit 2 Accident," *Nuclear Technology*, 87, August 1989, pp. 34-53.
- A12-3. J. R. Wolf et al., *TMI-2 Vessel Investigation Project Integration Report*, NUREG/CR-6197, TMI V(93)EG10, EGG-2734, March 1994.
- A12-4. D. A. Brownson, L. N. Haney, and N. D. Chien, *Intentional Depressurization Accident Management Strategy for Pressurized Water Reactors*, NUREG/CR-5837, EGG-2688, April 1993.
- A12-5. E. W. Coryell et al., *SCDAP/RELAP5/MOD3.2 Code Manual Volume III: User's Guide and Input Manual*, NUREG/CR-6150, INEL-95/6422, Revision 1, November 1996.
- A12-6. R. W. Brower L. J. Fackrell, D. W. Golden, M. L. Harris, and C. L. Olaveson, *ICBC Version 3.1, TMI-2 Initial and Boundary Conditions Data Base*, GEND-INF-078, January 1988.
- A12-7. Y. Nomura, *PORV Discharge Flow During the TMI-2 Accident*, EGG-TMI-7825, July 1987.
- A12-8. D. Coleman, "As-Built Design and Material Characteristics of the TMI-2 Core," *Part III in TMI-2 Accident Core Heatup Analysis, A Supplement*, NSAC-25, June 1981.

- A12-9. J. L. Anderson, *TMI-2 Once Through Steam Generator Secondary Level Analysis*, EGG--TMI-7359, January 1987.
- A12-10. P. Dumaz, "Three Mile Island Unit 2 Analysis Exercise: CATHARE Computations of Phases 1 and 2 of the Accident," *Nuclear Technology*, 87, December 1989, pp. 946-955.
- A12-11. J. L. Anderson, *Recommended HPI Rates for the TMI-2 Analysis Exercise (0 - 300 Minutes)*, EGG-TMI-7833, September 1987.
- A12-12. D. W. Golden and N. Ohnishi, *SCDAP/RELAP5 Demonstration Calculation of the TMI--2 Accident*, EGG-TMI-8473, March 1989.
- A12-13. F. E. Motley and R. P. Jenks, "Modeling of the Three Mile Island Unit 2 Accident with MELPROG/TRAC and Calculation Results for Phases 1 and 2," *Nuclear Technology*, 87, August 1989, pp. 302-309.
- A12-14. T. R. England and W. B. Wilson, *TMI-2 Decay Power: LASL Fission-Product and Actinide Decay Power Calculations for the President's Commission on the Accident at Three Mile Island*, LA-8041-MS, Revised, March 1980.
- A12-15. E. L. Tolman et al., *TMI-2 Accident Scenario Update*, EGG-TMI-7489, December 1986.
- A12-16. J. K. Hohorst et al., *TMI-2 Analysis using SCDAP/RELAP5/MOD3.1*, INEL-94/0157, November 1994.
- A12-17. A. Annunziato, A. Franceschini, and C. Addabbo, "TMI-2 Simulation by RELAP5/SCDAP and COMETA Codes," 8th International Conference on Nuclear Engineering, April 2-6, Baltimore, MD USA.

Reference 10.23

Letter from ITS Corporation (K. Ross)

to

OPPD (F. James Jensen)

September 9, 2002

**“ITS Corporation’s Cursory Review of OPPD’s LTOP
Analysis”**



Innovative Technology Solutions Corporation

Merging Innovation with Technology

September 9, 2002

F. James Jensen III
Nuclear Design Engineer
Fort Calhoun Nuclear Station
OPPD
P. O. Box 550
Fort Calhoun, NE 68023

Subject: ITS Corporation's Cursory Review of OPPD's LTOP Analysis

Reference: Fort Calhoun Low Temperature Overpressure Protection Final Report, Revision 1, 3/15/02,
Enercon Services

Dear Mr. Jensen:

ITS Corporation has performed a cursory review of the RELAP model developed by Enercon for OPPD for analyzing postulated Fort Calhoun transients having the potential to exercise the Low Temperature Overpressure Protection (LTOP) System. This letter report documents the review. In summary, no modeling concerns have been identified which question the conclusions of OPPD's current LTOP analysis. The RELAP model seems well designed and the LTOP analysis seems thorough and well conceived. NRC LTOP analysis requirements appear to have been followed. A few modeling specifics that might be improved upon have been identified. They are discussed below. Suggested modeling changes are made in context.

Injection Water Temperature

The temperature of the injection water in the mass addition scenarios was taken to be 250 °F. This temperature is unrealistically high for safety injection water and for makeup (charging) water under cold shutdown conditions. The reasoning behind the use of elevated injection water temperature seems questionable. However, the LTOP report argues convincingly that the elevated temperature is conservative; the reasons being that:

1. Injection mass flow rates were specified assuming that the injection water was cold.
2. The peak reactor coolant system (RCS) pressure predicted by RELAP for a particular scenario was compared to the allowable pressure on the P/T curve given the temperature of the RCS at the beginning of the scenario (as opposed to the higher allowable pressure on the P/T curve given the higher temperature of the RCS at the time the peak pressure occurred).

The argument that the use of elevated injection water temperature is conservative is believable. However, a review recommendation is that any future RELAP LTOP calculations be made with realistic injection water temperatures.

PORV Flow Resistance

A hand calculation was made to verify the flow resistance offered by the PORV in the RELAP model. This was done to address questions that arose in the course of the review regarding the adequacy of the PORV modeling for subcooled liquid flow. In several of the mass-addition LTOP scenarios, RCS temperature remains below the



Innovative Technology Solutions Corporation

Merging Innovation with Technology

saturation temperature downstream of the PORV. In these scenarios, the PORV is flowing liquid water. The hand calculation is included as Attachment 1. The results of the hand calculation were compared to the results of the RELAP calculation for the base mass-addition LTOP scenario. The RELAP calculation had to be extended for a comparison to be made. The specific comparison was of the steady-state pressure drop across the PORV given a cold water-solid RCS and a fixed charging flow rate. Critical in considering the mass addition scenarios involving the charging pumps is realizing that these pumps at FCS are positive displacement pumps (as opposed to centrifugal pumps). Such pumps develop a certain flow irrespective of head. As such, the pressure excursion that would be experienced by FCS given spurious operation of all charging pumps (and one operating PORV) in a cold shutdown condition would be largely different (smaller) than what would be experienced by a plant having centrifugal charging pumps. For 132 gpm charging flow, the hand calculation and the RELAP calculation predict a pressure drop across the PORV of 36.6 and 57.0 psid, respectively. The RELAP modeling then of the flow resistance offered by the PORV to subcooled liquid flow shows to be on the conservative side. (A review recommendation is, however, that PORV modeling be done differently in future RELAP LTOP calculations. The current RELAP modeling of the PORV for subsonic single-phase flow (e.g., cold liquid water flow) is not clean. Use of the abrupt expansion model should be replaced by the inclusion of a physical flow coefficient (C_v) table. The current PORV modeling is conservative because the area of the orifice in the valve has been defined 18% smaller than physical. Were a physically representative orifice area defined, the conservatism in flow resistance offered to cold flowing liquid would be lost. A physically representative C_v value of 24.58 for a full-open FCS PORV is calculated in Attachment 1.)

RCS Pressurization Rate in Mass-Addition Scenarios

A hand calculation was made to verify the time taken for the RCS to pressurize to the PORV set point in the base mass-addition LTOP case. This was done on account of questions that arose in the course of the review regarding the seemingly slow pressurization rate in the RELAP calculation of further water addition to a water-solid system. The calculation is included as Attachment 2. It simply relates the charging flow rate to the volume of the RCS and the compressibility of liquid between the initial RCS pressure and the PORV set point. The hand calculation and the RELAP calculation predict an elapse of 16.9 and 18.3 sec, respectively, from the time charging flows initiate to the time the PORV set point is reached. This good comparison satisfied the review questions regarding pressurization rate.

Reactor Coolant Pumps

The heating of RCS inventory associated with irreversible flow losses in the system is accounted for in the RELAP LTOP model by depositing energy in the fluid as it flows through the reactor coolant pumps. This is appropriate but there is a conservatism here that may have been overlooked. As part of the thermal hydraulic solution performed by RELAP, irreversible losses associated with wall friction are deposited in the fluid locally as heat. Typically wall friction accounts for roughly half of the flow loss in an RCS; the other half being attributed to "minor"-type flow losses through fittings, abrupt expansions and contractions, etc. Minor-type flow losses are not deposited in the fluid as part of the thermal hydraulic solution performed by RELAP. Thus, the heat additions made to the RELAP LTOP calculations to account for reactor coolant pump operation are roughly 50% higher than realistic.

It was noticed that in cases where a reactor coolant pump was not operating, the pump component was removed from the RELAP model and a simplistic control-volume component was substituted. It is unclear why this was done. A substantial effort was clearly made in the modeling of the pumps as evidenced by the complete set of homologous curves defined. It would be good to take advantage of the thorough pump modeling given the



Innovative Technology Solutions Corporation

Merging Innovation with Technology

reverse loop flows that develop in many (all?) of the LTOP scenarios. If the reason for removing the pumps was robustness-related (e.g., code stops), it would have been good to state this in the LTOP report. In any case, it would have been good to include a description of how the resistance offered by a stopped reactor coolant pump to reverse flow was captured in the surrogate component.

Volume Control Flags

It was noticed in the course of the review that a handful of control volumes had the calculation of wall friction disabled. It is unclear why this was the case. If this was inadvertent, it would be good to enable friction in these control volumes for consistency.

Pressurizer

The pressurizer is modeled as a single stack of 6 control volumes. With respect to interfacial heat and mass transfer considerations, it would be better to use either 2 or more adjacent stacks of cells or simply a single cell to represent the pressurizer. The reason for this is the tendency for unrealistic stratification to develop. In an actual pressurizer, the liquid inventory is well mixed by circulative natural convection flows. In a single stack of control volumes, RELAP has no way to develop such flows. Consequently, stratified layers of largely varying temperature can develop. Relatively cold layers can unrealistically sit atop relatively hot layers. This unphysical stratification can impact the realism of the interfacial heat and mass transfer calculated by RELAP between the liquid region and vapor space of the pressurizer.

The pressurizer inventory in the heat addition LTOP scenarios was appropriately initialized as saturated. In the mass addition cases, however, the pressurizer inventory was initialized at the initial temperature of the RCS. This seems questionable given that 1) before the spurious injection, the pressurizer inventory would have been saturated at the initial pressure of the RCS, and that 2) the pressurizer heaters are assumed to be operating as the pressurizer fills with liquid. It might be more defensible to start mass-addition scenarios with a realistic pressurizer condition (i.e., saturated with level in the nominal range) and then allow the pressurizer to fill with the heaters operating. It could be that the pressure drop across the PORV differs meaningfully dependent upon the temperature of the liquid in the pressurizer. (This might especially be true if the liquid temperature were greater than the saturation temperature downstream of the PORV.)

Steady State

A review recommendation is that in future LTOP analyses documentation, results be presented of an extended steady-state RELAP calculation. The objective of including the steady-state results would be to identify close correspondence between the RELAP LTOP model and actual FCS monitored parameters. The calculation should have reactor power at the full operating value, and should include realistic feedwater temperature, active steam generator level control, and active RCS pressure control. The goal here would be to convincingly illustrate the base realism of the RELAP model.

Steam Generators

The secondary side of the steam generators and the steam generator tubing metal mass were conservatively excluded from the mass-addition scenarios. In the heat addition scenarios, the generators were initialized entirely full of liquid which was hot relative to RCS temperature. Initializing the steam generators full of liquid seems



Innovative Technology Solutions Corporation

Merging Innovation with Technology

unrealistically conservative. A suggestion of the review is that future heat addition LTOP calculations be initialized with steam generator level in the nominal range consistent with where the operators would maintain it.

Summary

In summary, the model shortcomings identified in the course of the review are not thought to have the potential to meaningfully impact the conclusions of OPPD's current RELAP LTOP calculations. The RELAP model seems well suited to performing LTOP transients and is very well documented. Modeling uncertainties appear to have been consistently addressed in a conservative manner.

It needs to be emphasized that ITS Corporation's review of the OPPD LTOP model was cursory only. As such ITS Corporation can not attest that the model is physically representative of FCS or that the LTOP analysis is valid. It does seem though that the model and the analysis performed with it are sound.

ITS Corporation appreciates this opportunity to support OPPD and looks forward to providing future support.

Sincerely:

A handwritten signature in dark ink, appearing to read 'Kyle Ross'.

Kyle Ross
Senior Engineer

cc: Jan Bostelman
Jack Dallman



Attachment 1: Hand Calculation of Fort Calhoun PORV Pressure Drop and Determination of PORV C_v for Liquid Flow

Problem

1. What would the pressure drop across an FCS PORV be given a 132 gpm flow of 80 °F water.
2. What would the appropriate flow coefficient (C_v) be for such flow.

Given

A 2.5 in valve body with a 0.94 in² (1.0940 in dia) orifice

Basic Equations

[Per Crane Technical Paper No. 410 - see attached]

The rate of flow of an incompressible fluid through an orifice may be expressed by:

$$q = C \cdot A \sqrt{\frac{2 \cdot g \cdot 144 \cdot \Delta P}{\rho}} \quad \text{Eq. 1}$$

where:

q = rate of flow in units of ft³/s

C = orifice flow coefficient

A = orifice area in units of ft²

g = 32.2 ft/s²

ΔP = upstream gauge pressure in units of psig

ρ = incompressible fluid density in units of lbm/ft³

C in the above is given by the attached chart as a function of Reynolds Number and diameter ratio β which are expressed as:

$$\beta = \frac{d_1}{d_2} = \frac{\text{orifice diameter}}{\text{valve body diameter}} \quad \text{Eq. 2}$$

$$\text{Re} = \frac{\rho \cdot \bar{V} \cdot d}{\mu} \quad (\text{based on } d_2) \quad \text{Eq. 3}$$

The resistance coefficient K in the formula:

$$h_L = K \cdot V^2 / 2 \cdot g \quad \text{Eq. 4}$$

is given by:



$$K_{orifice} \cong \frac{1 - \beta^2}{C^2 \beta^4} \quad \text{Eq. 5}$$

The flow coefficient is given by:

$$C_v = \frac{29.9 \cdot d^2}{\sqrt{K}} \quad (\text{based on } d_2) \quad \text{Eq. 6}$$

Solution

Solving Eq. 1 for ΔP :

$$\Delta P = \frac{\rho}{2 \cdot g \cdot 144} \left(\frac{q}{C \cdot A} \right)^2 \quad \text{Eq. 7}$$

Eq. 2 gives:

$$\beta = \frac{1.0940 \text{ in}}{2.5 \text{ in}} = 0.44 \quad \text{Eq. 8}$$

Assuming $\rho = 62.2586 \text{ lbm/ft}^3$ and $\mu = 1.791\text{e-}5 \text{ lb}_r\text{-sec/ft}^2$, Eq. 3 gives $Re = 194,163$. Per the attached chart for the above β and Re , C is 0.61. Substituting into Eq. 7 gives $\Delta P = 36.6 \text{ psid}$.

Substituting for β and C in Eq. 5 gives $K_{orifice} = 57.82$. Substituting into Eq. 6 gives $C_v = 24.58$.

Flow Through Nozzles and Orifices

Orifices and nozzles are used principally to meter rate of flow. A portion of the theory is covered here. For more complete data, refer to Bibliography sources 8, 9, and 10... or to information supplied by the meter manufacturer.

Orifices are also used to restrict flow or to reduce pressure. For liquid flow, several orifices are sometimes used to reduce pressure in steps so as to avoid cavitation. Overall resistance coefficient K for an orifice is given on page A-20. For a sample problem, see page 4-7.

The rate of flow of any fluid through an orifice or nozzle, neglecting the velocity of approach, may be expressed by:

$$q = C_d A \sqrt{2g h_L} \quad \text{Equation 2-21}$$

Velocity of approach may have considerable effect on the quantity discharged through a nozzle or orifice. The factor correcting for velocity of approach,

$$\frac{1}{\sqrt{1 - \beta^4}}$$

may be incorporated in Equation 2-21 as follows:

$$q = \frac{C_d A}{\sqrt{1 - \beta^4}} \sqrt{2g h_L} \quad \text{Equation 2-22}$$

The quantity

$$\frac{C_d}{\sqrt{1 - \beta^4}}$$

is defined as the flow coefficient C . Values of C for nozzles and orifices are shown on page A-20. Use of the flow coefficient C eliminates the necessity for calculating the velocity of approach, and Equation 2-22 may now be written:

$$q = C A \sqrt{2g h_L} = C A \sqrt{\frac{2g(1.44) \Delta P}{\rho}} \quad \text{Equation 2-23}$$

Orifices and nozzles are normally used in piping systems as metering devices and are installed with flange taps or pipe taps in accordance with ASME specifications. The values of h_L and ΔP in Equation 2-23 are the measured differential static head or pressure across pipe taps located 1 diameter upstream and 0.5 diameter downstream from the inlet face of the orifice plate or nozzle, when values of C are taken from page A-20. The flow coefficient C is plotted for Reynolds numbers based on the internal diameter of the upstream pipe.

Flow of liquids: For nozzles and orifices discharging incompressible fluids to atmosphere, C values

may be taken from page A-20 if h_L or ΔP in Equation 2-23 is taken as the upstream head or gauge pressure.

Flow of gases and vapors: The flow of compressible fluids through nozzles and orifices can be expressed by the same equation used for liquids except the net expansion factor Y must be included.

$$q = Y C A \sqrt{\frac{2g(1.44) \Delta P}{\rho}} \quad \text{Equation 2-24}$$

The expansion factor Y is a function of:

1. The specific heat ratio, k .
2. The ratio (β) of orifice or throat diameter to inlet diameter.
3. Ratio of downstream to upstream absolute pressures.

This factor^{8,10} has been experimentally determined on the basis of air, which has a specific heat ratio of 1.4, and steam having specific heat ratios of approximately 1.3. The data is plotted on page A-21.

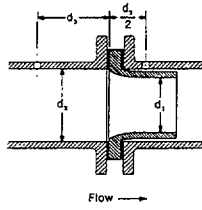
Values of k for some of the common vapors and gases are given on pages A-8 and A-9. The specific heat ratio, k , may vary slightly for different pressures and temperatures, but for most practical problems the values given will provide reasonably accurate results.

Equation 2-24 may be used for orifices discharging compressible fluids to atmosphere by using:

1. Flow coefficient C given on page A-20 in the Reynolds number range where C is a constant for the given diameter ratio, β .
2. Expansion factor Y per page A-21.
3. Differential pressure ΔP , equal to the inlet gauge pressure.

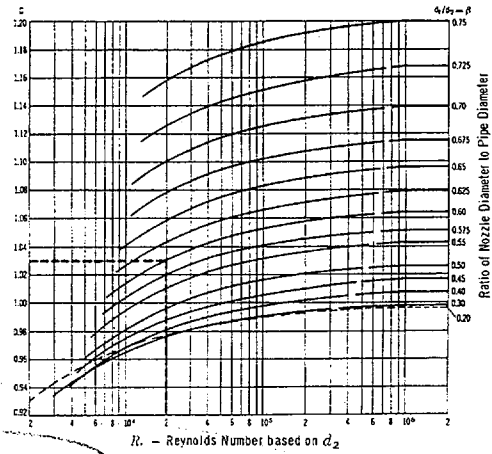
This also applies to nozzles discharging compressible fluids to atmosphere only if the absolute inlet pressure is less than the absolute atmospheric pressure divided by the critical pressure ratio r_c ; this is discussed on the next page. When the absolute inlet pressure is greater than this amount, flow through nozzles should be calculated as outlined on the following page.

Flow Coefficient C for Nozzles⁹

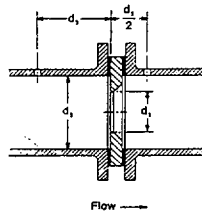


$$C = \frac{C_d}{\sqrt{1 - \beta^4}}$$

Example: The flow coefficient C for a diameter ratio β of 0.60 at a Reynolds number of 20,000 (2×10^4) equals 1.03.

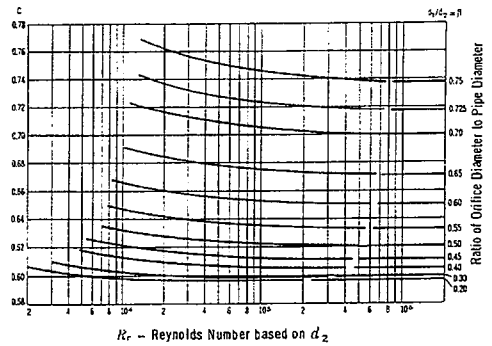
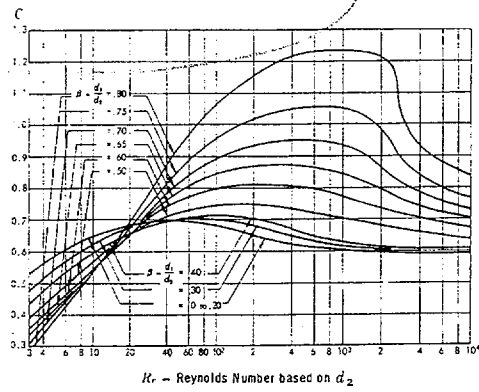


Flow Coefficient C for Square-Edge Orifices^{9,17}



$$C = \frac{C_d}{\sqrt{1 - \beta^4}}$$

$$K_{\text{orifice}} \approx \frac{1 - \beta^2}{C^2 \beta^4}$$



**Resistance Coefficient K , Equivalent Length L/D ,
And Flow Coefficient C_v - continued**

The friction factors for clean commercial steel pipe with flow in the zone of complete turbulence (f_T), for nominal sizes from 1/2 to 24-inch, are tabulated at the beginning of the "K" Factor Table (page A-26) for convenience in converting the algebraic expressions of K to arithmetic quantities.

There are some resistances to flow in piping, such as sudden and gradual contractions and enlargements, and pipe entrances and exits, that have geometric similarity between sizes. The resistance coefficients (K) for these items are therefore independent of size, as indicated by the absence of a friction factor in their values given in the "K" Factor Table.

As previously stated, the resistance coefficient K is always associated with the diameter in which the velocity in the term $v^2/2g$ occurs. The values in the "K" Factor Table are associated with the internal diameter of the following pipe schedule numbers for the various ANSI Classes of valves and fittings.

| | |
|-----------------------------------|--------------|
| Class 300 and lower..... | Schedule 40 |
| Class 400 and 600..... | Schedule 80 |
| Class 900..... | Schedule 120 |
| Class 1500..... | Schedule 160 |
| Class 2500 (sizes 1/2 to 6")..... | XXS |
| Class 2500 (sizes 8" and up)..... | Schedule 160 |

When the resistance coefficient K is used in flow equation 2-2, or any of its equivalent forms given in Chapter 3 as Equations 3-14, 3-16, 3-19 and 3-20, the velocity and internal diameter dimensions used in the equation must be based on the dimensions of these schedule numbers regardless of the pipe with which the valve may be installed.

An alternate procedure which yields identical results for Equation 2-2 is to adjust K in proportion to the fourth power of the diameter ratio, and to base values of velocity or diameter on the internal diameter of the connecting pipe.

$$K_a = K_b \left(\frac{d_a}{d_b} \right)^4 \quad \text{Equation 2-5}$$

Subscript "a" defines K and d with reference to the internal diameter of the connecting pipe.

Subscript "b" defines K and d with reference to the internal diameter of the pipe for which the values of K were established, as given in the foregoing list of pipe schedule numbers.

When a piping system contains more than one size of pipe, valves, or fittings, Equation 2-5 may be used to express all resistances in terms of one size. For this case, subscript "a" relates to the size with reference to which all resistances are to be expressed, and subscript "b" relates to any other size in the system. For sample problem, see Example 4-14.

It has been found convenient in some branches of the valve industry, particularly in connection with control valves, to express the valve capacity and the valve flow characteristics in terms of the flow coefficient C_v . The C_v coefficient of a valve is defined as the flow of water at 60 F, in gallons per minute, at a pressure drop of one pound per square inch across the valve.

By the substitution of appropriate equivalent units in the Darcy equation, it can be shown that,

$$C_v = \frac{29.0d^2}{\sqrt{K}} \quad \text{Equation 2-6}$$

Also, the quantity in gallons per minute of liquids of low viscosity* that will flow through the valve can be determined from:

$$Q = C_v \sqrt{\Delta P \left(\frac{62.4}{\rho} \right)} \quad \text{Equation 2-7}$$

$$Q = 7.9 C_v \sqrt{\frac{\Delta P}{\rho}}$$

and the pressure drop can be computed from the same formula arranged as follows:

$$\Delta P = \frac{\rho}{62.4} \left(\frac{Q}{C_v} \right)^2 \quad \text{Equation 2-7}$$

Since Equations 2-2 and 2-7 are simply other forms of the Darcy equation, the limitations regarding their use for compressible flow (explained on page 1-7) apply. Other convenient forms of Equations 2-2 and 2-7 in terms of commonly used units are presented on page 3-4.

*When handling highly viscous liquids determine flow rate or required valve C_v as described in the ISA Handbook of Control Valves.

* * * * *



Innovative Technology Solutions Corporation

Merging Innovation with Technology

Attachment 2: Hand Calculation of Fort Calhoun Pressurization Rate Given a Water-Solid RCS and Full Charging Flow

Problem

If the FCS RCS were water solid at 200 psig and 80 °F, how long would it take to pressurize the system to the LTOP setpoint of 459 psig if all charging pumps were operating?

Solution

$$V = m / \rho$$

where:

V = volume

m = mass

ρ = density

Since the volume of the RCS is constant:

$$m_1 / \rho_1 = m_2 / \rho_2$$

where the subscripts 1 and 2 associate with the lower and higher pressures, respectively.

Solving for m_2 :

$$m_2 = m_1 \rho_2 / \rho_1 = 3.88877e5 \text{ lbm} \times 62.31098 \text{ lbm/ft}^3 / 62.26142 \text{ lbm/ft}^3$$

$$m_2 = 3.89187e5 \text{ lbm}$$

So the mass associated with the higher pressure is 310 lbm greater than the mass associated with the lower pressure. And so, at a charging flow rate of 132 gpm or 18.356 lbm/s, it would take 16.9 sec to pressurize the RCS from 200 to 459 psig.

Reference 10.25

**Letter from Westinghouse (C. L. Stuart)
to OPPD (F. James Jensen)**

September 11, 2002

**“Calculation of the Pressure-Temperature Limits and
Minimum Temperature Requirements for Core Critical
Operation”**



Westinghouse Electric Company
Nuclear Services
Windsor Service Center
20 International Drive
Windsor, Connecticut 06095
USA

Mr. F. James Jensen III
Omaha Public Power District
Fort Calhoun Station
P.O. Box 399
Fort Calhoun, NE 68023

Direct tel: (860) 731-1613
Direct fax: (860) 731-1674 & 1675
e-mail: Charles.l.stuart@us.westinghouse.com

Our ref: CFTC-02-1

September 11, 2002

Subject: Calculation of the Pressure-Temperature Limits and the Minimum Temperature Requirements for Core Critical Operation

Reference: OPPD Job Order Notice Number RE-02-001
Attachment: Westinghouse Letter LTR-02-CI-134 dated September 11, 2002

Dear Mr. Jensen:

The purpose of this letter is to formally transmit the information requested in the referenced JON. The attached document provides a clarification for the calculation of the pressure-temperature limits and the minimum temperature requirements for core critical operation. If you have any questions or need additional information, please do not hesitate to contact me or the Project Manager, Boris Nadgor, at (860) 731-6728.

Sincerely,

Charles L. Stuart, Jr.
Customer Projects Manager
Nuclear Services

cc: John Ghergurovich
Carl Gimbrone
Bruce Hinton
Boris Nadgor



Memorandum

To: File
cc: John Ghergurovich
Bruce Hinton

Date: September 11, 2002

From: Boris Nadgor
WIN: 265-6728

Our Ref: LTR-CI-02-134

Subject: Calculation of the Pressure-Temperature Limits and the Minimum Temperature Requirements for Core Critical Operation

This purpose of this letter is to respond to OPPD Job Order Notice Number RE-02-001 in order to provide a clarification for the calculation of the pressure-temperature limits and the minimum temperature requirements for core critical operation. These requirements are defined by two criteria specified in 10 CFR Part 50 Appendix G.

According to 10 CFR Part 50 Appendix G, the Reactor Vessel (RV) must be at a temperature equal to or greater than the minimum temperature required for the inservice hydrostatic test and at least 40°F higher than the minimum pressure-temperature curve for normal operation heatup or cooldown.

In addition, in the case when the RCS pressure is greater than 20% of the preservice hydrostatic test pressure (PHTP) and the reactor core is critical, the minimum temperature requirement for the RV must be at least as high as

- the initial RT_{NDT} for the limiting material in the closure flange region which is highly stressed by bolt preload plus 160°F, or
- the minimum permissible temperature for the inservice hydrostatic pressure test, whichever is larger.

Based on these requirements, Westinghouse calculation A-FC-PS-0001, Rev. 000 defines the minimum temperature for the inservice hydrostatic pressure test as 300°F (Section 7.4). This temperature is larger than $\text{Initial } RT_{NDT} + 160^\circ\text{F} = 10^\circ\text{F} + 160^\circ\text{F} = 170^\circ\text{F}$, where $\text{Initial } RT_{NDT} = 10^\circ\text{F}$ is obtained from Letter No. LTR-CI-01-3, S. Byrne (W) to F. J. Jensen (OPPD), "Fort Calhoun RPV Flange Region Initial RT_{NDT} ," dated September 28, 2001.

In order to obtain the data points for the core criticality curve above the minimum temperature for the inservice hydrostatic pressure test, data from Tables 1 and 2 of the calculation are used. The minimum pressure value for each RCS temperature above 260°F will correspond to the temperature point of RCS temperature + 40°F, i.e. the core criticality curve will be parallel to the minimum pressure-temperature curve for normal operation heatup or cooldown with the offset of 40°F to the right.

Therefore, a core criticality curve on Figures 7 and 8 of the calculation may be represented by a vertical line at 300°F and the portion above this temperature of a +40°F offset curve of the minimum pressure-temperature limits.

Note, that the core critical limits established above are solely based upon fracture mechanics considerations, and do not consider core physics safety analyses which can control the temperature at which the core can be brought critical.